

Spectroscopic Studies of Solvation;

Part 1 : Solvation of Thiols.

Part 2 : Hydration of Deoxyribonucleic Acid.

A thesis submitted by
Geoffrey Philip Archer
for the degree of
Doctor of Philosophy
in the
Faculty of Science
of the
University of Leicester.

UMI Number: U497325

All rights reserved

INFORMATION TO ALL USERS

The quality of this reproduction is dependent upon the quality of the copy submitted.

In the unlikely event that the author did not send a complete manuscript and there are missing pages, these will be noted. Also, if material had to be removed, a note will indicate the deletion.



UMI U497325

Published by ProQuest LLC 2015. Copyright in the Dissertation held by the Author.
Microform Edition © ProQuest LLC.

All rights reserved. This work is protected against
unauthorized copying under Title 17, United States Code.



ProQuest LLC
789 East Eisenhower Parkway
P.O. Box 1346
Ann Arbor, MI 48106-1346



7500478674

x25169385x

Statement of Originality

The experimental work described in this thesis was carried out solely by the author during the period November 1984 to January 1988.

The work in this thesis is not being presented for any other degree. All work herein is original unless stated in the text or by reference.

Date : 31/7/1989

Signed

A handwritten signature in cursive script that reads "Geoff. Archer" with a horizontal line extending to the right.

Geoffrey Philip Archer

Acknowledgements

A complete list of those to whom I am indebted for their support, friendship, and advice, would be too long to include here. However, I would like to express my thanks to the following in particular.

Prof. Martyn Symons for his guidance and encouragement. But most of all for managing to convey to me, at least a fraction of his enthusiasm for life in general, and science in particular.

Dr. Graham Eaton for helping me avoid many chemical pitfalls, only to see me become inextricably entwined with a coat hanger.

Dr. David Turner for his advice on N. M. R.

Maggie Pitts for all her love and patience.

The following for providing light (and sometimes heavy !) relief from laboratory bench: Don Jones, John D. McClymont, David 'the fish' Keeble, Chris Rhodes, Rob Janes, Ian Podmore and all other 'lab walkers'.

Dr. Carmen Carmona for introducing me to the delights of tapas and the Spanish way of life.

Mr. A. R. Griffiths and Mrs. A. Crane for their skill in producing the diagrams for this thesis.

The Cancer Research Campaign is thanked for the provision of funds for these studies.

Last, but by no means least, I wish to thank my parents for their unwavering support and love.

Quotations

"The conviction of certainty is a sure proof of nonsense and extreme uncertainty."

- Montaigne.

"What does it matter ? Science has shaped some wonderful things of course, but I'd far rather be happy than right any day."

- Slartibartfast in the Hitchhikers Guide to the Galaxy.

Table of Contents

	Page
1.1 Preview and Introduction	1
1.2 Types of Chemical Bonds	2
1.2.1 The Covalent Bond	2
1.2.2 Ionic Bonding	2
1.2.3 Metallic Bonding	3
1.3 van der Waals Interactions	3
1.3.1 Dipole-Dipole Interactions	3
1.3.2 Induced Dipole-Dipole Interactions	4
1.3.3 Induced Dipole-Induced Dipole Interactions	5
1.4 Repulsion Forces and Combined Interactions	5
1.5 Relative Strengths of Chemical Bonds and van der Waals Interactions	6
1.6 The Hydrogen Bond	6
1.6.1 Background History	6
1.6.2 Criteria for Hydrogen Bonding	7
1.6.3 Types of Hydrogen Bond	9
1.6.4 The Theory of The Hydrogen Bond	10
1.7 The Structure of Water	14
1.7.1 The Continuum Model	15
1.7.2 The Mixture Models	15
1.7.3 Continuum vs. Mixture Models - The Arguments and Evidence	17
1.7.4 The Concept of Free Lone-Pair and OH Groups	20
1.8 Hydrogen Bonding in Alcohols and Thiols	22
1.9 Solvation of Electrolytes	24
1.10 Hydration of Macromolecules	27
1.11 Current Developments and a Summary	31
References for chapter 1	34
2.1 Purification of Materials	41
2.2 Preparation of Samples	41
2.3 Spectroscopic Techniques	42
2.3.1 Infrared Spectroscopy	42
2.3.2 Near Infrared Spectroscopy	42
2.3.3 Nuclear Magnetic Spectroscopy	43
References for chapter 2	44
3.1 Introduction	45
3.2 Previous Work	45
3.3 Experimental	52
3.3.1 Infra-red Spectra	52
3.3.2 Nuclear Magnetic Resonance Spectra	52
3.3.3 First Overtone Near Infra-Red Spectra	53
3.3.4 Purification of Materials	53
3.4 Results and Discussion	54
3.4.1 Fundamental Infra-red Spectroscopy	55
3.4.2 Nuclear Magnetic Resonance Spectroscopy	56
3.4.3 First Overtone Near Infra-Red Spectroscopy	59
3.5 Concluding Remarks	61
References for chapter 3	63

4.1 Introduction	65
4.2 Previous Work	65
4.3 Experimental	69
4.3.1 Infra-red Spectra	69
4.3.2 Nuclear Magnetic Resonance Spectra	69
4.3.3 First Overtone Near Infra-red Spectra	69
4.3.4 Purification of Materials	69
4.4 Results and Discussion	70
4.5 Concluding Remarks	75
References for chapter 4	77
5.1 Introduction	79
5.2 Previous Work	79
5.3 Results and Discussion	84
5.3.1 Solvation of the Dimethylthiophosphate Anion	84
5.3.2 Metal Binding to Dimethylthiophosphate and Dimethylphosphate Anions	86
5.4 Concluding Remarks	92
References for chapter 5	96
6.1 Introduction	98
6.2 Previous Work	98
6.3 Experimental	108
6.3.1 Nuclear Magnetic Resonance Spectra	108
6.3.2 Sample Preparation	109
6.4 Results and Discussion	109
6.5 Concluding Remarks	114
References for chapter 6	116
Appendix I	119

Chapter 1

Introduction.

1.1 Preview and Introduction

Chemistry as a science, is largely concerned with the making and breaking of chemical bonds. A great deal of the work presented in this thesis is concerned with one particular type of bond - the hydrogen bond. Much of the importance of hydrogen bonds is derived from the fact that they have a range of energies (strictly enthalpies) such that, at room temperature they are constantly being broken and reformed.¹ This property has several important biological ramifications, particularly since the physical and chemical behaviour of water is so greatly influenced by hydrogen bonding.² Hydrogen bonds between water and biomolecules such as DNA and proteins have been shown to be important in stabilising conformations in such systems.³⁻⁵

In chapters 3 and 4 the role of hydrogen bonding in systems containing thiol groups is investigated. In particular the studies concentrate upon determining the extent to which ethanethiol is associated in the pure liquid and whether or not thiol groups form hydrogen bonds with water molecules. The second part of this thesis highlights the importance of hydrogen bonding in DNA and DNA related systems. Chapter 5 concentrates upon ion-pairing between various metal di-cations and the dimethylphosphate and analogous thiophosphate anions. Chapter 6 describes the use of high-field fourier transform NMR as a method of obtaining information about the degree of hydration in DNA.

In view of the central role that hydrogen bonding plays in the above studies, it is important to describe and, if possible,

define what is meant by a hydrogen bond and show how the concept of hydrogen bonding fits in with that of chemical bonding and other interactions between molecules.

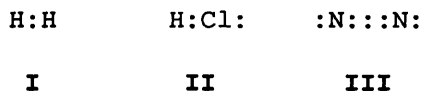
1.2 Types of Chemical Bonds

It is generally considered that there are three forms of chemical bonding: covalent, ionic and metallic.

6

1.2.1 The Covalent Bond

Lewis theory proposes that chemical bonds are formed as a result of the sharing of one or more pairs of electrons between two atoms. This is illustrated for H_2 and HCl in schemes I and II respectively. In the case of nitrogen (N_2) three pairs of electrons are shared between two nitrogen atoms (III).



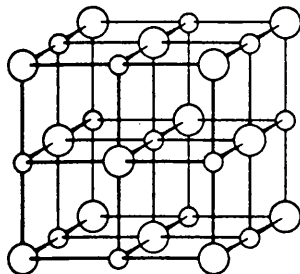
These bonds are described as covalent bonds. It is possible to distinguish between polar and non-polar covalent bonds. In homo-nuclear diatomic molecules, the bonding electrons are shared equally and hence there is no net polarity. However, if the component atoms have different affinities towards electrons the bond will be polarised and a permanent dipole results.

7

1.2.2 Ionic Bonding

In the extreme case of polarised covalent bonds, the difference in electronegativity between component atoms is sufficiently great for the bonding electrons to be transferred completely to one

component, thus creating negatively and positively charged ions which then interact to form an ionic structure. e.g. NaCl (IV).



IV

6

1.2.3 Metallic Bonding

A further bonding type is exhibited by metals. It can be envisaged as individual atoms bearing a positive charge which are surrounded by delocalised electrons. It is these delocalised electrons which are responsible for the observed high electrical and thermal conductivity in metals.

1.3 van der Waals Interactions

This term refers to the sum of all interactions between uncharged molecules. ⁷ These can be conveniently divided into: dipole-dipole, dipole-induced dipole and induced dipole-induced dipole interactions.

1,7

1.3.1 Dipole-Dipole Interactions

In the vicinity of each other, polar molecules exert a force on each other. In liquids and gases the molecules rotate through all angles relative to each other and therefore it might be expected

that the attractive forces ($\rightarrow \rightarrow$) will be cancelled out by the repulsive forces ($\rightarrow \leftarrow$). This argument however, does not allow for the tendency of one dipole to align the other into the favourable orientation. This results in the attractive orientations slightly outweighing the repulsive orientations and hence a net attractive force between the dipoles. The average energy of interaction is given by equation 1.1.

$$E(r) = -\frac{2}{3} \left\{ \frac{\mu_1^2 \mu_2^2}{(4\pi\epsilon_0)^2} \right\} (1/r^6) (kT)^{-1} \quad (1.1)$$

Where μ_1 and μ_2 are the permanent dipole moments of the molecules and r is the separation between them. ϵ_0 , being the vacuum permittivity. From equation 1.1 it is clear that raising the temperature tends to disrupt the alignment of the dipoles and lower the interaction energy. Also it is clear that the energy of interaction is inversely proportional to the sixth power of the separation. The latter relationship is true for all van der Waals forces.

1,7

1.3.2 Induced Dipole-Dipole Interactions

If a polar molecule is introduced into the vicinity of another molecule it has the effect of inducing a dipole in that molecule. This induced dipole will then interact with the permanent dipole of the first molecule. The magnitude of the interaction depends upon both the size of the permanent dipole in the first molecule and the polarisability of the second molecule. The average interaction energy for the two molecules is given by equation 1.2 where: μ_1 is the permanent dipole moment of molecule 1 and α_2 is

the polarisability of molecule 2.

$$\mathbf{E}(r) = -2(\mu_1^2/4\pi\epsilon_0) (\alpha_2/r^6) \quad (1.2)$$

1.3.3 Induced Dipole-Induced Dipole Interactions ^{1,7}

The fact that all aggregates of molecules/atoms can be liquified by cooling to sufficiently low temperatures, irrespective of whether or not they possess a permanent dipole, indicates that additional attractive forces are present. These attractive forces (sometimes known as London forces) arise from the average interaction of an instantaneous moment on one molecule/atom brought about by fluctuations in charge density, and the electric moment induced on the other molecule/atom. An approximation of the energy of interaction of two isotropic groups of polarisability is given by equation 1.3, where r is the distance between the two interacting species and I_1 and I_2 their ionisation potentials.

$$\mathbf{E}(r) \approx \left(\frac{3I_1 I_2}{2(I_1 + I_2)} \right) \left(\frac{\alpha_1 \alpha_2}{r^6} \right) \quad (1.3)$$

1.4 Repulsion Forces and Combined Interactions ^{1,7}

Repulsion effects are always present between molecules/atoms in any system. These electronic and nuclear repulsions increase very rapidly as the separation decreases. The precise behaviour of the forces, at short separations, is very complicated and depends upon the nature of the species. Despite the complexities involved in calculating repulsion forces, a good approximation of total

interaction is given by the Lennard-Jones potential (equation 1.4). Generally a value of 12 is used for n in which case it is referred to as the Lennard-Jones (12,6) potential.

$$E(r) = C_n / r^n - C_6 / r^6 \quad (1.4)$$

1.5 Relative Strengths of Chemical Bonds and van der Waals Interactions

Some typical bond strengths are presented in table 1.1. In comparison, van der Waals forces are very weak, being only in the order of a few tenths of a kcal/mole. Intermediate in strength between chemical bonds and van der Waals interactions are interactions between molecules which fulfil certain criteria. This interaction is known as the hydrogen bond and has an interaction energy usually in the region of a few kcal mol⁻¹.

1.6 The Hydrogen Bond

1.6.1 Background History

Towards the end of the last century, scientists began to realise that in order to explain the behaviour of some associated compounds such as acetic, benzoic and hydroxybenzoic acids some new theories were necessary. It soon became apparent that compounds containing certain functional groups such as the hydroxyl group were more likely to form complexes than other molecules

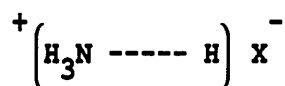
Werner proposed that ammonium salts have structures in which a hydrogen atom lies between the ammonia molecule and the

Table 1.1

Some typical chemical bond strengths

Bond	Bond Enthalpy (kcal mol ⁻¹)
C—C	83
C=C	146
C—H	99
H—H	104
O—H	111
S—H	88
N—H	93

counter-ion in some way bridging the two (V). The same kind of structure was proposed by Moore and Winmill¹² to account for the observation of low dissociation of trimethyl ammonium hydroxide $(\text{CH}_3)_3\text{NHOH}$ when compared with tetramethyl ammonium hydroxide $(\text{CH}_3)_4\text{NOH}$. Later the first intra-molecular hydrogen bonds were^{13,14} observed.



v

Despite these observations, and subsequent proposals of structures which today would be considered as hydrogen bonds, it was not until Latimer and Rodebush in 1920¹⁵ recognised the existence and importance of hydrogen bonding in water, that the true extent of hydrogen bonds in chemistry became apparent.

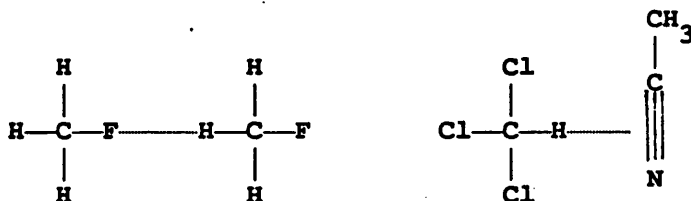
1,8,9

1.6.2 Criteria for Hydrogen Bonding

Given the wide range of systems which display hydrogen bonding, it might be thought that trying to produce a list of criteria necessary for hydrogen bonding to occur, which satisfy all cases, would be difficult. In practice however, it is clear that hydrogen bonding involves two functional groups, one of which must be able to act as a base (or electron donor) and the other have an acidic proton. The two groups may be in the same molecule, in which case intramolecular hydrogen bonding occurs, or in separate molecules whence intermolecular hydrogen bonds are formed.

So far no mention of an energy criterion has been made but it is

clear that some cutoff point must be made which can differentiate between, for example, the interaction between two methyl fluoride molecules (CH_3F) (VI) and that between chloroform (CHCl_3) and acetonitrile (VII).



VI

VII

In the case of the former the interaction is so weak that it might not be considered as a hydrogen bond even though it might be thought to satisfy the requirement concerning functional groups. A simple solution may be to state that ¹⁶ "...to be a 'hydrogen bond,' the energy of complex formation must be greater than dipolar or London dispersion force energies."

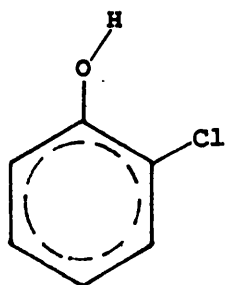
Other criteria arise from the techniques used to probe hydrogen bonding. If crystallographic methods are employed then a suitable criterion may be the distance $r(\text{A}-\text{H})$ between the electronegative atom of the electron donor group (A) and the acidic proton. If this is equal to or less than the van der Waals radii of the two atoms, then a hydrogen bond can be said to have been formed i.e. the contraction in bond length caused by hydrogen bond formation is greater than or equal to twice the van der Waals radius of the proton. Low frequency shifts in B—H stretching frequency upon formation of a hydrogen bond B—H—A with an electronegative

donor group (A) in infra-red and Raman spectra, have been used to determine relative hydrogen bond strength.^{17,18} Similarly, downfield shifts in proton resonance are also associated with hydrogen bonding and have been extensively studied.¹⁸

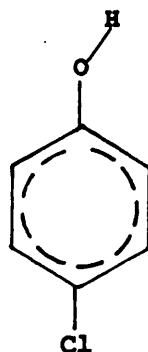
1.6.3 Types of Hydrogen Bond

Essentially, hydrogen bonds can be divided into two groups; one in which the bond is intermolecular, and the other in which it is intramolecular. Further differentiation can be made between compounds which can form intermolecular hydrogen bonds in their pure state e.g. water, alcohols and hydrofluoric acid; and those which require the presence of another species to provide the functional group (either electron acceptor or donor) which they do not possess, for example dimethylsulphoxide, triethylphosphine oxide and chloroform. When molecules of the latter type are mixed with suitable species so as to form hydrogen bonds, surprisingly large enthalpy changes occur. Those molecules that can form intermolecular hydrogen bonds in the pure state are said to have bifunctionality, i.e. act as both an electron donor and acceptor.

The effect of intramolecular hydrogen bonding can be demonstrated by examining the boiling points of the series; chlorobenzene, *o*-chlorophenol and *p*-chlorophenol which are, respectively, 132°C, 175°C and 217°C.⁹ Quite clearly the introduction of intramolecular hydrogen bonding with the hydroxyl and chloro groups ortho to each other (VIII) decreases the amount of intermolecular bonding relative to that shown when the groups are in the para configuration (IX).



VIII



IX

1.6.4 The Theory of The Hydrogen Bond

According to simple valence theory, hydrogen is capable of forming
¹⁶
 only one bond. This makes it necessary to examine the nature of
 hydrogen bonds so as to explain how hydrogen, in certain
 circumstances, forms a second bond.

¹⁹

The first explanation for this was put forward by Pauling and
 involved an electrostatic model. It noted that the "...hydrogen
 bond is a bond by hydrogen between two atoms...". This was
 explained by considering the hydrogen ion as a extremely small
 cation, which would attract one anion (considered as a rigid
 sphere of finite radius). The hydrogen ion might then attract a
 second ion. However a third anion would be prevented from
 complexing by anion-anion repulsion forces (see figure 1.1). This
 concept of hydrogen bonds being akin to weak ionic bonds also
 explains why the most electronegative atoms (F, O and N) form the
 strongest hydrogen bonds.

Despite the above general 'rule of thumb', there are several
²⁰⁻²²
 examples of bifurcated hydrogen bonds in which the hydrogen atom

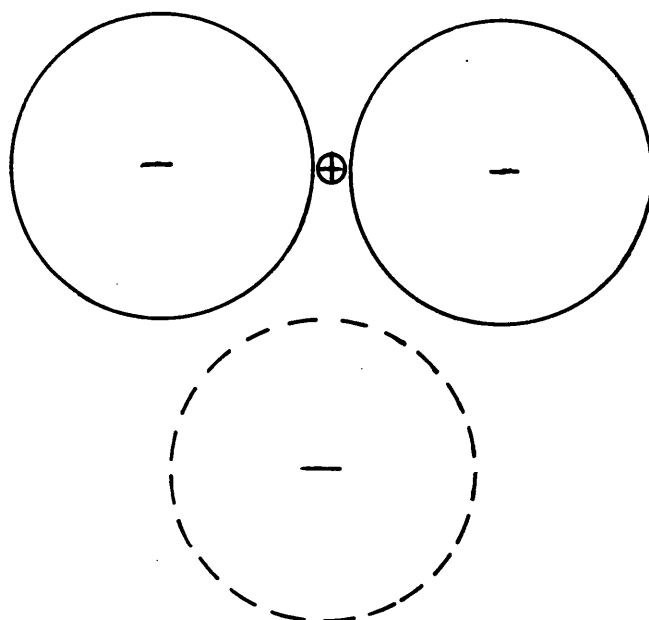
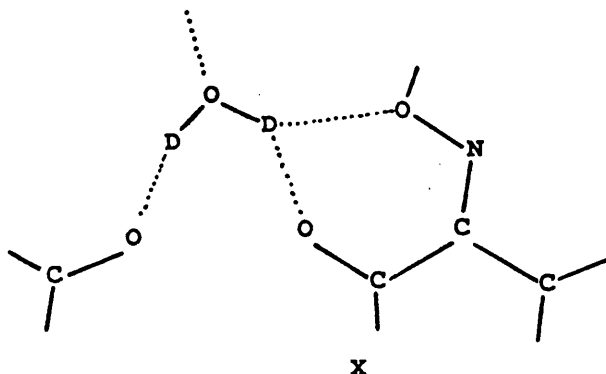


Fig. 1.1. Diagrammatic representation of Pauling's electrostatic model of hydrogen bonding¹⁹.

is effectively coordinated to three other atoms (X).



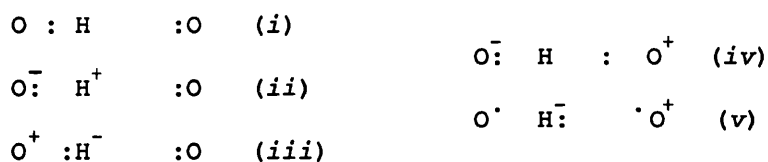
This model however, runs into difficulty when an explanation is sought for the relative strength of hydrogen bonds formed by acetonitrile (MeCN) and triethylamine (Et₃N)^{9,23}. If hydrogen bonding is determined to be solely an electrostatic interaction, MeCN with a dipole moment (μ) of 3.44 should form stronger hydrogen bonds than Et₃N ($\mu = 0.7$).¹⁶ This is not found experimentally. Kollman and Allen point out that this observation does not necessarily rule out the electrostatic model because *"At the distance where hydrogen bonding occurs, the dipole-moment approximation is a poor one and higher multipoles must be considered."* They suggest that an explanation of why amines form stronger hydrogen bonds than nitriles, lies in the shape of the orbitals in which the lone-pair electrons reside (sp^3 in amines and sp in nitriles).

A more serious flaw in the simple electrostatic model is revealed by spectroscopic methods, particularly infra-red.²⁴ This technique shows that hydrogen bond formation is accompanied by charge redistribution in the A—H bond.

¹⁶ Another objection raised is that at the hydrogen bonded distance, there must exist considerable repulsion forces between hydrogen

bonded groups. When a term reflecting these forces is included in calculations based on the electrostatic model, the previously good agreement between calculated hydrogen bond energies and those obtained experimentally is lost.

In order to explain these anomalies a model was developed by Coulson and Danielson,^{25,26} and Tsubomura²⁷ which tried to determine all the contributions rather than just the electrostatic term. They considered that the hydrogen bond in water can be described using five resonance hybrids (i - v):



They concluded that at long O—H—O distances, the electrostatic term dominates the interaction energy. At shorter distances however, repulsion forces and charge delocalisation increase and may become important.

Another approach involves the use of molecular orbital theory. In principle it is possible to describe a system by means of a wavefunction which is the solution of the appropriate Schrodinger equation. In practice however, for all but the most simple molecules, these are very difficult to solve exactly. For this reason a series of approximations have been developed from which nonempirical descriptions of hydrogen bonds can be obtained. The most popular of these is the self consistent field (SCF) method developed by Hartree²⁸ and improved by Fock.²⁹ In essence this

technique first, guesses the wavefunctions of all electrons in the system, and then calculates the potential of a selected electron by summing the interactions it experience with all the remaining electrons. This is repeated for all electrons in the system thereby creating a new set of wavefunctions. The process is then repeated, each time starting from the newly calculated wavefunctions until further repetition makes no significant difference to the wavefunctions. From this description it is obvious why the advent of high speed computers has greatly increased research in this area. Most pertinent to the studies contained in this thesis are the ab initio molecular orbital calculations of water dimers and polymers, dimethylphosphate anion - cation interactions, dimethylphosphate - water interactions.

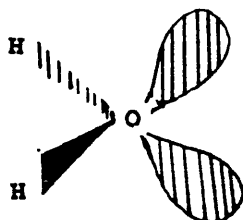
In their review of hydrogen bonding, Kollman and Allen refer to the following generalisations about hydrogen bond formation :-

- 1) Electron density is withdrawn from the hydrogen atom involved in a hydrogen bond and deposited on the electronegative atoms, the majority going to the electronegative atom of the proton donor group.
- 2) Atoms adjoining the proton acceptor groups suffer the greatest loss of electrons. Protons attached to the electronegative atom (other than the proton involved in the hydrogen bond) of the proton donor group gain electrons.

These generalisations prove to be very useful when the hydrogen bonding in complicated systems such as water and alcohols is examined.

1.7 The Structure of Water

In spite of the fact that water is of the greatest importance to man, easy to handle, abundant and relatively inexpensive, there is still no general consensus as to its precise structure in the liquid phase. An examination of the water molecule (XI) shows that it is approximately tetrahedral in geometry with two lone pairs of electrons and two slightly acidic protons. These properties give water a bi-bifunctionality and hence it's ability to form a three dimensional hydrogen bonded structure (figure 1.2), unlike alcohols which have near linear hydrogen bonded structures.



XI

In general, two major classifications of water models have emerged; one (the continuum model) in which water is described as being essentially completely hydrogen bonded with a broad range of hydrogen bond energies and geometries, and another (mixture models) in which a mixture of distinct types of water molecule environments are envisaged.

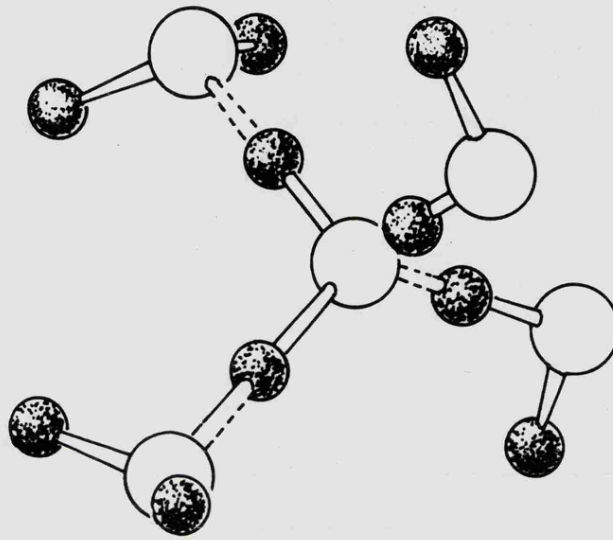


Fig. 1.2. Tetrahedral structure of water molecules.

1.7.1 The Continuum Model

37

Pople put forward a model for the structure of water based upon a 'picture' of ice melting. As ice melts the hydrogen bonding becomes more flexible. Changes in temperature would then cause hydrogen bonds to distort rather than break. The major consequence of this being that any regular structure water has, only extends to a few molecular diameters of any given molecule.

1.7.2 The Mixture Models

Many models for the structure of water come under this umbrella. Indeed, the idea that water may be described as a mixture of at least two molecular species is a historical one. Dating back to 1892 and Roentgen's explanation for the occurrence of a density maximum in water at 4°C.

37,39

As with the continuum model's development, early mixture models were developed by examining, and then in some way 'relaxing' the structure of ice, thereby obtaining a structure for the liquid phase. Samoilov suggested that water can be thought of as a distorted version of ice in which the increased translational mobility of water causes water molecules to move from their 'ice-like' equilibrium positions and pass into nearby interstitial spaces.

Another model based on the filling of interstitial spaces by non-associated molecules was proposed by Forslind. This described water as having an expanded ice-I lattice with spaces large enough to accommodate non-hydrogen bonded molecules without the lattice

being distorted greatly. Forslind calculated that at 0°C. around 16% of the water molecules are in the interstitial sites.

Pauling proposed a model for water based upon water polyhedra similar to those observed in gas hydrates ⁴⁵ e.g. methane hydrate. It was envisaged that water consists of a mixture of two units; the pentagonal dodecahedron (figure 1.3), and the tetrakaidecohedron. These have cavities with diameters of 0.52 nm and 0.59 nm respectively, in which are sited rotationally free water molecules.

One concept which has gained widespread acceptance is that of 'flickering clusters' postulated by Frank and Wen. ⁴⁶ This describes (see figure 1.4) ^{47, 48} water as consisting of groups of water molecules which are essentially fully hydrogen bonded (in the interior) interspersed with monomeric water molecules. At the surface of these clusters water molecules have either one, two or three hydrogen bonds. The clusters are being continuously, and cooperatively, broken and reformed with a timescale of ca. 10^{-11} s. The average size of the clusters, and hence the concentration of monomers, varies with temperature.

Very recently, Watterson postulated a 'wave' model for water structure. This model suggests that clusters of water molecules are formed in the condensed phase. These clusters, however, do not just flicker on and off transiently and randomly, rather, they travel as wave through the liquid. Watterson goes on to suggest that these clusters are cubic with edges about 3.3 nm long and

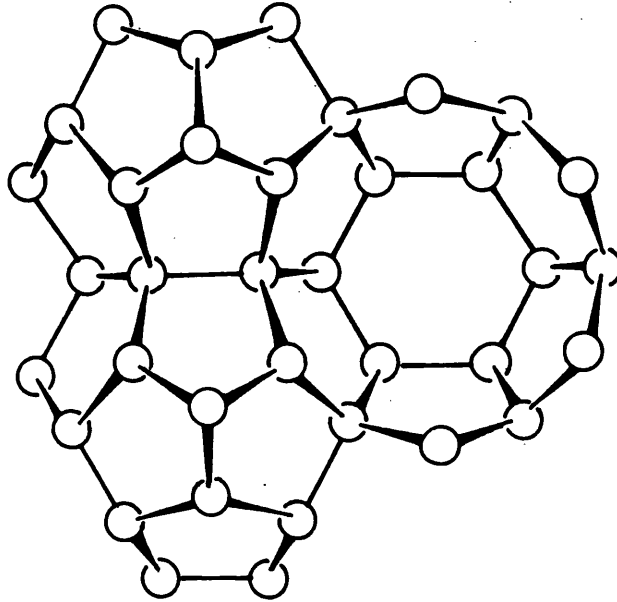


Fig. 1.3. A model for water put forward by Pauling⁴⁴. Water forms clathrate cages. Non bonded water molecules are able to jump in and out of the cages depending upon temperature.

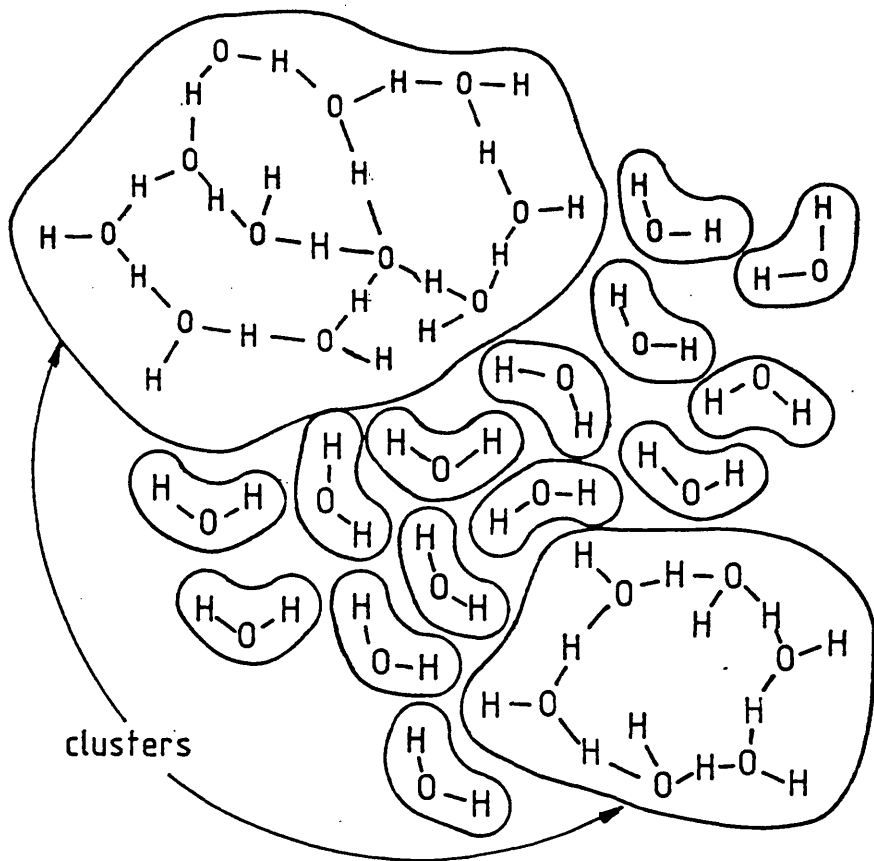


Fig. 1.4. Water cluster model of Nemethy and Scheraga^{47,48} based on the concept of "flickering clusters" outlined by Frank and Wen⁴⁶.

contain approximately 1000 molecules. In another paper,⁵¹ concerning the role of water in cell structure, Watterson notes that for a diverse range of systems this distance (3.3 nm) crops up remarkably frequently as the extent of influence that solutes have in water.⁵² Watterson then states his view that *"...this basic domain size corresponds to that of the basic unit in water structure."*⁵¹

1.7.3 Continuum vs. Mixture Models - The Arguments and Evidence

The very fact that this section is included implies that the question of which model is most appropriate has not yet been settled.³² The continuum model has been successfully used by various groups of workers to reproduce the observed properties of water such as; dielectric constant,⁵³ radial distribution functions² and ice/water density changes.²

Experimental support for this model has come from Falk et al.⁵⁴ who observed no asymmetry in the fundamental stretching bands of HOD and concluded that the results *"...are incompatible with the existence in water of any discrete molecular species differing in the extent of hydrogen bonding."*⁵⁵ Another study of H₂O/D₂O showed that stretching bands are symmetrical and that the OD stretch could be reproduced by a single Gaussian band or 10 to 15 Lorentzian component bands which also suggests a continuous distribution of oscillator environments.

Using the same technique,⁵⁶ Senior and Verral came to the opposite conclusion,⁴⁶ namely that a mixture model was more appropriate.

Their reasoning for this was based on the observation of asymmetry in the differentiated IR spectra (ν O—D stretching region) of HOD. The degree of asymmetry was found to be temperature dependent, with the higher frequency component increasing with temperature. In addition, an isosbetic point was observed in the undifferentiated spectra at 2575 cm^{-1} . This coincided almost exactly with one found by Walrafen⁵⁷ in a Raman study of the ν O—D band. Walrafen⁵⁷ assigned the high frequency (2645 cm^{-1}) component to the O—D stretch of monomer molecules, an assignment which Gorbunov and Naberukhin⁵⁸ disagreed with. They argued that the monomer band should occur at a frequency close to that of the monomer band in inert solvents^{54, 59} i.e. around 2700 cm^{-1} .

The use of fundamental IR spectroscopy in the above way (i.e. in trying to determine whether or not bands due to water are made up of more than one component band) suffers from the dependence of band intensity upon oscillator polarisation. Because the O—H / O—D bonds are more polar when involved in hydrogen bonding, they absorb much more strongly than a free oscillator.³⁵ Therefore if hydrogen bonded species are present in large concentrations, they will tend to dominate the spectrum and make the observation of any free (or weakly bound) oscillators, very difficult.

In the overtone regions the relative intensity of bands is reversed with free or weakly bound oscillators having greater^{35, 60} extinction coefficients than those more strongly bound. This is thought to be due to decreased electric anharmonicity.⁶¹ The overtone region has another advantage over fundamental IR

spectroscopy. The separation between bands is almost double that
of the fundamental region. The use of the overtone region to study
water is complicated (as a result of its triatomic nature) by the
possibility of combination tones contributing to observed bands.
In HOD the problem is largely eliminated.

In the 2ν spectrum of HOD in D_2O (figure 1.5) a narrow feature is
observed at about 7050 cm^{-1} which, due to its proximity to the
frequency of 2ν OH stretch of monomer HOD in inert solvents, has
been assigned by several groups of workers as arising from the
stretching of free O—H oscillators ($(OH)_{\text{free}}$). Raising the
temperature increases the intensity of this feature. It was
suggested that this feature and its temperature dependency is
proof of the existance of $(OH)_{\text{free}}$ groups in water. Others have
suggested that this feature is due to very weakly bound OH
groups.

Sceats and Besley showed that the observed temperature dependent
spectral changes could be simulated without any change in the
intensity of the band at 7050 cm^{-1} . They found that a decrease in
intensity around 6800 cm^{-1} reproduced the observed spectra.

Further evidence against the 'flickering cluster' model has come
from statistical mechanics experiments performed by Rahman and
Stillinger who concluded that the existence of one temperature
dependent maximum in the distribution of numbers of molecules with
0, 1, 2, 3 and 4 hydrogen bonds is not consistent with mixture
models. Also they found that "...the liquid seems to show no

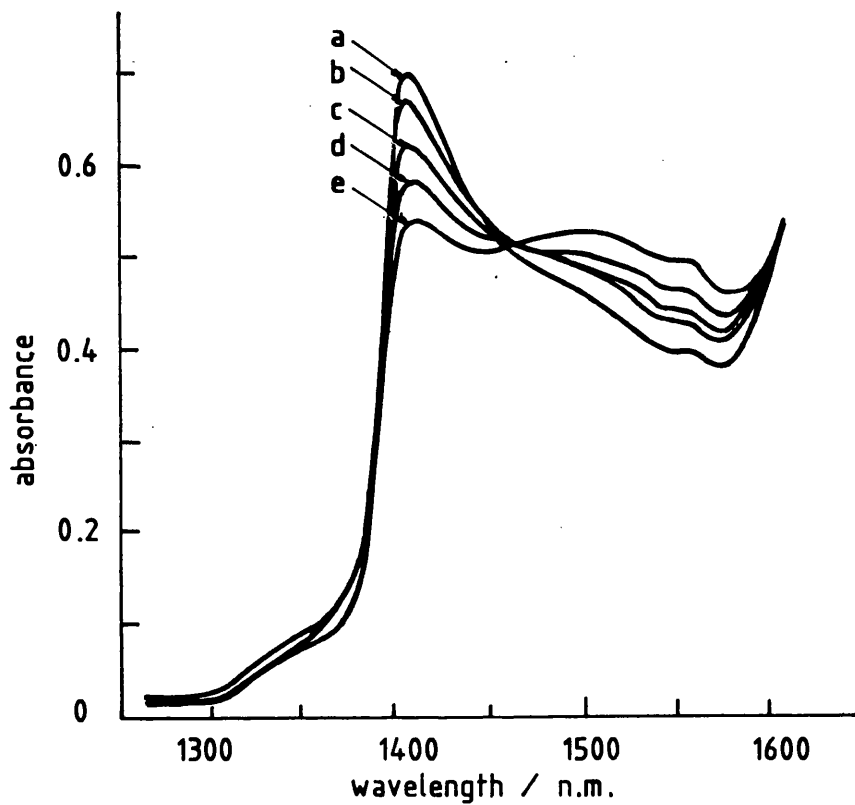


Fig. 1.5. Absorption spectrum in the $2\nu_{\text{O-H}}$ region for HOD in D_2O as a function of temperature⁶³. The narrow band at Ca. 1416 nm (7052 cm^{-1}) is assigned to free OH groups. (a) 65°C., (b) 55°C., (c) 45°C., (d) 35°C., (e) 25°C.

marked tendency anywhere to organize the beginnings of ice nuclei.''

67, 68

Stevenson estimated, using ultraviolet spectrophotometry, that at 25°C. water has, at most, a concentration of 0.15% monomer. As monomers are an integral part of the 'flickering cluster' model^{46,47} their presence in such small concentrations (when compared with the concentrations predicted) must be seen as an obstacle to the acceptance of that particular mixture model. Other estimates of the concentration of monomers in water, derived from measurements of 'free' OH bands in fundamental and overtone regions⁶⁹⁻⁷¹ suggest an upper limit of between 5% and 10%.

47

Proponents of the 'flickering cluster' model point out that the continuum model does not account the 'structure promoting' effect that non polar solutes have upon water. They also criticise the rigidity of the Lennard-Jones/Pople model³⁷, which (they suggest) cannot account for the whole entropy term in liquid water.

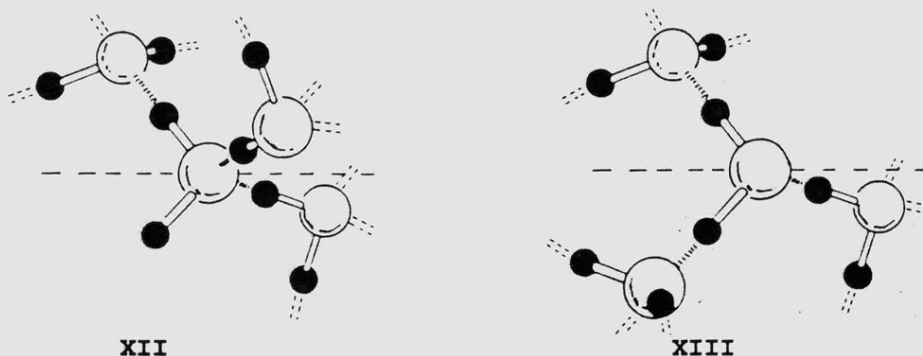
1.7.4 The Concept of Free Lone-Pair and OH Groups

35

This concept was first proposed by Symons in 1972, although the idea of non-hydrogen bonded OH groups had been discussed earlier by Luck and Ditter and other workers^{60,61}, who have since broadly endorsed it.⁷¹ Symons suggested that instead of observing the properties of liquid water and then developing models which reproduce them, a better starting point would be examine carefully the electronic structure of the monomer molecule and its chemical

properties and develop a description of the liquid structure based on those properties.

Because water is bi-bifunctional and tends to form hydrogen bonds in approximately tetrahedral directions, it will attempt to form four hydrogen bonds which would result in a rigid polymeric structure. However, as has been stated earlier, hydrogen bonds are continually being broken and reformed at ambient temperatures and pressures. This leads to the observed fluidity in water. Whenever a hydrogen bond is broken, two units will be formed; $(OH)_{free}$ and $(LP)_{free}$ with the structures (XII) and (XIII) respectively. These, Symons contends are "...of major importance and need to be considered seriously as contributing both to the physical and the chemical properties of water."



The importance of these units stems from their unsatisfied hydrogen bonding capacity which makes them very reactive, relative to a fully hydrogen bonded water molecule. The mobility of these groups is expected to be very high. The mechanism for this mobility (figure 1.6) is analogous to that of hydroxyl (OH^-) and hydroxonium (H_3O^+) ions, involving bifurcated intermediates. Symons points out the importance which is accorded to these ionic species and suggests that, in view of the much greater

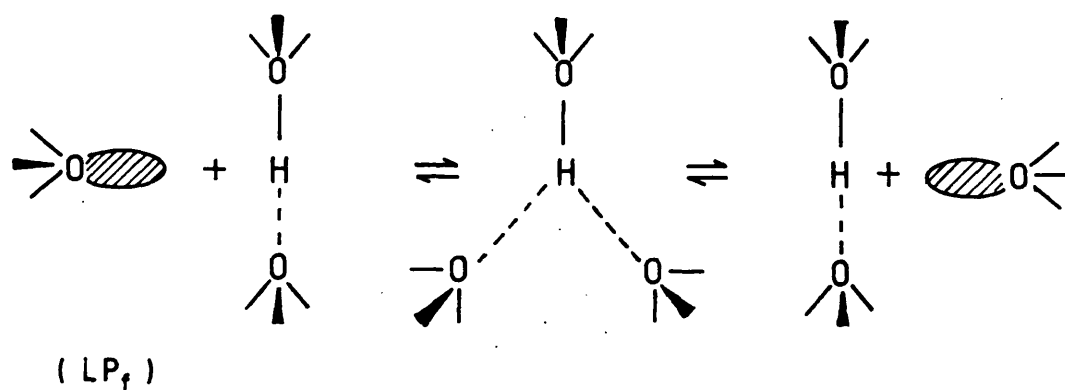
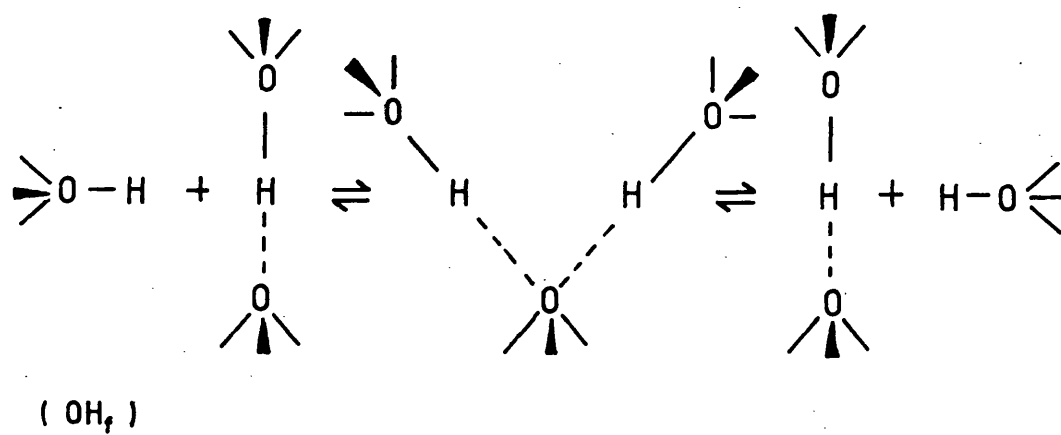


Fig. 1.6. Mechanism for the mobility of OH_{free} and LP_{free} groups ⁶⁴.

concentrations of $(\text{OH})_{\text{free}}$ and $(\text{LP})_{\text{free}}$ groups, these have "...a significance at least as great...".

By using a kind of law of mass action this model successfully predicts spectral changes observed (see figures 1.7 and 1.8) in overtone studies of the OH stretch of HOD in D_2O when electrolytes are added. In addition it explains the initial downfield shift in the hydroxyl proton's chemical shift upon addition of a base to water.⁷² In methanol, addition of a base results only in a upfield shift in the hydroxyl proton resonance.^{73,74} This observation is hard to explain without postulating the presence of significant amounts of $(\text{OH})_{\text{free}}$ in water, (methanol has a two to one excess of acceptor sites over acidic protons, which results in the concentration of $(\text{OH})_{\text{free}}$ groups being very low) this difference in behaviour between alcohols and water is not 'seen' by computer simulations.⁶⁴

Criticism of this model has come from advocates of the continuum model who point out that theoretical studies show that the energy ($4-6 \text{ kcal mol}^{-1}$) needed to break the hydrogen bond in the dimer,⁷⁵ is not available from thermal fluctuations. Whether the situation which they envisage, in which two water molecules are taken from an equilibrium distance apart to an infinite separation is relevant to the very different situation which exists in the liquid phase,⁷⁶ has been questioned.

1.8 Hydrogen Bonding in Alcohols and Thiols

A major difference between alcohol molecules and water molecules

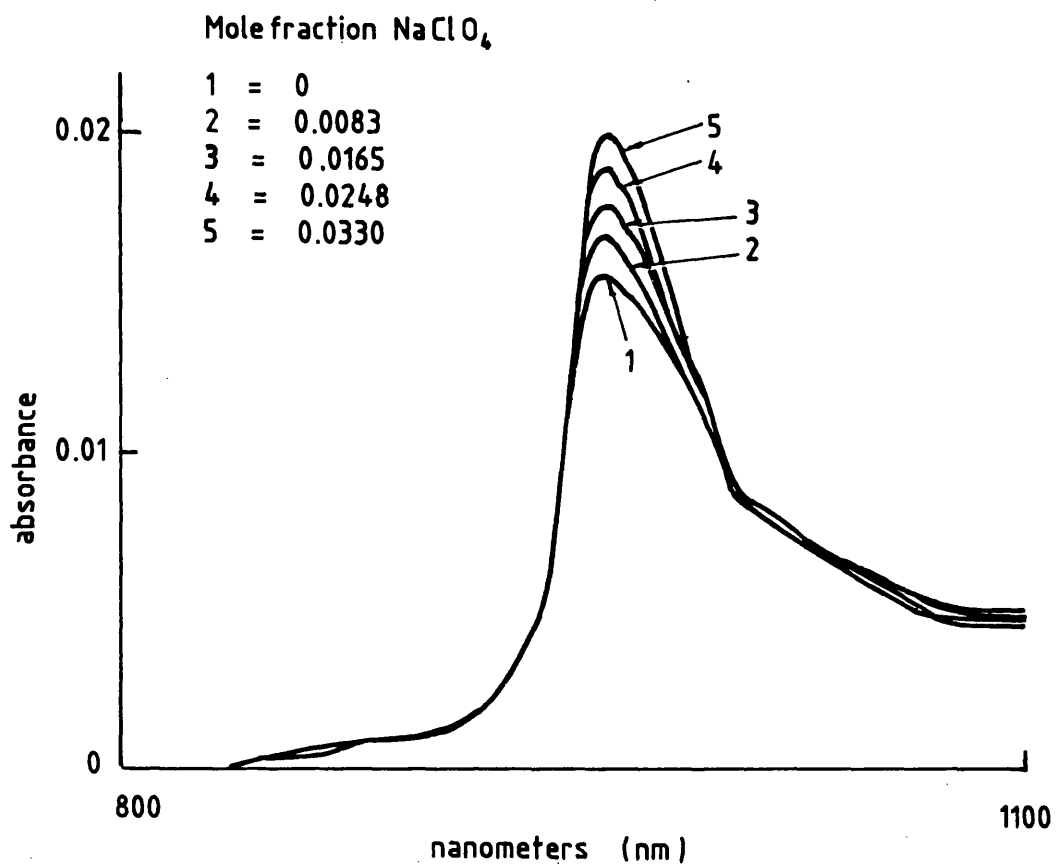


Fig. 1.7. The effect addition of NaClO_4 has upon the $3 \nu \text{O-H}$ peak of HOD^{D_3} (20% $\text{H}_2\text{O}/\text{D}_2\text{O}$ v/v).
 Temperature = 25°C .

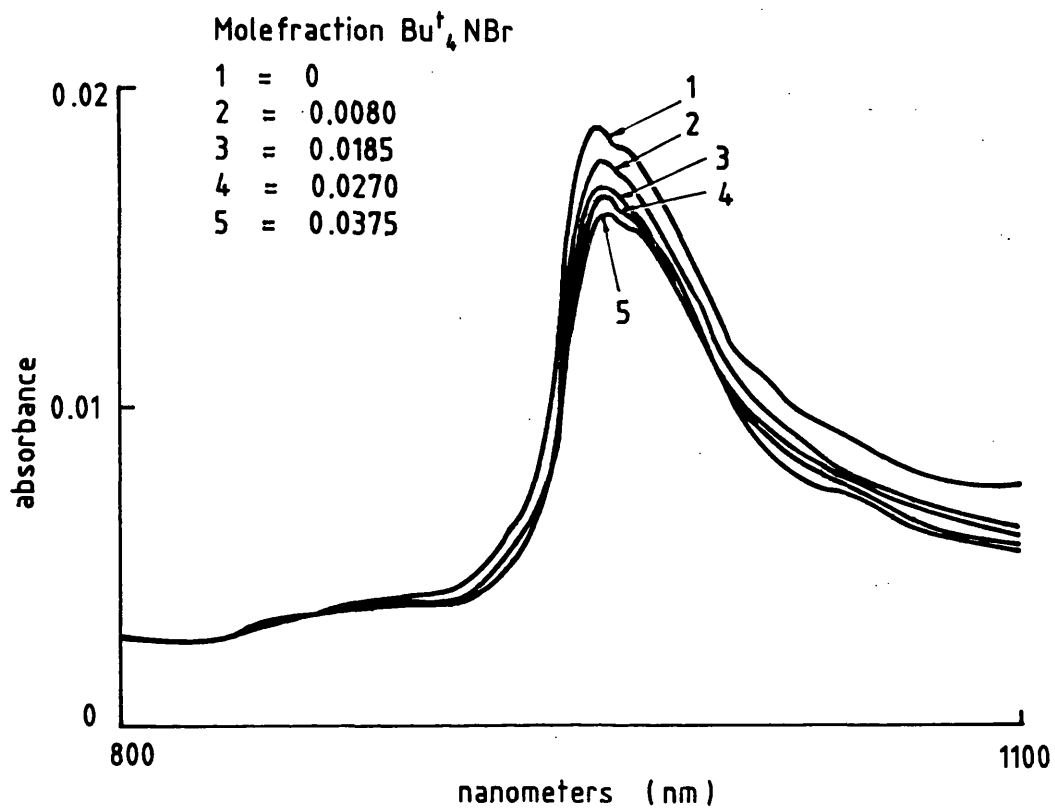


Fig. 1.8. The effect addition of Bu^t_4NBr has upon 3ν O-H peak of HOD (20% H_2O / D_2O v/v. Temperature = 25°C.

is that whilst water is bi-bifunctional with two electron donating sites and two accepting sites, alcohols are only trifunctional.

They possess two electron donating sites but only one electron accepting hydroxyl group.

Crystallographic studies of solid methanol show that it has a near linear arrangement of methanol molecules (XIV).

Matrix isolation studies in the far IR region have been very useful in determining the structure of the dimer and trimer as linear. Some earlier studies had concluded that the dimer was a closed structure (XV).



XIV



XV

Calculations have been made which suggested that methanol is only about 80% hydrogen bonded at room temperature.

It ought to be possible to detect the presence of such a quantity of non-hydrogen bonded species in the overtone region, however no sharp feature is observed.

Symons postulates that the presence of only a very indistinct shoulder at around 7100 cm⁻¹ which might be assignable to (OH)_{free} groups in the overtone region, suggests that the concentration of (OH)_{free} is very low.

The reason for this being the ability of the second free lone-pair to form weak hydrogen bonds to any (OH)_{free} groups.

Robinson found that it was possible to determine solvation numbers of anions and bases by measuring changes in absorbance assigned to (LP)_{free} groups at ca. 6790 cm⁻¹.

Thiols are not important solvents. However their hydrogen bonding ability is of great interest, in particular to biochemists. A major difference between the monomer structures of thiols and alcohols is the C—O—H / C—S—H bond angle. In thiols this is much lower, around 90° as compared with ca. 110° in alcohols.^{84,85}

This has been attributed to a smaller degree of hybridization in thiols.⁸⁵ Hallam suggests that although a bond angle of ca. 90° ⁸⁴ should favour the formation of cyclic tetramers, close inspection of matrix isolation IR spectra reveals evidence for dimers but not cyclic tetramers. A very broad band at lower frequency was also seen at higher concentrations which was assigned to higher oligomers.

From the relative boiling and melting points of thiols and alcohols¹⁷ it can be deduced that hydrogen bonding in thiols is not so extensive as in alcohols. Quite how extensive it is, however, is a subject which is examined in part 1 of this thesis and was, whilst this work was being undertaken, the subject of a timely paper in the literature reporting the results of a 'Monte Carlo' simulation experiment.⁸⁶

1.9 Solvation of Electrolytes

Whether or not an electrolyte dissolves in any particular solvent is determined by magnitude of the free energy of solvation which must be great enough to overcome the large ionic lattice energy of the electrolyte. This solvation energy is the energy difference between the gas phase and hydrated species. If the solvent is

assumed to be a dielectric continuum, the Born equation can be used to calculate the free energy of solvation:

$$\Delta G^{\ominus} = \frac{-N(e)^2}{8\pi\epsilon_0 r} \left(1 - \frac{1}{\epsilon}\right) \quad (1.5)$$

where: ΔG^{\ominus} = Partial molar free energy
 N = Avogadro's number
 Z = Ionic charge
 e = Electronic charge
 r = Ionic radius
 ϵ = Dielectric constant of the medium
 ϵ_0 = Vacuum Permittivity

The free energy comprises an enthalpy term and an entropy term:

$$\Delta G^{\ominus} = \Delta H^{\ominus} - T\Delta S^{\ominus} \quad (1.6)$$

where: ΔH^{\ominus} = Molar enthalpy change
 T = Temperature of the system
 ΔS^{\ominus} = Molar entropy change

Combining these relationships it can be seen that enthalpy and entropy changes are related to the dielectric constant (a property of the solvent) and the ionic charges and radii of the electrolyte.⁸⁸

Unfortunately, Walden's rule for ionic mobility is not obeyed in aqueous solutions which is taken to indicate that water is not a dielectric continuum.⁸⁹ Furthermore in order to calculate ΔG^{\ominus} it is

necessary to have a reliable value for the ionic radius (r). This parameter is also required if partial molal volumes are to be used as a tool with which to probe ion-solvent interactions.

Several multilayer hydration models have been proposed. The most widely referred to being that of Frank and Wen.⁹⁰ They suggested that water is divided into three regions around an ion (see figure 1.9). In region **A** water molecules have their orientation determined by the interaction of their dipole with the electronic charge of the ion. Region **C** consists of normal bulk water, in between these regions lies a third region (**B**) which is disordered and is a result of the incompatibility of the more ordered **A** and **B** regions. Closely related to this model is a description of ionic solvation put forward by Horne⁹¹ (see figure 1.10), which has, in addition to regions **A**, **B** and **C**, a further region (**A**^{*}) of Frank-Wen type clusters.

Changes in enthalpy of water which occur as a result of adding ionic species are rationalised by examining the effect of such species upon regions **A** and **B**. Small ions such as F^- , Li^+ and Na^+ and multivalent ions such as Ca^{2+} , Mg^{2+} , Ba^{2+} and Al^{3+} have large electric fields which tend to affect not just the water molecules of region **A**, but also molecules in region **B**. The effect of this is to decrease the net entropy of the water. Thus, these ions are said to be 'structure makers'. The extent of electrostatic influence of larger monovalent ions such as K^+ , Rb^+ , Cs^+ , Cl^- , Br^- and I^- , is less (generally not beyond the first hydration shell) and therefore they induce a net gain in entropy. Accordingly,

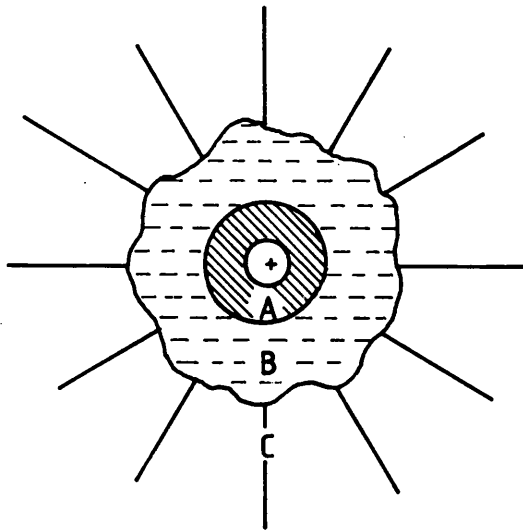


Fig. 1.9. Diagrammatic representation of the hydration of a small ion ⁹⁰.

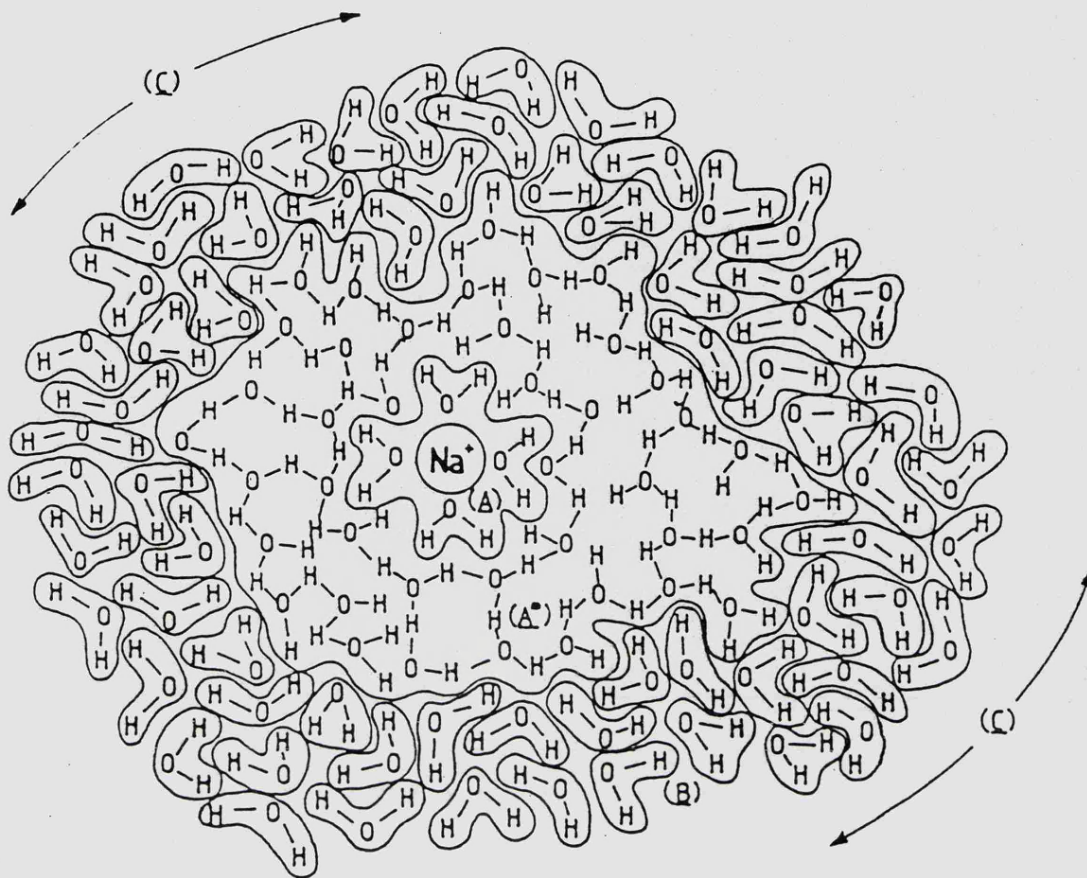


Fig. 1.10. Pictorial model of ionic solvation ⁹¹.

these are termed 'structure breakers'.

Models of this type have been criticised by Symons because they assign a too regular structure to region C. In his opinion this is erroneous. Symons postulates that there is enough disorder in bulk water for it to be able to hydrogen bond directly with those molecules which form the immediate hydration sphere which corresponds to the solvation number of the ion. Observed entropy changes are rationalised by considering changes in hydrogen bond strength rather than numbers.

Cation and anion solvation involves interaction with water's lone pairs (figure 1.11a and free hydroxyl groups (figure 1.11b) respectively. Cation solvation will therefore lead to an increase in $(OH)_{free}$. Similarly solvation of anions should produce $(LP)_{free}$. If the solvation numbers of cation and anion are the same, the quantities of $(OH)_{free}$ and $(LP)_{free}$ units produced will be comparable and hence no net change in concentration of either species will be observed. If however, one ion is very bulky and reluctant to form hydrogen bonds e.g. tetraalkylammonium (R_4N^+) or tetraphenylboron (BPh_4^-) ions, its counterion is therefore the only species forming hydrogen bonds to water. This leads to an imbalance in $(OH)_{free}$ and $(LP)_{free}$ groups after solvation has taken place. This imbalance has been observed spectroscopically.

1.10 Hydration of Macromolecules

Many attempts have been made to derive a theory to explain the

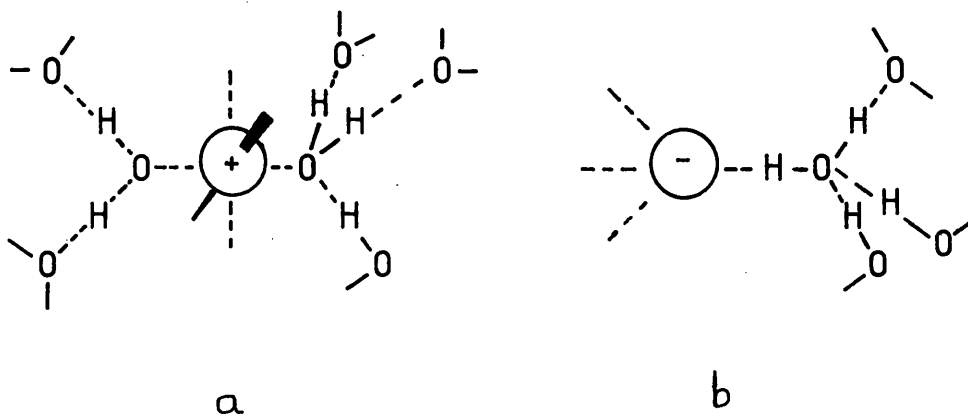


Fig. 1. 11. Solvation of cations and anions by LP_{free} and OH_{free}^{93} .

adsorption of gases onto surfaces. One of the earliest was the
 94
 'polarisation theory' developed by deBoer and Zwikker who proposed
 that charge centres on the surface induce dipoles in the first
 layer of gases adsorbed. This dipole then could influence the
 next layer and so on until a polarised multilayer of gases is
 formed on the surface of the solid. An isotherm was derived for
 this which took the form:

$$\log(\log \frac{p}{p_0} - K_3) = a \log K_1 + \log K_2 \quad (1.7)$$

where: K_1 , K_2 and K_3 are constants (under the specified
 experimental conditions)

a = amount of adsorbed gas

p = partial pressure of gas

p_0 = pressure of gas at saturation under same condition.

95
 Later Bradley derived a similar isotherm for the adsorption of
 polar gases (e.g. H_2O vapour) and showed that water adsorbed onto
 CuO crystal surfaces were characterised by it.

Because of doubts as to whether noble gases are polarisable enough
 to be able to form more than a monolayer, Brunauer, Emmett and
 96
 Teller suggested that the formation of multilayers of these gases
 could be considered in the same way as the condensation of gases.

96
 The isotherm they derived became known as the BET isotherm and has
 been widely used to analyse experimental data.

$$\frac{p}{V(p - p_0)} = \frac{1}{V_m c} + \frac{(c - 1)}{V_m c} \left(\frac{p}{p_0} \right) \quad (1.8)$$

Where: V = amount of gas absorbed at vapour pressure $\frac{p}{p_0}$

V_m = volume adsorbed in monolayer

c = a constant

plotting $p / V(p - p_0)$ against p / p_0 should result in a straight line from which c and V_m can be determined.

When experimentally obtained isotherm data is compared with the BET isotherm predictions reasonably good agreement is observed for low partial vapour pressures however at higher p / p_0 deviations from a straight line are observed. The deviations have been attributed to the fact that the BET isotherm assumes that all water molecules not in the monolayer behave as bulk water.

From the Grand Partition function for N_s primary sites (1.9),
98
Gascoyne and Pethig derive a general formula (1.10) describing sorption of gases on a surface which makes only two assumptions. Firstly, that the sites are identical and secondly, that they are non-interacting. The validity (or otherwise) of these assumptions is also discussed.

$$F(x) = (1 + a_1 x + a_1 a_2 x^2 + a_1 a_2 a_3 x^3 + \dots) N_s \quad (1.9)$$

where: a_i = coefficient relating to the activity of sorbed gas in the i^{th} layer.

x = activity of sorbed gas which can be related to the relative pressure of the gas (p / p_0)

$$V(x) = V_m x \frac{\delta}{\delta x} \ln f(x). \quad (1.10)$$

This is a versatile equation which relates total sorption, $V(x)$, to V_m and the partition function, $f(x)$. If, for example, only monolayer adsorption is considered thereby giving a partition function:

$$f(x) = 1 + ax \quad (1.11)$$

99

this yields the Langmuir isotherm for monolayer adsorption:

$$V(x) = V_m ax / (1 + ax). \quad (1.12)$$

Similarly if the activities of molecules in the second and subsequent layers are assumed to be equal i.e.

$$f(x) = 1 + abx + a(bx)^2 + a(bx)^3 + \dots \quad (1.13)$$

where: ab = activity of gas in monolayer

b = activity of all subsequent layers.

When substituted into (1.10) this gives an isotherm equation of the form:

$$V(x) = V_m abx / (1 - bx) [1 + b(a - 1)x]. \quad (1.14)$$

If, as is often assumed, the activity of molecules in the second sorption layer and beyond is the same as for the bulk condensed gas, i.e. is equal to 1, (1.14) simplifies to the BET isotherm:⁹⁶

$$V(x) = V_m ax / (1 - x) [1 + (a - 1)x]. \quad (1.15)$$

They then showed that deviations from BET isotherms at high partial pressure could be removed by giving b a non-unity value. Furthermore, they found that only DNA of the five biomolecules

studied (the others were; cytochrome-c, bovine serum albumin, lysozyme and lecithin) needed a value of b greater than one (1.05) to give a straight line 'BET like' isotherm. The others required values ranging from 0.81 to 0.88. This result implies that DNA alone amongst the biomolecules studied, has an outermost hydration shell which is already ⁹⁸ "...indistinguishable from bulk water...". In discussing the validity of the assumption made about the equivalence of primary adsorption sites, Gascoyne and Pethig, suggested that for biomolecules this is unreasonable (synthetic polypeptides may be suitable for this kind of treatment) and that this must seriously limit the information obtainable from such isotherms. Despite this they consider that *'The BET derived values will be of very much greater inaccuracy due to the erroneous assumption of having $b = 1$.'*

In general, hydration of large biomolecules follows the pattern one might expect from their component groups, with the following proviso added, in some large macromolecules (notably proteins) ¹⁰⁰ folded regions exist which exclude water. This leads to these areas being less than fully hydrated. Also adjacent groups may share water molecules, which will also lead to hydration being ¹⁰¹ economised. Hydration of proteins is discussed further in chapter 4 and a detailed description of the hydration of DNA is presented in chapter 6.

1.11 Current Developments and a Summary

The past two decades has seen a technological leap made in the development of computers with dramatically increased speeds of

execution and memory size. This has led to a flood of papers describing computer simulation experiments (Monte Carlo and molecular dynamics), these have described solvent-solvent and solute-solvent interactions as well as ion pairing. The trend has been towards more and more complicated systems. Hence, initial experiments concerning water were aimed at finding the energetics and geometry/structure of the dimer. This has progressed and current work considers systems containing many more molecules. This progression is observed in experiments pertaining to solute-solvent interactions with early studies concentrating upon simple ions. More recent studies have involved the simulation of such solutes as Vitamin B₁₂ coenzyme crystal hydrates and peptides. This work continues and is likely to proceed at an even faster rate with the introduction of computers utilising parallel processing.

Experimental techniques have also improved as result of computer development, notably fourier transform NMR, which has helped to elucidate the structure of large biomolecules e.g. substance P, physalaemin (small linear polypeptide) and cytochrome c (large protein). Multi-nuclear NMR has also been used to probe the dynamics of solutions, using relaxation times as a 'handle'. This aspect has been developed largely as a result of the ability of computers to generate the fast pulse sequences required to measure relaxation times accurately. Fourier transform IR allows the fast accumulation and manipulation of IR spectra. In particular resolution enhancement functions have allowed the separation of broad bands into component bands.

Despite the 'picture' of frantic development in the area of hydrogen bonded systems painted above, it is worth reflecting upon the words which Latimer and Rodebush used to introduce the concept of hydrogen bonding in liquid water in 1920:

'Water...shows tendencies both to add and give up hydrogen, which are nearly balanced. Then...a free pair of electrons on one water molecule might be able to exert sufficient force on a hydrogen held by a pair of electrons on another water molecule to bind the two molecules together...Indeed the liquid may be made up of large aggregates of molecules, continually breaking and reforming under the influence of thermal agitation. Such an explanation amounts to saying that the hydrogen nucleus held between 2 octets constitutes a weak 'bond.'

This description has stood the test of time remarkably well.

References for chapter 1

1. S. N. V. Vinogradov and R. H. L. Linnel, *Hydrogen Bonding*, Chapter 1, Van Nostrand Reinhold Co. New York, (1971).
2. J. L. Kavanau, *Water and Solute-Water Interactions* pp. 8-20, Holden-Day Inc. San Francisco, (1964).
3. R. Langridge, W. E. Seeds, W. E. Wilson, H. R. Hooper, M. H. F. Wilkins and L. D. Hamilton, *J. Biophys. Bioc.* 3, 767 (1957).
4. D. A. Marvin, M. Spencer, M. H. F. Wilkins and L. D. Hamilton, *Nature* 182, 387 (1958).
5. F. Franks, *Phil. Trans. Roy. Soc.* B278, 89 (1977).
6. F. A. Cotton and G. Wilkinson, *Advanced Inorganic Chemistry*, Third edition, Chapter 3, J. Wiley and Sons, London. (1972).
7. P. W. Atkins, *Physical Chemistry* (1st Edition) Chapters 15 and 23, Oxford University Press, Oxford (1978).
8. *Handbook of Chemistry and Physics* (67th Edition) F-178 - F181, CRC Press, Florida (1986).
9. G. C. Pimentel and A. L. McClellan, *The Hydrogen Bond*, p. 2, W. H. Freeman and Co. San Francisco, (1960).
10. W. Nernst, *Z. Physik. Chem.* 8, 110 (1891).
11. A. Werner, *Bev.* 36, 147 (1903).
12. T. S. Moore and T. F. Winmill, *J. Chem. Soc.* 101, 1635 (1912).
13. G. Oddo and E. Puxeddu, *Gazz (ii)* 36, 1 (1906).
14. P. Pfeiffer *Ann.* 398, 137 (1913).
15. W. M. Latimer and W. H. Rodebush, *J. Am. Chem. Soc.* 42, 1419 (1920).
16. P. A. Kollman and L. C. Allen, *Chem. Rev.* 72, 283 (1972).

17. L. J. Bellamy, *Advances in Infrared Group Frequencies*, Chapter 8, Methuen and Co. Ltd. London, (1968).
18. A. S. N. Murthy and C. N. R. Rao, *Appl. Spectrosc. Rev.* 2, 1 (1968).
19. L. Pauling, *Proc. Nat. Acad. Sci. U.S.A.* 14, 359 (1928).
20. B. M. Craven and W. J. Takei, *Acta Cryst.* 17, 415 (1964).
21. J. Gaultier and C. Hauw, *ibid.* 25B, 546 (1969).
22. J. Donohue, in *Structural Chemistry and Molecular Biology* (A. Rich and N.R. Davidson, Eds.), p. 443, W. H. Freeman and Co. San Francisco, (1968).
23. W. Gordy and S. C. Stanford, *J. Chem. Phys.* 9, 204 (1941).
24. C. M. Huggins and G. C. Pimental, *J. Phys. Chem.* 60, 1615 (1956).
25. C. A. Coulson and U. Danielson, *Ark. Fys.* 8, 205 (1955).
26. C. A. Coulson and U. Danielson, *ibid.* 8, 239 (1955).
27. H. Tsubomura, *Bull. Chem. Soc. Jap.* 27, 445 (1954).
28. D. R. Hartree, *Proc. Cambridge Phil. Soc.* 24, 89, 111, 426 (1928).
29. V. Fock, *Z. fur Phys.* 61, 126 (1930).
30. A. Rahman and F. H. Stillinger, *J. Chem. Phys.* 55, 2263 (1971).
31. A. Rahman and F. H. Stillinger, *J. Am. Chem. Soc.* 95, 7943 (1973).
32. A. Pullmann, B Pullmann and H. Berthod, *Theoret. Chim. Acta* 47, 175 (1978).
33. J. Langlet, P. Claverie, B. Pullmann and D. Piazzola, *Int. J. Quant. Chem. : Quant. Biol. Symp.* 6, 409 (1979).

34. See *Water and Aqueous Solutions - Colston Papers No. 37*, (G. W. Neilson and J. E. Enderby, Eds.) Discussion (2) Adam Hilger, Bristol, (1986).
35. M. C. R. Symons, *Nature* 239, 252 (1972).
36. N. J. Pay, *Ph.D. Thesis*, Leicester, (1981).
37. J. A. Pople, *Proc. Roy. Soc.* A205, 163 (1951).
38. W. K. Röntgen, *Ann. Phys. Chim (Wied)* 45, 91 (1892).
39. J. D. Bernal, *Proc. Roy. Soc.* A280, 299 (1964).
40. O. Ya. Samilov, *Zhur. Fiz. Khim.* 20, 12 (1946).
41. O. Ya. Samilov, *Disc. Fara. Soc.* 24, 141, 216 (1957).
42. E. Forslind, *Proc. 2nd Int. Congr. Rheology*, Butterworths, London (1953).
43. W. H. Barnes, *Proc. Roy. Soc.* A125, 670 (1929).
44. L. Pauling, in *Hydrogen Bonding*, (Hadzi and Thompson, Eds.) p. 1, Pergamon, London (1959).
45. G. A. Jeffrey and R. K. McMullan in *Progress in Inorganic Chemistry* (F. A. Cotton, Ed.), Wiley, New York (1967).
46. H. S. Frank and W. Y. Wen, *Disc. Fara. Soc.* 24, 133 (1957).
47. G. Nemethy and H. A. Scheraga, *J. Chem. Phys.* 36, 3382 (1962).
48. G. Nemethy and H. A. Scheraga, *ibid.* 36, 3401 (1962).
49. J. G. Watterson, *Phys. Chem. Liq.* 16, 313 (1987).
50. J. G. Watterson, *ibid.* 16, 317 (1987).
51. J. G. Watterson, *Biochem. J.* 248, 615 (1987).
52. B. W. Ninham, *J. Phys. Chem.* 84, 1423 (1980).
53. F. E. Harris and B. J. Alder, *J. Chem. Phys.* 21, 1031 (1953).
54. M. Falk and T. A. Ford, *Can. J. Chem.* 44, 1699 (1966).
55. W. Yellin and W. L. Courchene, *Nature* 219, 852 (1968).

56. W. A. Senior and R. E. Verrall, *J. Phys. Chem.* 73, 4242 (1969).
57. G. E. Walrafen, *J. Chem. Phys.* 43, 244 (1968).
58. B. Z. Gorbunov and Yu. I. Naberuhkin, *Zhu. Strukt. Khim.* (translation) 16, 703 (1975).
59. G. Herzberg, *Infrared and Raman Spectra Of Polyatomic Molecules* p. 280, Van Nostrand, Princeton NJ (1945).
60. W. A. P. Luck and W. Ditter, *J. Mol. Structure* 1, 339 (1967-68).
61. W. A. P. Luck and W. Ditter, *ibid.* 1, 261 (1967-68).
62. J. D. Worley and I. M. Klotz, *J. Chem. Phys.* 45, 2868 (1966).
63. W. A. P. Luck and W. Ditter, *Z. Naturf.* 24B, 482 (1969).
64. M. C. R. Symons in *Water and Aqueous Solutions - Colston Papers No. 37*, (G. W. Neilson and J. E. Enderby, Eds.) p. 41, Adam Hilger, Bristol, (1986).
65. Yu. Ya. Efimov and Yu. I. Naberuhkin, *Mol. Phys.* 36, 973 (1978).
66. M. G. Sceats and K. Besley, *Mol. Phys.* 40, 1389 (1980).
67. D. P. Stevenson, *J. Phys. Chem.* 69, 2145 (1965).
68. D. P. Stevenson, in *Structural Chemistry and Molecular Biology* (A. Rich and N. R. Davidson, Eds.), p. 490, W. H. Freeman and Co. San Francisco, (1968).
69. W. A. P. Luck and W. Ditter, *Ber. Bunsenges* 72, 365 (1968).
70. J. -J. Peron, C. Bourderon and C. Sandorfy, *Can. J. Chem.* 49, 3901 (1971).
71. W. A. P. Luck, in *The Hydrogen Bond* (P. Schuster, G. Zundel and C. Sandorfy, Eds.), Vol. III, Chapter 28, p. 1396, North Holland Publishing Co. Amsterdam, (1976).

72. M. C. R. Symons, J. M. Harvey and S. E. Jackson, *J. Chem. Soc. Fara. Trans. I* 76, 256 (1980).
73. M. C. R. Symons, N. J. Fletcher and V. K. Thompson, *Chem. Phys. Letts.* 60, 323 (1979).
74. M. C. R. Symons, N. J. Fletcher and V. K. Thompson, *J. Chem. Soc. Fara. Trans. I* 77, 1899 (1981).
75. J. L. Finney, in *Water and Aqueous Solutions - Colston Papers No. 37*, (G. W. Neilson and J. E. Enderby, Eds.) Discussion (2) Adam Hilger, Bristol, (1986).
76. T. H. Lilley, in *Water and Aqueous Solutions - Colston Papers No. 37*, (G. W. Neilson and J. E. Enderby, Eds.) Discussion (2) Adam Hilger, Bristol, (1986).
77. K. J. Tauer and W. N. Lipscombe, *Acta Cryst.* 5, 606 (1952).
78. B. Dreyfus-Alain and R. Viillard, *Comp. Rend.* 234, 536 (1952).
79. A. J. Barnes and H. E. Hallam, *Trans. Fara. Soc.* 66, 1920 (1970).
80. M. Van. Thiel, E. D. Becker and G. C. Pimentel, *J. Chem. Phys.* 27, 95 (1957).
81. W. A. P. Luck, in *The Hydrogen Bond* (P. Schuster, G. Zundel and C. Sandorfy, Eds.), Vol. II, Chapter 11, North Holland Publishing Co. Amsterdam, (1976).
82. Referred to in H. L. Robinson, *Ph.D. Thesis*, Leicester, (1985).
83. H. L. Robinson, *Ph.D. Thesis*, Leicester, (1985).
84. W. S. Fife, *J. Chem. Phys.* 21, 2 (1953).
85. H. E. Hallam, in *The Hydrogen Bond* (P. Schuster, G. Zundel and C. Sandorfy Eds.) Vol. III, Chapter 22, North Holland Publishing Co. Amsterdam, (1976).

86. W. L. Jorgensen, *J. Phys. Chem.* 90, 6379 (1986).
87. M. Born, *Z. Physik* 1, 45 (1920).
88. P. W. Atkins, *Physical Chemistry* (1st Edition) Chapter 8, Oxford University Press, Oxford (1978).
89. H. S. Frank, in *Chemical Physics of Ionic Solutions* (B. E. Conway and R. G. Barradas, Eds.), J. W. Wiley, New York, (1966).
91. R. A. Horne, *Adv. Hydrosci.* 6, 107 (1970).
92. M. C. R. Symons, *Phil. Trans. Roy. Soc.* 272, 13 (1973).
93. S. E. Jackson and M. C. R. Symons, *Chem. Phys. Letts.* 37, 551 (1976).
94. J. H. de Boer and C. Zwicker, *Z. Physik. Chem.* B3, 407 (1929).
95. R. S. Bradley, *J. Chem. Soc.* 1467 (1936).
96. S. Brunauer, P. H. Emmett and E. Teller, *J. Am. Chem. Soc.* 60, 309 (1938).
97. E. A. Guggenheim, *Applications of Statistical Mechanics*, Chap. 11, pp. 186 - 206, Clarendon Press, Oxford (1966).6).
98. P. R. C. Gascoyne and R. Pethig, *J. Chem. Soc. Fara. Trans. I* 31, 171 (1977).
99. I. Langmuir, *J. Am. Chem. Soc.* 40, 1361 (1918).
100. A. L. Lehninger, *Principles of Biochemistry*, Chap 8, pp. 178-179, Worth, New York (1982).
101. W. Saenger, W. N. Hunter and O. Kennard, *Nature*, 324, 385 (1986).
102. H. Popkie, H. Kistenmacher and E. Clementi, *J. Phys. Chem.* 59, 1325 (1973).
103. P. Rossky and M. Karplus, *J. Am. Chem Soc.* 101, 1913 (1979).

- 104 A. T. Hagler, D. J. Osguthorpe and B. Robson, *Science* 208, 599 (1980).
- 105 J. M. Goodfellow, F. Vovelle, J. E. Quinn, H. F. J. Savage and J. L. Finney, in *Water and Aqueous Solutions - Colston Papers No.37*, (G. W. Neilson and J. E. Enderby, Eds.) p. 251, Adam Hilger, Bristol, (1986).
- 106 V. Madison, D. J. Osguthorpe, P. Dauber and A. T. Hagler, *Biopolymers* 22, 57 (1983).
- 107 G. Chassaing, O. Convert and S. Lavielle, *Bioc. Biop. Acta* 873, 397 (1986).
- 108 A. R. Cross and C. Anthony, *Biochem. J.* 192, 421 (1980).
- 109 H. Santos and D. L. Turner, *FEBS Letts.* 194, 73 (1980).
- 110 O. Jardetzky and G. C. K. Roberts, *NMR in Molecular Biology*, Academic Press, (1981).

Chapter 2

Materials and Methods.

2.1 Purification of Materials

Organic solvents used in this work were purified and dried using standard procedures¹. Typically this involved distillation off an appropriate drying agent, usually calcium hydride (CaH_2) or activated molecular sieve. Such solvents were then stored over a drying agent. Regular analysis (IR / NMR) of solvents was performed. Water was purified, firstly by deionisation, and then by passage through a Millipore 'Milli-Q' system.

DNA was stored in a desiccator over silica gel at $0 - 5^\circ\text{C}$. In order to obtain consistent results, DNA of a single batch number was used throughout the duration of the experiment. The DNA was periodically checked for denaturation using electron spin resonance spectroscopy².

Thiols were stored over 4A Molecular sieve and the extinction coefficient of the νSH stretching band monitored to determine the extent of oxidation, no significant deterioration was observed.

2.2 Preparation of Samples

All solutions of thiols, phosphates and thio-phosphates were made up immediately before the recording of their spectra. Solutions were made up by volume or weight, whichever proved the more convenient. This was done under nitrogen in a 'glovebag' if the samples were hygroscopic enough to make this necessary.

DNA samples were prepared by the addition of water to weighed out

DNA and were left for 24 - 36 hours at 5°C. to form homogeneous gels. The samples were then transferred into NMR tubes using a wide tipped pipette and any air bubbles observed in the samples removed by gentle centrifugation.

2.3 Spectroscopic Techniques

2.3.1 Infrared Spectroscopy

All spectra were recorded on a Perkin - Elmer 681 double beam spectrophotometer.³ The ordinate scale is controlled by an ordinate microprocessor. This allowed the amplitude of resulting signals to be easily adjusted. Resolution was determined by the monochromator slit width. A micro-computer was linked to the spectrophotometer and data pertaining to most spectra were stored on floppy disk. This facilitated the analysis of spectra, for example averaging, resolution enhancement and peak picking. Furthermore data could be transferred onto the mainframe computer to allow bandshape analysis to be performed. Temperature was controlled using a "SPECAC 2000" vacuum jacketed cell holder. With this apparatus temperatures could be varied between ca. -200 and + 250°C. Temperature stability was around $\pm 1^\circ\text{C}$.

2.3.2 Near Infra-red Spectroscopy

All spectra were recorded using a Perkin-Elmer Hitachi 340 Spectrophotometer.⁴ This double beam spectrophotometer is capable of operating in the ultra-violet, visible and near infra-red regions of the spectrum. Near infra-red and visible light is generated by a tungsten filament and is detected by a lead

sulphide detector. The machine has a built in microprocessor which was capable of subtracting out differences in sample and reference cells. The spectrophotometer has variable temperature capability and was linked to the same micro computer as the infra-red spectrometer described above.

2.3.3 Nuclear Magnetic Spectroscopy

This work made use of three spectrometers. For ^{31}P measurements a "Jeol FX-60" spectrometer was utilised. This operates in the pulsed fourier transform mode at a frequency of 60 MHz (protons). Sample solutions were put into 10 mm OD tubes along with a coaxial 5 mm OD containing the reference compound made up in D_2O . This served as an internal hetero-nuclear lock signal.

Proton magnetic resonance work presented in chapter 3 was obtained using a "Jeol PS-100" continuous wave spectrometer operating at 100 MHz. This spectrometer has variable temperature capability and uses an internal homo-nuclear lock signal, usually TMS.

All Spectra and relaxation time measurement presented in Chapter 6 were obtained from a Bruker AM 300 spectrometer⁵ with an operating frequency of 300.134 MHz for protons. The probeheads are equipped for an internal deuterium lock and variable temperature operation. A superconducting cryomagnet is used to produce the high field required. This is kept below its critical temperature by an inner liquid helium filled jacket. To reduce the rate of boil-off, an outer jacket is filled with liquid nitrogen.

The rf frequencies and associated offset frequencies are synthesised from a single quartz oscillator. The data produced is handled by an "Aspect 3000" computer which is capable of multitasking. This means that up to 3 jobs can be performed simultaneously. Complex experiments (e.g. pulse sequences) can be automated by using simple micro-programs.

References for Chapter 2

1. G. Riddick and E. R. Bunger, *Techniques of Chemistry - Organic Chemistry*, Volume II, Wiley-Interscience, New York, (1970).
2. G. D. D. Jones, Personal Communication, (1985).
3. Instruction Manual for Model 580, Perkin-Elmer Ltd. (1975).
4. Instruction Manual for Model 340, Hitachi Ltd. (1977).
5. Instruction Manual for AM Series, Bruker Ltd. (1984).

Chapter 3

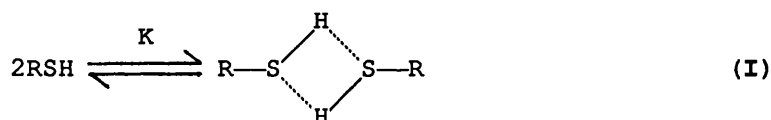
*Hydrogen Bonding in
Ethanethiol.*

3.1 Introduction

This work is concerned with the ways in which ethanethiol (EtSH) forms hydrogen bonds. The techniques used were ^1H nuclear magnetic resonance (NMR), infra-red (IR) and near infra-red (NIR) spectroscopy. The spectra obtained by IR and NIR spectroscopy were curve analysed by computer to separate the free ν S-H band from the band(s) due to bound species.

3.2 Previous Work

On the basis of techniques such as cryoscopy¹, solubility², dipole moments^{3,4} and also NMR and IR spectroscopy^{5,6}, earlier workers claimed that thiols do not self-associate. However, Spurr and Byers⁷ studied the IR S-H stretching band for several thiols in tetrachloromethane (CCl_4) solutions and observed changes in the shape and position of this band on changing the concentration of the solutions. They interpreted these changes in terms of a monomer-dimer equilibrium, written as (I);

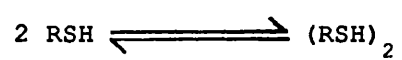


for which they derived relationship (3.1), which they used to calculate the dimerisation constant K and the integrated absorption coefficient for the dimer. The value they obtained for K and those values obtained by subsequent workers are presented in table 3.1.

$$\frac{1}{A - A_M} = \frac{2}{A_D - A_M} \frac{K}{2(A_D - A_M)} \frac{1}{C} \quad (3.1)$$

Table 3.1

Dimerisation equilibrium constants (K_d) / M^{-1} for the equilibrium



Ref.	K_d
Spurr & Byers ⁷	0.021
Forsen ⁸	0.012
Marcus & Miller ¹⁰	0.0056
This work	0.038

Where: A - Apparent integrated absorption coefficient

A_M - Monomer integrated absorption coefficient

A_D - Dimer integrated absorption coefficient

C - Concentration of thiol

8

Forsen in an NMR study, reported a linear dilution curve in CCl_4 for the chemical shift of the SH proton in ethanethiol. By guessing the chemical shift of the dimer and using it in the limiting slope expression (3.2), they obtained a dimerisation equilibrium constant (K_2).

$$\frac{d\delta}{dC} = 2K_2(\delta_2 - \delta_1) \quad (3.2)$$

Where: C - Concentration of thiol

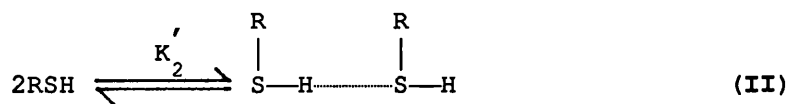
δ_2 - Chemical shift of the dimer

δ_1 - Chemical shift of the monomer

K_2 - Dimerisation equilibrium constant

9

In an IR study of thiols and thioethers Bulanin et al. concluded that the equilibrium involving the closed dimer (I) is inappropriate and that the unassociated S-H bond in the open dimer of process (II) contributes to the intensity of the monomer band.



10

In 1966 Marcus and Miller, studied the dilution curves in CCl_4 and C_6H_{12} of the chemical shift of the SH proton for several thiols. They treated the results by three different methods and obtained dimerisation equilibrium constants K_2 and K_2' . The

first method used applied to process (I), for which they derived expression (3.3);

$$\frac{1}{\delta - \delta_2} = \frac{1}{\delta_2 - \delta_1} \left(\frac{1}{2K_2 C} + 2 \right) \quad (3.3)$$

and for process (II) they derived expression (3.4)

$$\frac{1}{\delta - \delta_2} = \frac{1}{\delta_2 - \delta_1} \left(\frac{1}{K_2' C} + 4 \right) \quad (3.4)$$

From these expressions δ and K_2 (or K_2') were calculated. They decided that both of these expressions are unsatisfactory because they presuppose that the solution only contains monomers and dimers. As $1/C$ approaches zero this assumption breaks down because of the formation of higher polymers. Previously Josien et al.¹¹ had reported the stretching frequencies of the IR bands corresponding to monomer, dimer and polymer species of thiols.

The third method of analysis was based on that of Saunders and Hyne¹², this applied to process (III);



for which

$$K_n = \frac{M_n}{M_1^n} \quad (3.5)$$

and $C = M_1 + nK_n M_1^n \quad (3.6)$

Where: C - Total solute concentration
 M_1 - Molar concentration of monomer
 M_n - Molar concentration of n-mer
n - Number of monomer units

This method led to the following expressions (3.7 - 3.10):

$$\frac{d\delta}{d \log C} = 2.303 (\delta_1 - \delta_n) \left[\frac{1}{1 + n^2 K_n M_1^{n-1}} - \frac{1}{1 + n K_n M_1^{n-1}} \right] \quad (3.7)$$

$$\frac{d^2\delta}{d(\log C)^2} = \frac{d}{dM_1} \left(\frac{d\delta}{d \log C} \right) \frac{dM_1}{dC} \frac{dC}{d \log C} \quad (3.8)$$

At the point of inflection $\frac{d^2\delta}{d(\log C)^2} = 0$

since neither $\frac{dM_1}{dC}$ nor $\frac{dC}{d \log C}$ can equal zero

the inflection point condition (ip) is given by

$$\frac{d}{dM_1} \left(\frac{d\delta}{d \log C} \right)_{ip} = 0 \quad \text{and} \quad (M_1^{n-1} K_n)_{ip} = n^{-3/2} \quad (3.9)$$

therefore
$$\left(\frac{d\delta}{d \log C} \right)_{ip} = 2.303 (\delta_1 - \delta_n) \left[\frac{n^{-1/2} - n^{1/2}}{n^{-1/2} + n^{1/2} + 2} \right] \quad (3.10)$$

10

Marcus and Miller reasoned that if all shifts are measured from δ_1 then the slope of δ vs Log C curve is proportional to δ_n at the inflection point and the proportionality constant K_n is a function of n only. For each value of n a value of δ_n can be obtained from (3.10). K_n was then set to unity and plots of δ vs log C are

constructed, the value of n , which gave the best fit of the theoretical curve to the experimental, being accepted as the degree of association.

For thiols Marcus and Miller found that the inflection point occurred at concentrations so close to that of the pure thiol that the slope was difficult to measure. Consequently they adapted the method by guessing $\left(\frac{d\delta}{d \log C}\right)_{ip}$ obtaining δ_n from expression (3.10) and by iteration converging on consistent values of δ_n and K_n .

By this method, Marcus and Miller, found that for ethanethiol the best fit occurred if $n = 2$ i.e. a monomer/dimer equilibrium. Also that δ_n was 3.8 . δ_n is the average resonance of both dimer located protons in the open dimer, and the unassociated proton in the open dimer of process (II) can be expected to contribute to the monomer resonance frequency. Therefore, from the results of Marcus and Miller, it can be calculated that the associated proton in the dimer has a chemical shift of x where;

$$\frac{1.04 + x}{2} = 3.8$$

$$\text{i.e. } x = 6.16$$

Also in 1966 Rousselot et al. produced a series of papers in which they reported the dilution curves of the chemical shift of the S^1H proton of several thiols in various solvents. For basic solvents such as acetone, DMSO and HMPA, there is a downfield shift of the S^1H proton's resonance which is attributed to:-

- i) the partial withdrawal of the proton from its electronic environment by the electronegative acceptor atom of the base.
- ii) the inhibition of electronic circulation about the proton by the electric field of the electronegative atom.

The limiting values of these shifts at infinite dilution ranged from 1.04 in CCl_4 to 2.72 in HMPA. ¹⁴⁻¹⁶ These shifts are for the species;



If the value for the associated proton's chemical shift in the open dimer is examined i.e. for;



¹⁰
The value of 6.16 obtained by Marcus and Miller for the shift of the hydrogen bonded proton in the open dimer suggests this is a much stronger hydrogen bond than that formed to HMPA. ¹⁴⁻¹⁶ This result seems to be highly improbable.

¹⁷
Alencastro and Sandorfy studied self-association in thiols using fundamental and first overtone infra-red Spectroscopy. By lowering the temperature of dilute solutions of thiols in a 1:1 mixture of CCl_3F and $\text{C}_2\text{F}_4\text{Br}_2$ (FR) they observed that the fundamental free S-H band increased in intensity as the solutions were cooled and that a band grew in at lower wavenumber which they

assigned to the dimer. They explained this apparent paradox in terms of :-

- a) overlap of the dimer band boosting the apparent intensity of the free band
- b) contribution from the free S-H endgroup of an open dimer enhancing the intensity of the free band
- c) temperature dependent changes in the proportions of rotamers which would increase the intensity of the free band if the rotamer favoured by low temperatures was the more intense band.

This new band shifted to lower wavenumber as the temperature was lowered until at -184°C . it was positioned at 2535 cm^{-1} . For Propane-2-thiol they observed two distinct associated bands at 2543 and 2525 cm^{-1} at temperatures of -157°C and below. They concluded that these bands were due to the formation of dimers and higher polymers respectively. Upon cooling pure liquid thiols, the S-H band became more intense and shifted to lower frequency. Similar studies were also performed in the first overtone infra-red region of the spectrum. In conclusion they reported that their results confirmed the existence of S-H \cdots S hydrogen bond as postulated by previous authors, and that upon cooling the proportion of dimers increased. However, even at the lowest temperatures free molecules exist.

Recently a computer simulation study was performed on H_2S , MeSH and EtSH the conclusions of which were that for EtSH there is an extensive occurrence of linear dimers and trimers at 25°C with an average of one hydrogen bond per molecule. This result is completely incompatible with previous ideas on the structure of thiols in which the monomer - dimer equilibrium was thought to be highly displaced in favour of the monomer.

3.3 Experimental

3.3.1 Infra-red Spectra

IR spectra were recorded on a Perkin-Elmer 681 double beam spectrometer. Demountable cells with teflon spacers and calcium fluoride plates were used for the sample solutions. Identical cells containing solvent only were used in the reference beam. Pathlengths of 0.5 mm or 0.025 mm were used depending on the concentration of the solution being recorded.

Spectra were recorded at appropriate vertical expansions using a scan time of 3 x 16 minutes and a horizontal expansion of x5. Spectral band wavenumbers were measured from the noted wavenumber of the edges of the spectra.

3.3.2 Nuclear Magnetic Resonance Spectra

All Proton resonance spectra were recorded using a Jeol PS 100 spectrometer operating at 100 MHz. Frequencies were measured relative to that of the protons of the internal TMS reference. The spectra were calibrated using TMS sidebands induced at a known frequency from TMS. Chemical shifts are the average of three or

more measurements for each concentration. A variable temperature probe cooled by nitrogen gas generated from liquid nitrogen was used for all variable temperature work. The temperature was thermostatically maintained by electric heating coils to within $\pm 0.5^{\circ}\text{C}$.

3.3.3 First Overtone Near Infra-Red Spectra

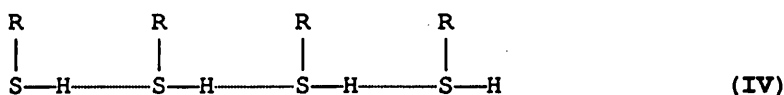
All first overtone spectra were recorded on a Perkin Elmer 340 spectrometer. Spectra were recorded at $25 \pm 0.1^{\circ}\text{C}$ and a photometric scale of 0 - 1.40 was used unless otherwise stated. Silica cells of 1 cm pathlength were used. The sample cell contained pure EtSH or EtSH in solution. The corresponding reference cell was left empty or contained the solvent only. For variable temperature work the cells were cooled by applying Drikold or liquid nitrogen to the copper cell mountings. The temperature was thermostatically maintained to within $\pm 0.1^{\circ}\text{C}$ by a heating coil which surrounds the mountings.

3.3.4 Purification of Materials

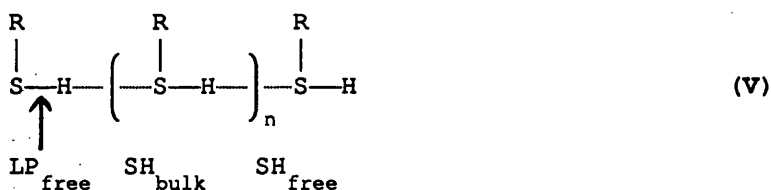
EtSH, used without further purification, was obtained from Aldrich Chemical Company Ltd. at 98%+ purity. Solvents were of the purest grade available and were purified further, usually by fractional distillation over CaH_2 and storing over CaH_2 or molecular sieves. Water was purified by deionisation followed by passage through a millipore "Milli-P" system.

3.4 Results and Discussion

Pure thiols can be thought to exist as short chain-like polymers (IV) with the thiol molecules linked together by hydrogen bonding similar to that in alcohols.



One important difference between the liquid structure of thiols and that of alcohols, lies in the strength of the hydrogen bonding which is much weaker for thiols than for alcohols. This difference is expected to lead to an increase in the number of non-bonded units, or "broken" hydrogen bonds for thiols. In general, it might be expected to find monomers, dimers and oligomers in liquid thiols. An open polymer chain should comprise three different types of S-H oscillators; a) $(\text{SH})_{\text{free}}$, b) $(\text{LP})_{\text{free}}$ and c) $(\text{SH})_{\text{bulk}}$ as in insert (V). Each unit in this group is expected to have a different infra-red frequency and chemical shift. If $n = 0$, the $(\text{SH})_{\text{bulk}}$ unit is absent.



The terminal groups, $(\text{SH})_{\text{free}}$ and $(\text{LP})_{\text{free}}$ are formed whenever hydrogen bonds are broken and must be present in equal concentrations. The infra-red spectra of thiols in CCl_4 show the S-H stretching bands between 2585 cm^{-1} and 2559 cm^{-1} , depending on the concentration. These spectra can be deconvoluted into bands assigned to the individual types of S-H oscillator. This was done

for ethanethiol and the results of this and other spectroscopic techniques, notably NMR, were used to investigate the hydrogen bonding in EtSH.

3.4.1 Fundamental Infra-red Spectroscopy

Dilute solutions of EtSH in CCl_4 and $\text{c-C}_6\text{H}_{12}$ have S-H stretching band maxima at 2585 cm^{-1} . As the ability of the solvent to form hydrogen bonds with the thiol group increases, so the wavenumber of the S-H stretching band decreases. This is due to the lengthening and weakening of the S-H bond on forming a hydrogen bond with the base.

One solvent parameter which measures the electron donating ability of various solvents is its Donor Number (DN)¹⁸. Figure 3.1 shows that there is a good linear relationship between the frequency of the S-H stretching band and the DN of the solvent, for dilute solutions of EtSH in various solvents.

The extinction coefficient of the monomer S-H stretching band was calculated from figure 3.2 using Beer's Law and was found to be $9.4 \text{ mol}^{-1} \text{ dm}^{-2}$ in CCl_4 . The shape, wavenumber and intensity of the S-H stretching band in CCl_4 solution varied with concentration, figure 3.3. As the concentration increased, ν_{max} shifted from 2585 cm^{-1} to 2560 cm^{-1} and the extinction coefficient increased.

The S-H stretching band was analysed by computer using the

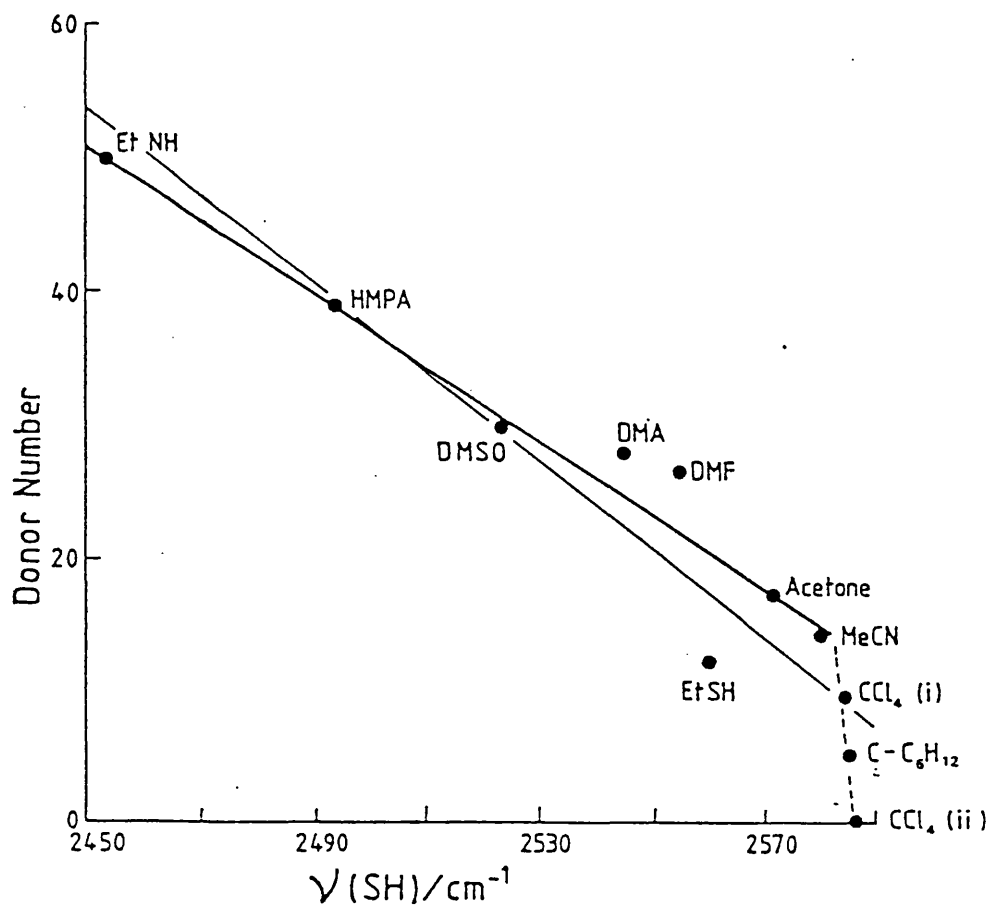


Fig. 3.1. Relationship between frequency of $\nu\text{S-H}$ of EtSH and solvent Donor Number (DN).

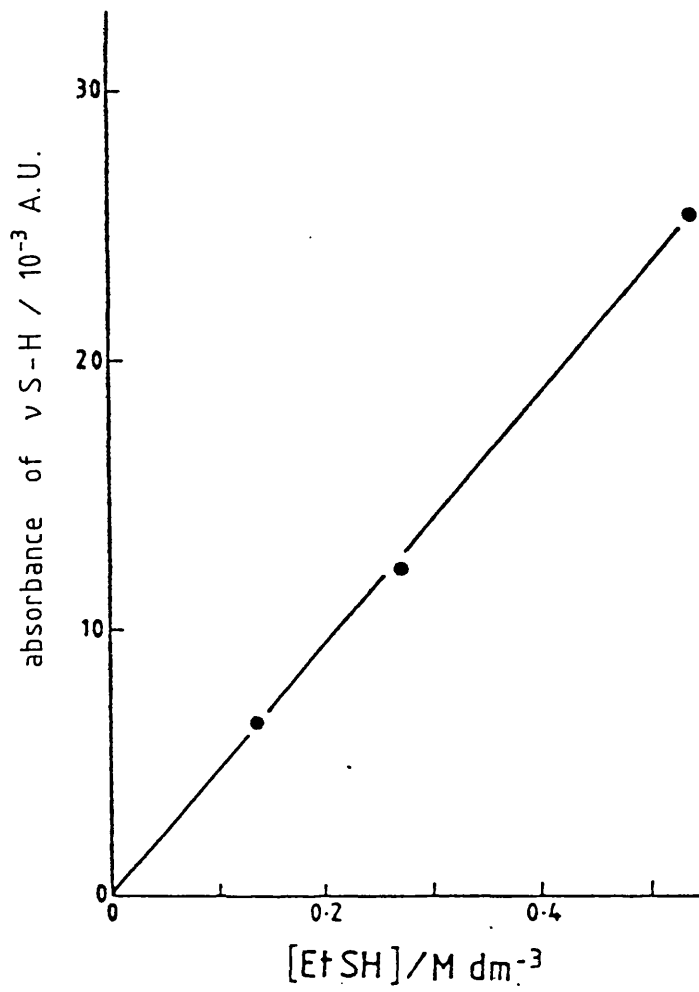


Fig. 3.2. Beer's law plot for ν S-H of EtSH in CCl_4 at 25°C.

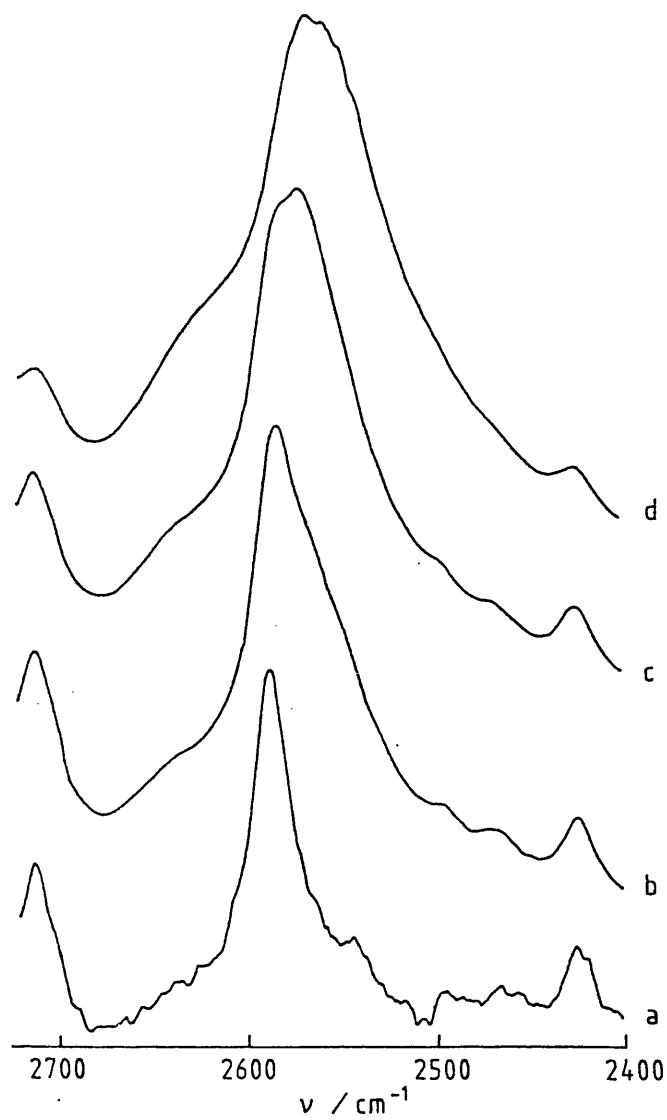


Fig. 3.3. Infrared spectra of solutions of EtSH in CCl_4 and pure EtSH in the $\nu_{\text{S-H}}$ region. (a) 0.33M, (b) 2.25 M, (c) 4.50 M and (d) 13.5 M.

V.I.D.C.A. program at various concentrations, figures 3.4, 3.5, 3.6, 3.7. For very dilute solutions of EtSH in CCl_4 , the monomer band at 2585 cm^{-1} was the only band present. At higher concentrations the $(\text{SH})_{\text{free}}$ oscillator of the polymer must also contribute to this band. On increasing the concentration, a second band grew in at 2570 cm^{-1} ; this was assigned to the $(\text{LP})_{\text{free}}$ S-H oscillator. At higher concentrations, a third band at 2559 cm^{-1} was observed and assigned to the $(\text{SH})_{\text{bulk}}$ oscillator. This band could only be due to polymers higher than dimers. The $(\text{LP})_{\text{free}}$ units of such oligomers are thought to contribute to the 2570 cm^{-1} band.

3.4.2 Nuclear Magnetic Resonance Spectroscopy

The chemical shift of the S-H proton was measured for very dilute solutions of EtSH in various solvents and plotted against the DN of the solvent. As with the wavenumber of the S-H stretching band, this plot is reasonably linear, figure 3.8. Furthermore, a plot of chemical shift $\delta(\text{S}^1\text{H})$ against $\nu(\text{S-H})$ is linear (a) figure 3.9. A better correlation (b) can be obtained if CCl_4 and $\text{c-C}_6\text{H}_{12}$ are not included in the least square fitting of the correlation line. The wavenumbers of the infra-red bands assigned to $(\text{LP})_{\text{free}}$ and $(\text{SH})_{\text{bulk}}$, (2570 cm^{-1} and 2559 cm^{-1} respectively) were used together with correlation (b) in figure 3.9 to give the chemical shifts for $(\text{LP})_{\text{free}}$ and $(\text{SH})_{\text{bulk}}$. They were found to have chemical shifts of 1.75 and 1.89 respectively. The observed chemical shift of EtSH is the weighted average of the chemical shifts of the three types of SH groups i.e.

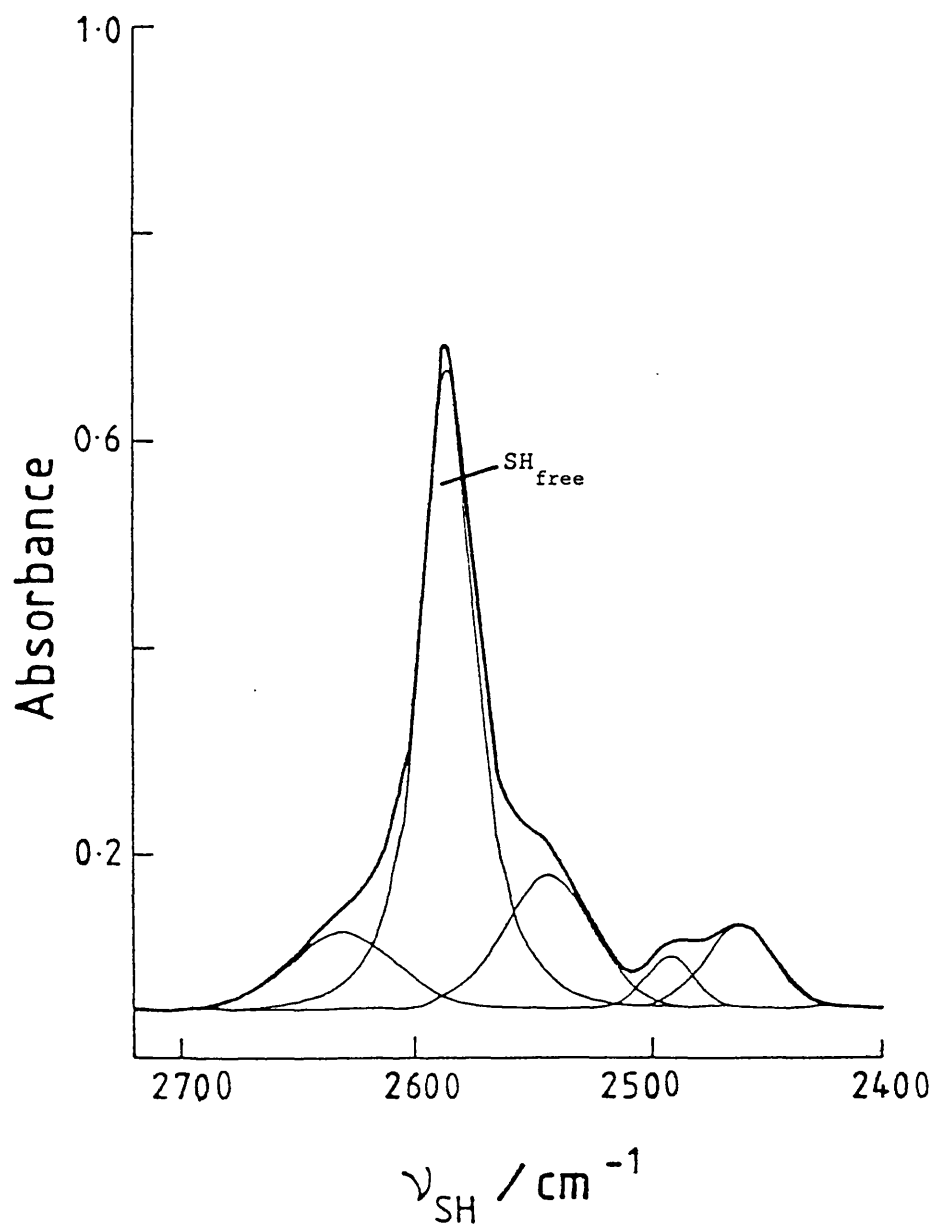


Fig. 3.4. Curve analysed infrared spectrum of 0.33 M EtSH in CCl₄ in the ν S-H region at 25°C.

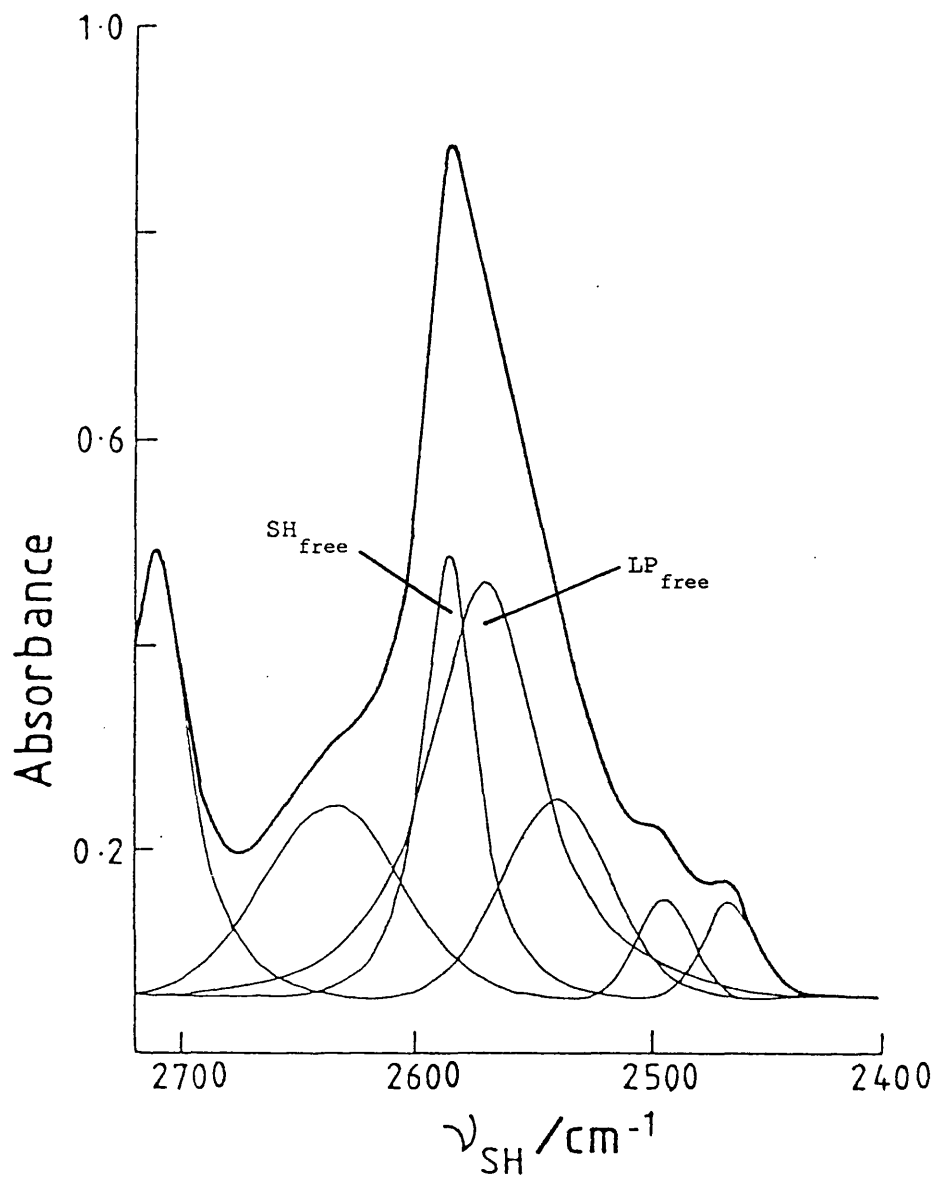


Fig. 3.5. Curve analysed infrared spectrum of 2.25 M EtSH in CCl₄ in the ν S-H region at 25°C.

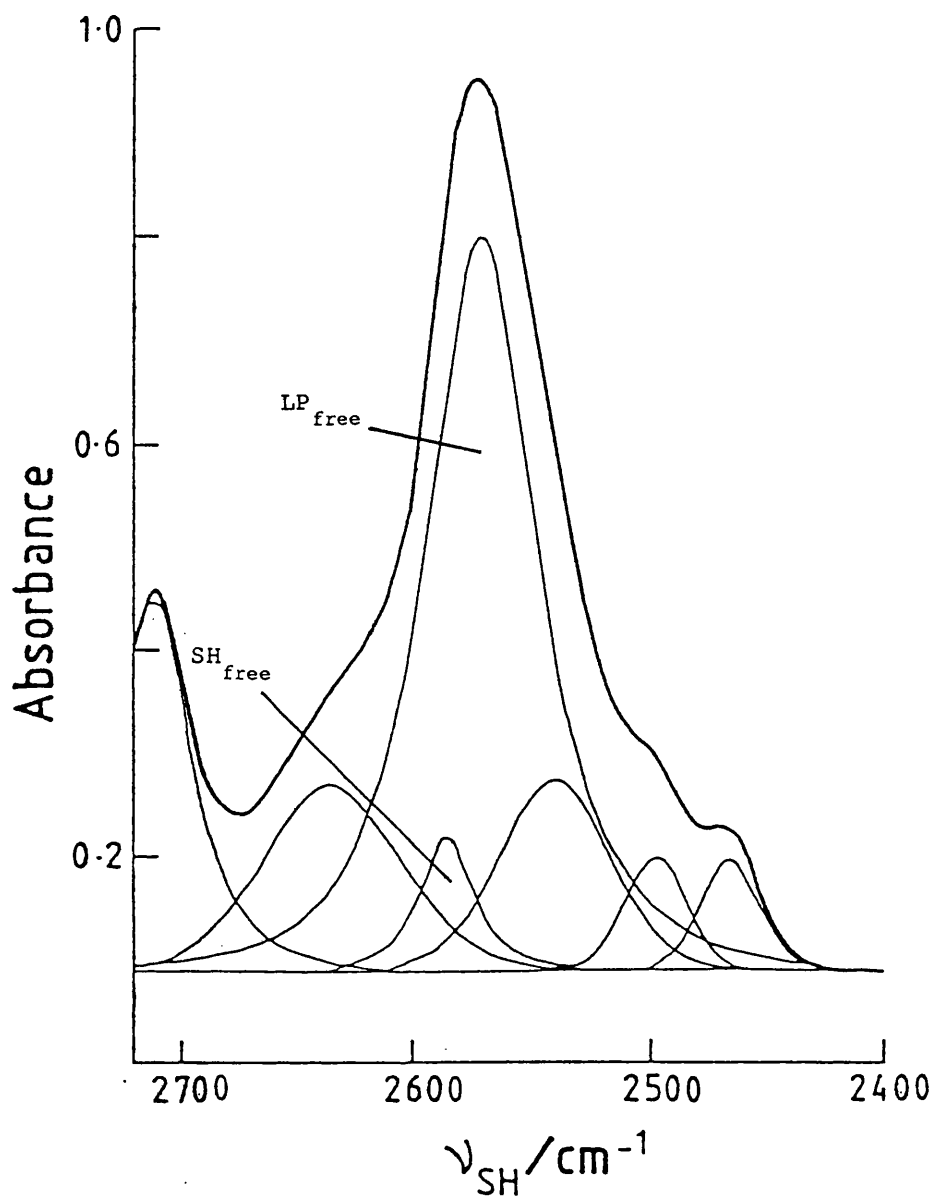


Fig. 3.6. Curve analysed infrared spectrum of 4.50 M EtSH in CCl₄ in the ν_{S-H} region at 25°C.

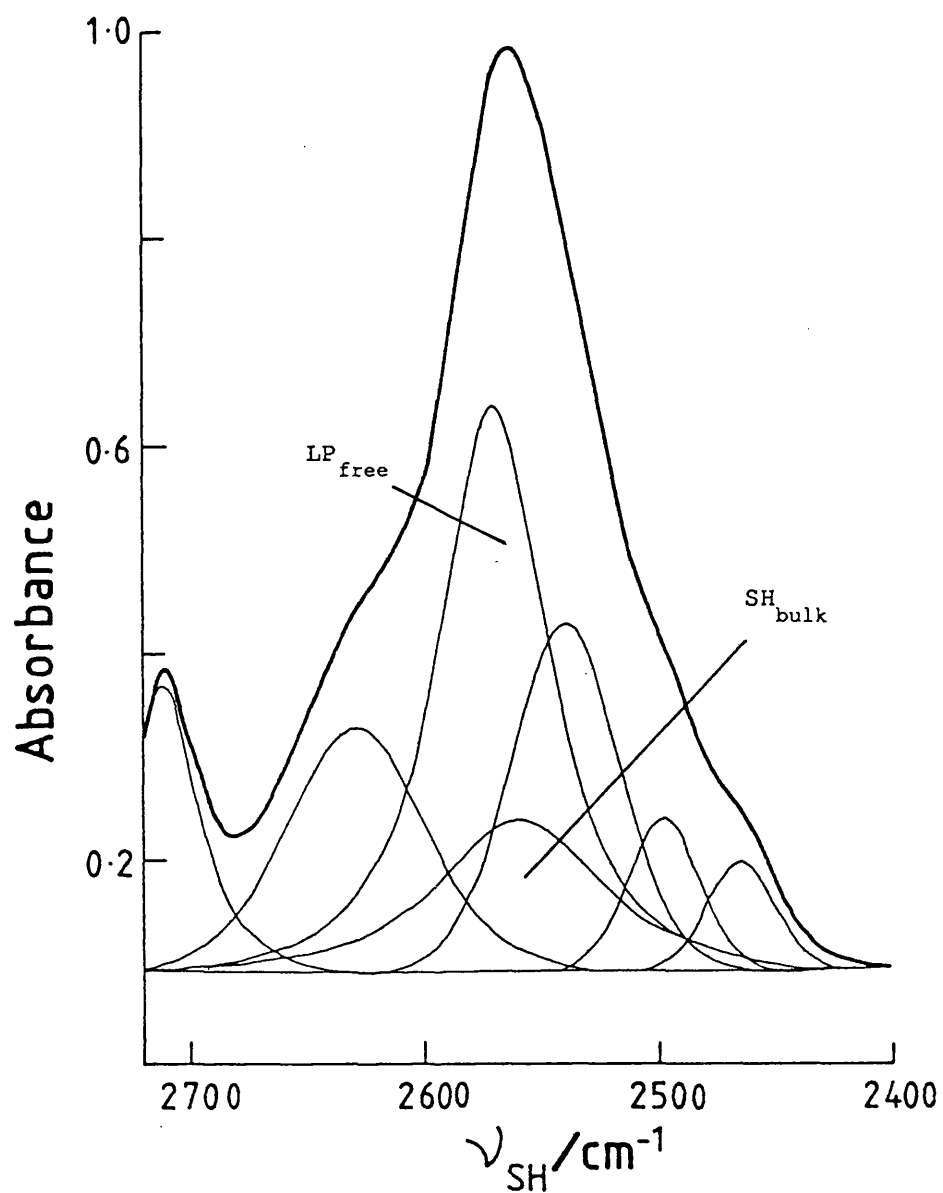


Fig. 3.7. Curve analysed infrared spectrum of pure EtSH (13.5 M) in the ν S-H region at 25°C.

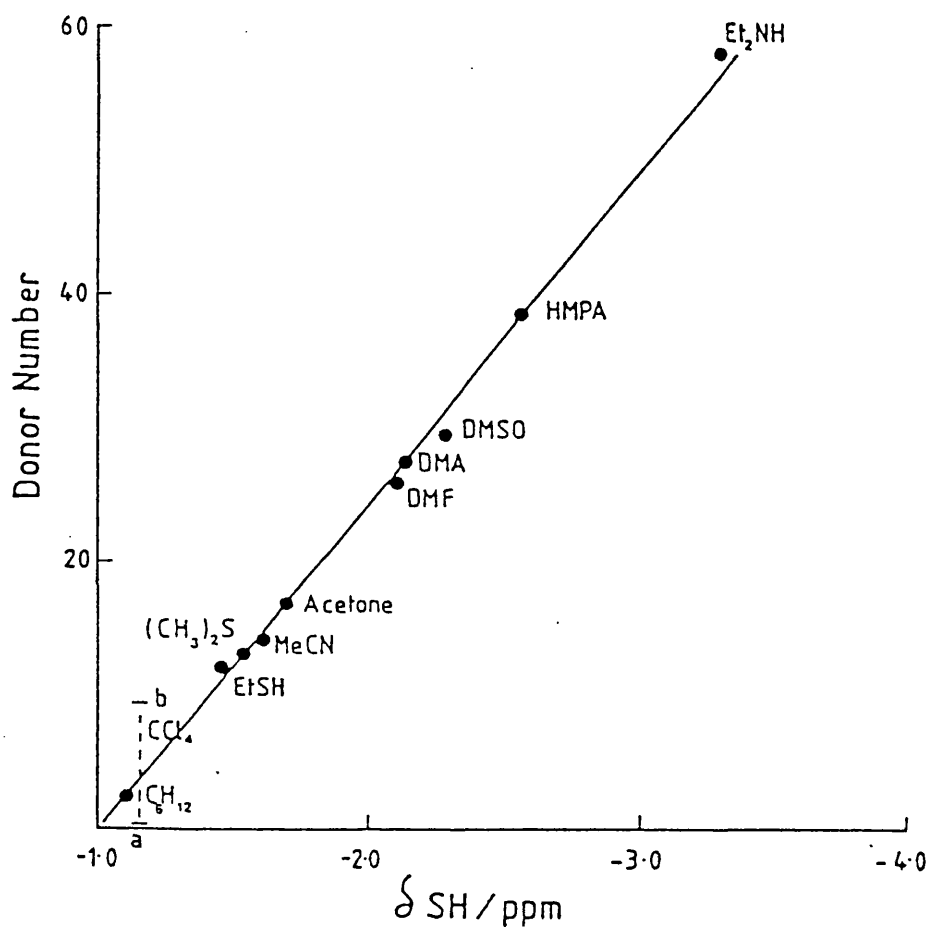


Fig. 3.8. Plot of chemical shift of the sulphydryl proton of EtSH in various solvents against the Donor Number of Solvent.

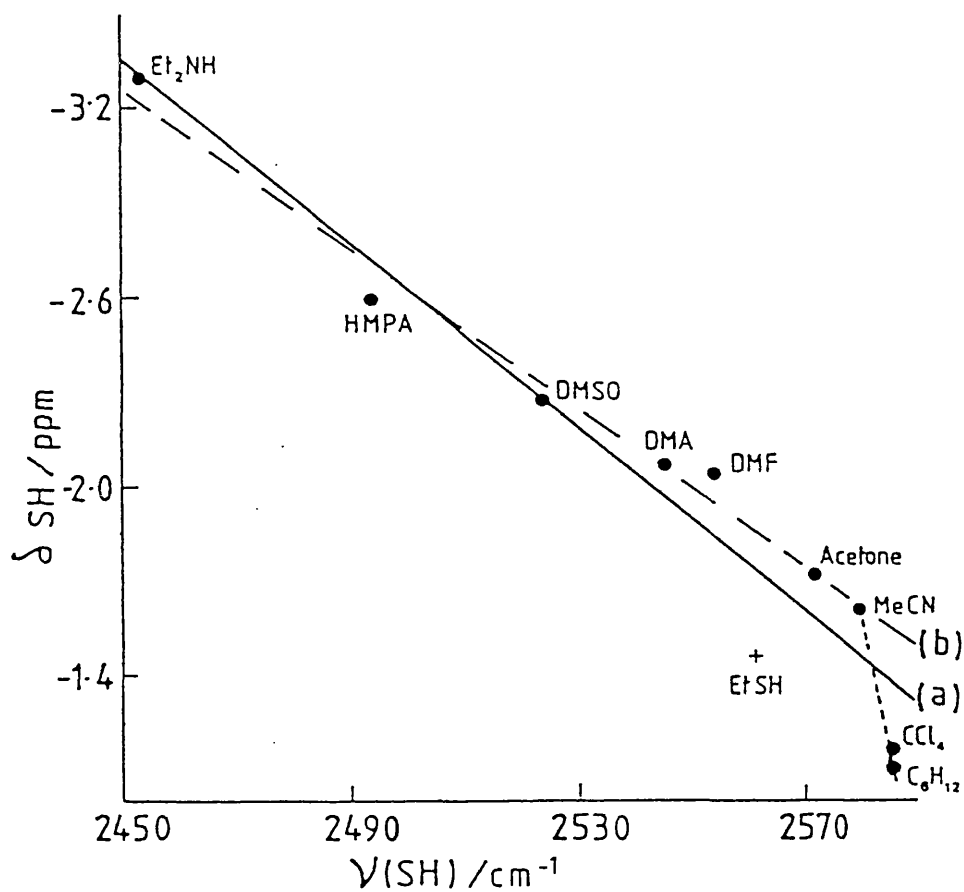
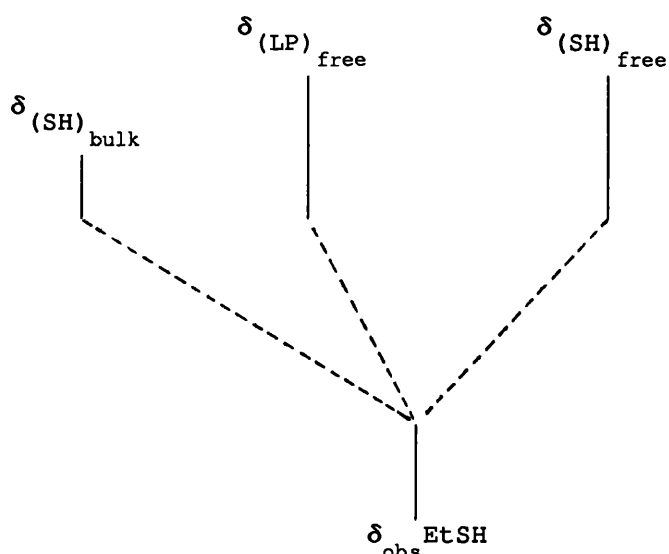


Fig. 3.9. Plot of the chemical shift of the sulphhydryl proton against the frequency of $\nu\text{S-H}$ of EtSH in various solvents.



Therefore, an estimation of the amount of $(SH)_{free}$ can be obtained from the following expression (3.11)

$$\delta_{obs} = x \delta_{(SH)_{free}} + x \delta_{(LP)_{free}} + (1-2x) \delta_{(SH)_{bulk}} \quad (3.11)$$

At 22°C $1.46 = x 1.16 + x 1.75 + (1-2x) 1.89$

$$x = 0.49$$

i.e. there is ca. 49% $(SH)_{free}$ at 22°C

This result suggests that in the pure liquid at 22°C the average size of the polymer is two, implying that dimers dominate. If correlation (a) is used to estimate the chemical shifts of $(LP)_{free}$ and $(SH)_{bulk}$, the percentage of $(SH)_{free}$ is calculated to be ca. 39%. Figure 3.10 shows that the temperature dependence of the chemical shift for pure EtSH in the temperature range -100°C to +20°C is linear. As the temperature falls the number of hydrogen bonds increases, therefore the observed chemical shift tends towards that of the $(SH)_{bulk}$ species. The correlation line

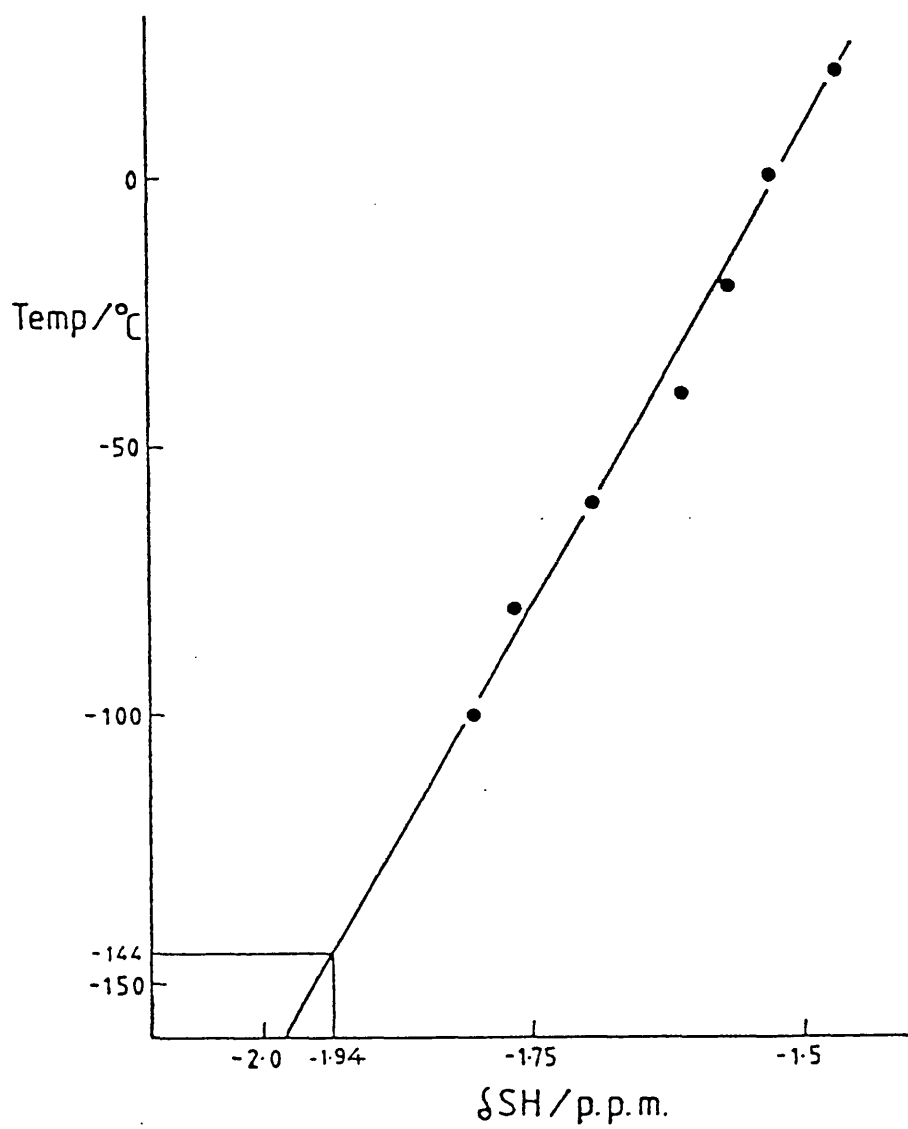


Fig. 3.10. Temperature dependency of the chemical shift of the sulphydryl proton of EtSH.

was extrapolated to the freezing point temperature of EtSH (-144°C), giving a chemical shift of 1.94. This value is close to that estimated for the (SH)_{bulk} at room temperature (1.89) which implies that hydrogen bonding is extensive at the freezing point. Using the chemical shift for (LP)_{free} obtained from the NMR/IR correlation and the measured chemical shift for (SH)_{free}, a value δ_d can be obtained for the average chemical shift for the open dimer;



$$\delta_d = \frac{\delta_{(\text{SH})_{\text{free}}} + \delta_{(\text{LP})_{\text{free}}}}{2}$$

$$\delta_d = \frac{1.16 + 1.75}{2}$$

$$\delta_d = 1.45$$

By assuming that in dilute solutions of EtSH in CCl₄ only monomer and dimer units are present, the limiting slope expression (3.12) can be used to calculate the dimerisation constant K_d for equilibrium (III).

$$\left(\frac{d\delta}{dC} \right)_{C \rightarrow 0} = 2K_d (\delta_d - \delta_{(\text{SH})_{\text{free}}}) \quad (3.12)$$

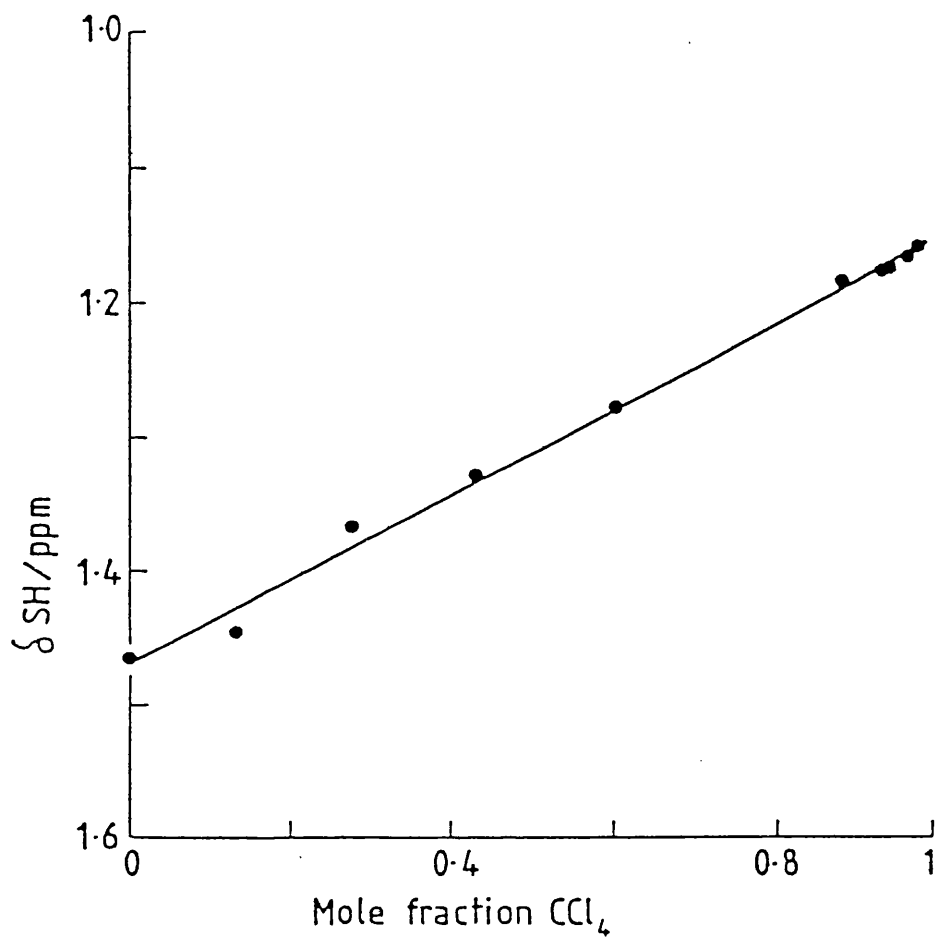


Fig. 3.11. Plot showing the concentration dependency of the chemical shift of the sulphydryl proton of EtSH in CCl₄.

$\left(\frac{d\delta}{dC}\right)_{c \rightarrow 0}$ is obtained from figure 3.11

$$\frac{1.184 - 1.16}{1.061} = 2K_d (1.45 - 1.16)$$

$$K_d = 0.038 \text{ mol}^{-1} \text{ dm}^3$$

This method affords a value of K_d which is nine times greater than the one obtained by Marcus and Miller.¹⁰ It must be stressed that K_d is only valid for solutions at concentrations at which higher polymers can be ignored.

The Acceptor Number (AN)²³ for EtSH was determined to be 16.1 by measuring the ³¹P chemical shift of Triethylphosphine Oxide Et₃PO at different concentrations and then using relationship (3.13).

$$AN = \delta_{\text{corr}} \times 2.348 \quad (3.13)$$

Where δ_{corr} is the ³¹P shifts of Et₃PO extrapolated to infinite dilution and measured relative to hexane solution.

The Donor Number (DN) of EtSH was estimated to be 12 using the method of Hahn et al.²⁴ These two results suggest that EtSH should be capable of intermolecular hydrogen bonding.

3.4.3 First Overtone Near Infra-Red Spectroscopy

The NIR spectrum of EtSH was studied in the region between 5175

cm^{-1} and 4825 cm^{-1} which contains the first overtone S-H stretching bands, figure 3.12. For solutions of EtSH in CCl_4 this region of the spectrum comprises several bands figures 3.13, 3.14, 3.15. The highest frequency band (1), absorbing at 5056 cm^{-1} , is assigned to $(\text{SH})_{\text{free}}$ units and band 2, at 4993 cm^{-1} , to the $(\text{SH})_{\text{bound}}$ stretch. As with alcohols the band assigned to the free species in the first overtone is much more intense relative to the bound band than in the fundamental spectrum. Because of this it proved difficult to resolve the band at 4993 cm^{-1} into two bands arising from two different bound (SH) units. It is therefore assumed in view of the fundamental infra-red results that band 2 must arise predominantly from the $(\text{LP})_{\text{free}}$ unit. The other bands in the region were found to be virtually unaltered by temperature, solvent and concentration changes, they are assumed to be combination bands not involving the S-H oscillator.

On lowering the temperature, figures 3.16, 3.17, 3.18, the intensity of band 1 fell whilst that of band 2 increased. On dilution with CCl_4 , band 1 increased in height relative to band 2. Both these spectral changes are in accord with expected changes in the amount of hydrogen bonding between the EtSH molecules. Lowering the temperature causes less hydrogen bonds to be broken by thermal motion. Upon dilution the polymer chains are broken down forming more of the $(\text{SH})_{\text{free}}$ species. Figure 3.19 is a plot of absorbance of the monomer S-H stretching band for solutions in CCl_4 against concentration. Using Beer's Law this gives an extinction coefficient of $0.53 \text{ mol}^{-1} \text{ dm}^2$ for the monomer S-H band.

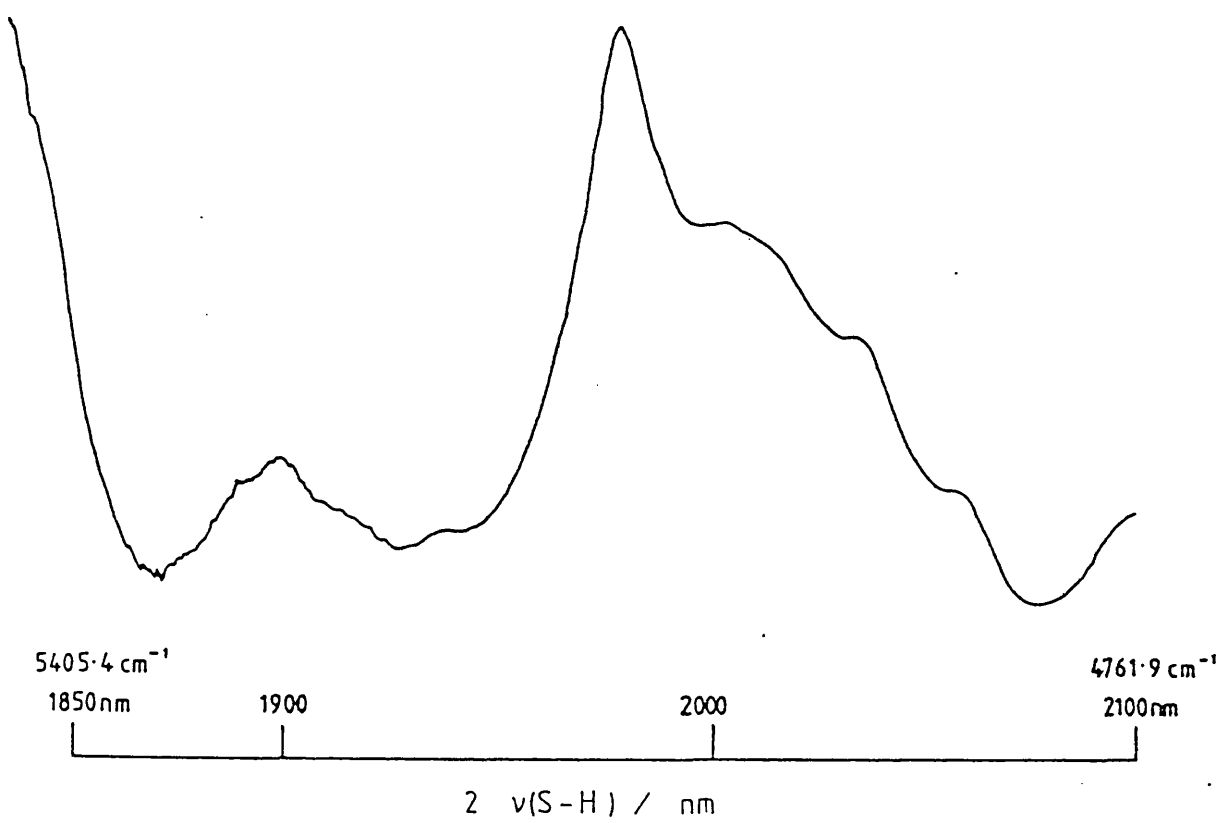


Fig. 3.12. Near infrared spectrum of EtSH in the 2ν S-H region at 25 °C.

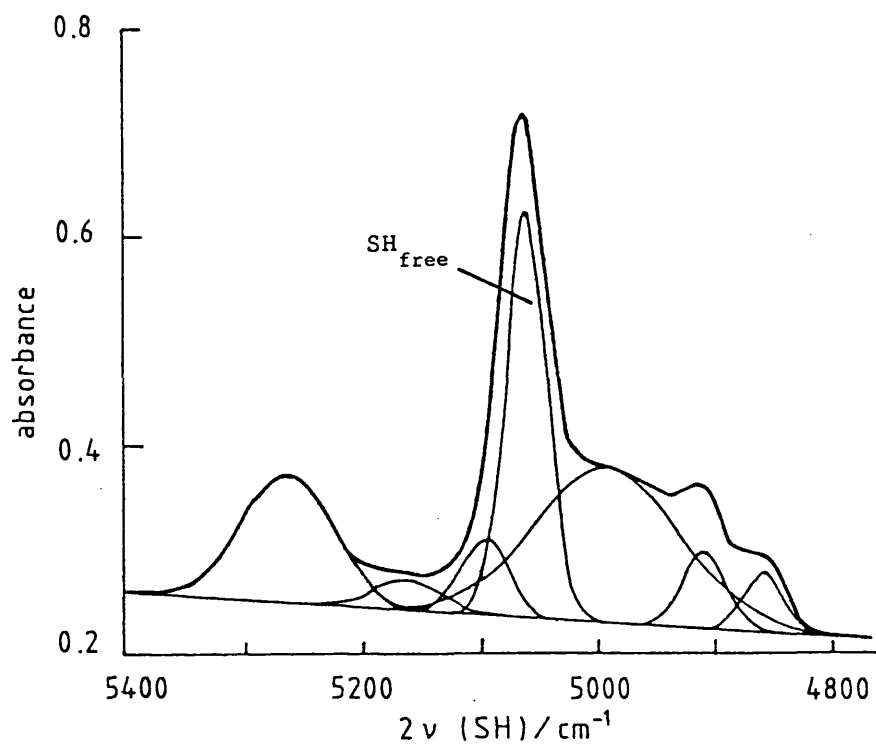


Fig. 3.13. Curve analysed near infrared spectrum of 0.115 M EtSH in CCl₄. Temperature = 25°C.

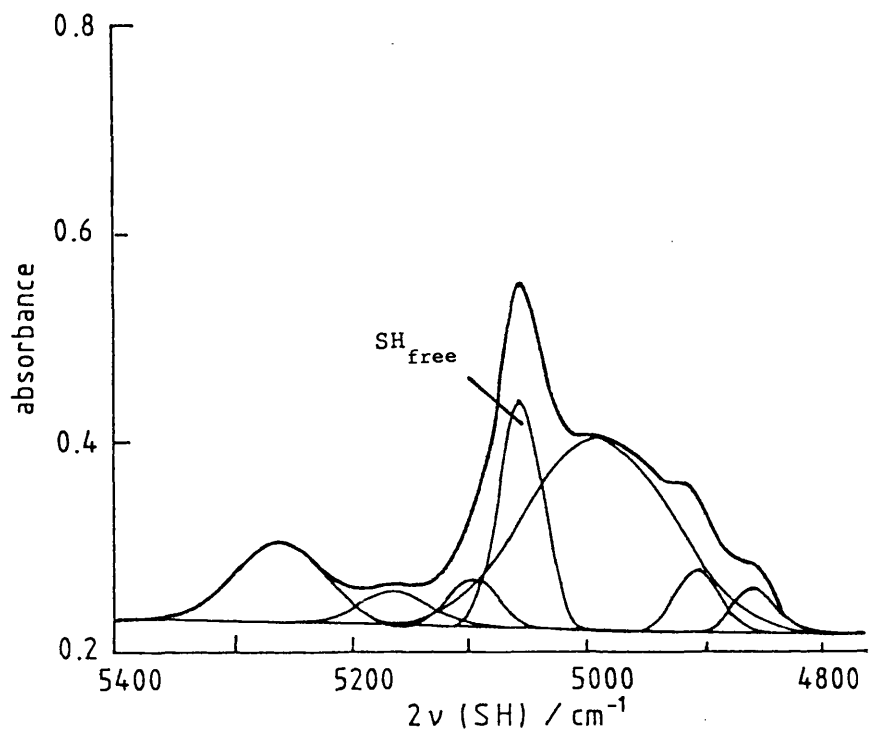


Fig. 3.14. Curve analysed near infrared spectrum of 0.622 M EtSH in CCl₄.
Temperature = 25°C.

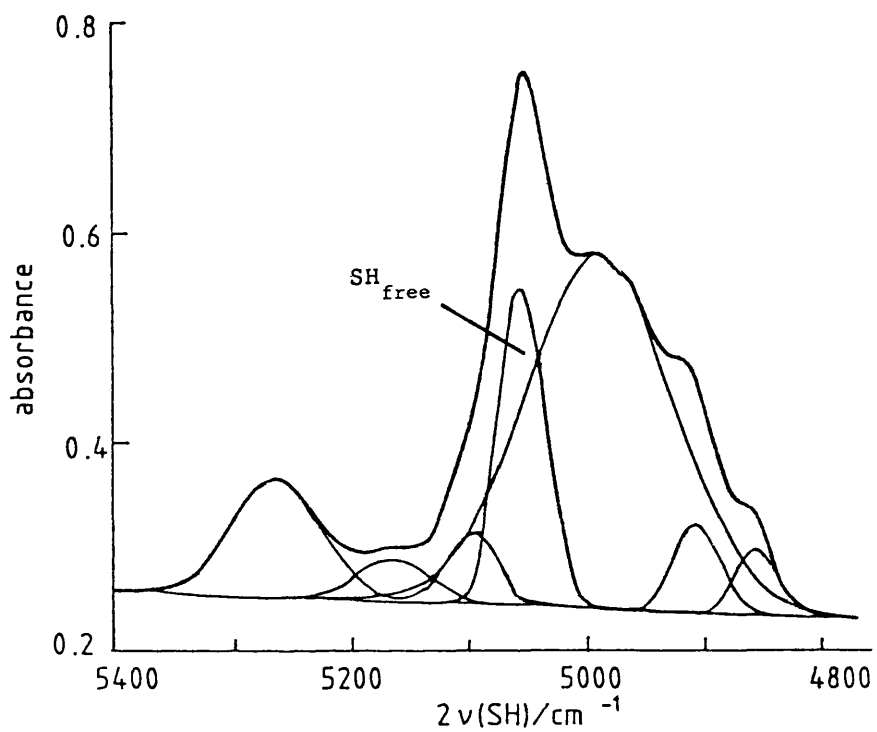


Fig. 3.15. Curve analysed near infrared spectrum of pure EtSH (13.5 M).
Temperature = 25°C.

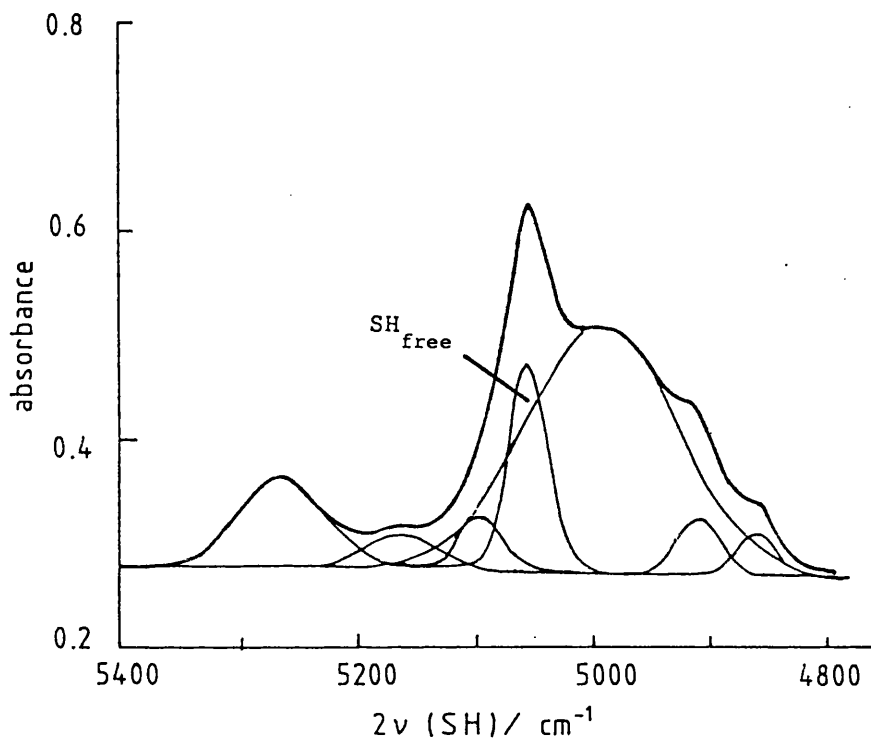


Fig. 3.16. Curve analysed near infrared spectrum of pure EtSH (13.5 M).
Temperature = 25°C.

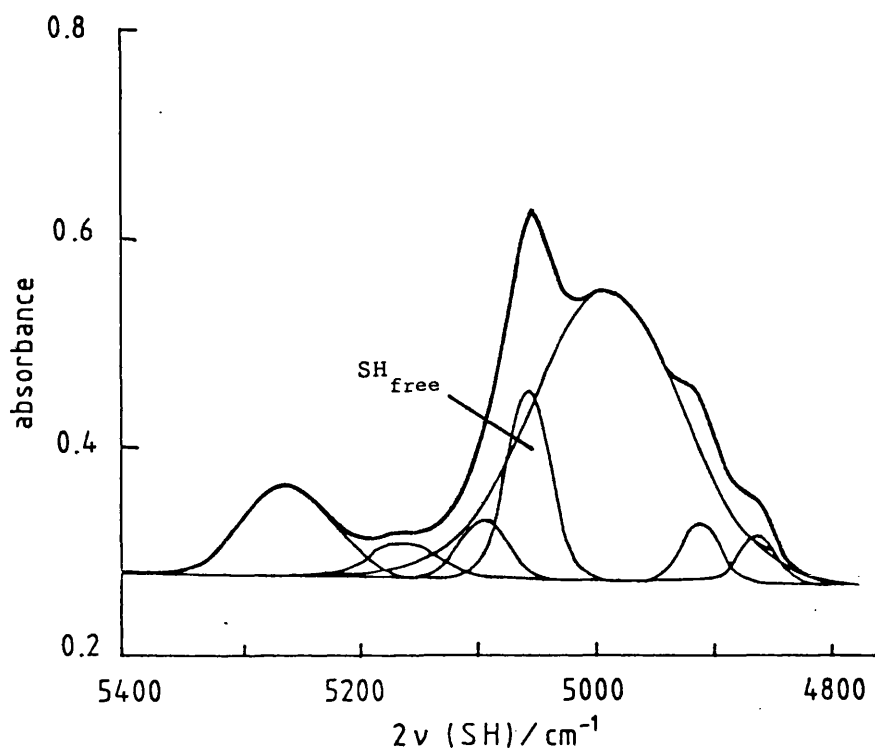


Fig. 3.17. Curve analysed near infrared spectrum of pure EtSH (13.5 M).
Temperature = 5°C.

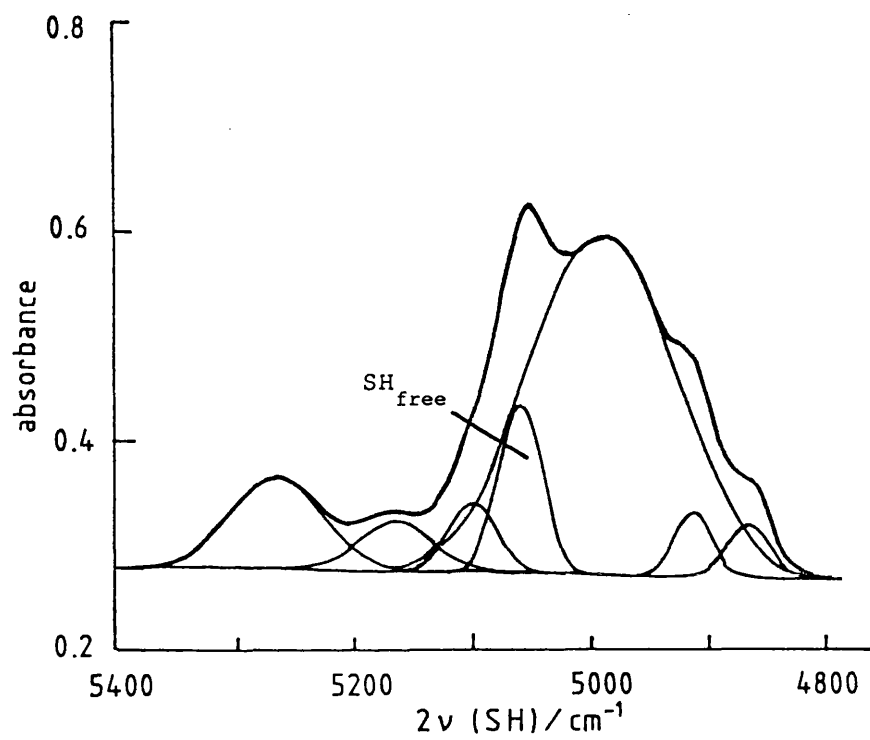


Fig. 3.18. Curve analysed near infrared spectrum of pure EtSH (13.5 M).
Temperature = -15°C.

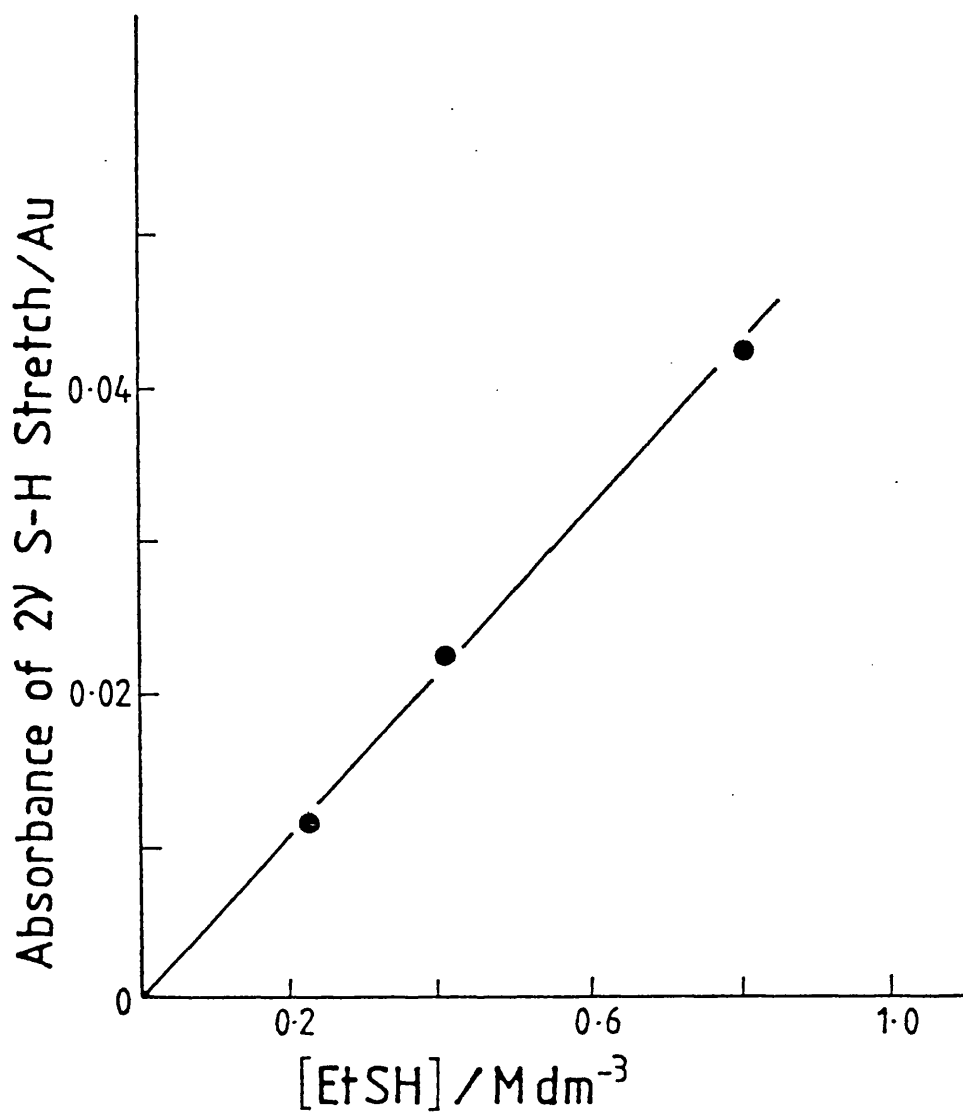


Fig. 3.19. Beer's law plot for 2ν S-H of EtSH in CCl₄ at 25°C.

Using this as an estimation of the extinction coefficient of the $(SH)_{\text{free}}$ band in pure EtSH and by using Beer's Law, an estimation of ca. 30% $(SH)_{\text{free}}$ can be made for the pure liquid. This is a lower percentage than was derived from the NMR/IR correlation method, however, this was not entirely unexpected because the same ²⁵ method when adapted to alcohols also underestimated the amount of free species present in pure alcohols. The reason for this is almost certainly due to a difference in the extinction coefficients of the monomer S-H band in CCl_4 and that of the $(SH)_{\text{free}}$ band in the pure liquid. If this is so, then the value of ca. 49% $(SH)_{\text{free}}$ is to be preferred.

3.5 Concluding Remarks

The approach to thiols adopted by previous workers concentrated on the estimation of equilibrium constants for the monomer and dimer species. Whichever method was used to obtain K_d the values obtained were not valid at high concentrations because of the formation of higher polymers. The NMR/IR correlation method used herein is useful for obtaining values for the concentration of $(SH)_{\text{free}}$ and therefore the average size of the polymer in the pure liquid. Also the value obtained for the chemical shift of the dimer can be used to obtain a dimerisation constant valid for low concentrations of EtSH in CCl_4 .

The comparison between the value of K_d obtained by the NMR/IR correlation method; $0.038 \text{ mol}^{-1} \text{ dm}^3$, and that obtained by Marcus and Miller; ¹⁰ $0.0056 \text{ mol}^{-1} \text{ dm}^3$, shows that K_d is extremely sensitive

to the magnitude of the chemical shift of the dimer used in the calculation. Marcus and Miller used a value of 3.8 which appears to be far too large when the chemical shifts of EtSH in bases are compared with it. The temperature dependence of the observed chemical shift in pure EtSH also seems to rule out such a high value of for the dimer.

The method by which Marcus and Miller obtained δ_d appears to be flawed, and this explains how the error in estimating K_d could be so great. In order to obtain δ_d Marcus and Miller estimated $\left(\frac{d\delta}{d \log C}\right)_{ip}$ and hence obtained δ_d and K_d . However, one of the assumptions in the Saunders and Hyne treatment which they used is that there is only one hydrogen bonding equilibrium. This assumption breaks down at high concentrations and therefore because the inflection point occurs at a concentration close to that of the pure thiol, the value of $\frac{d\delta}{d \log C}$ at the inflection point cannot reliably be used to find δ_d or K_d . Therefore Marcus and Miller's value for K_d must be rejected.

The results outlined above indicate that hydrogen bonding in EtSH is far more extensive than had been indicated by experiments involving the determination of monomer/dimer equilibrium constants, and confirm experimentally the suggestion made by Jorgensen that in the pure liquid at room temperature EtSH has an average of one hydrogen bond per molecule.

References for chapter 3

1. E. N. Lassetre, *Chem. Rev.* 20, 259 (1937).
2. G. F. Zellhoefer, M. J. Copley and C. S. Marvel, *J. Am. Chem. Soc.* 60, 1337 (1938).
3. H. Lumbrosco and R. Passerinini, *Bull. Soc. Chim. France*, 311, (1957).
4. S. Kondo, *Bull. Chem. Soc. Japan*, 38, 527 (1965).
5. A. S. N. Murthy C. N. R. Rao, B. D. N. Rao and P. Venkateswarlu, *Trans. Faraday Soc.* 58, 855 (1962); *Can. J. Chem.* 40, 963 (1962).
6. D. Plant, D. S. Tarbell and C. Whiteman, *J. Am. Chem. Soc.* 77, 1572 (1955).
7. R. A. Spurr and H. F. Byers, *J. Phys. Chem.* 62, 425 (1958).
8. S. Forsen, *Acta. Chem. Scand.* 13, 1472 (1959).
9. M. O. Bulanin, G. S. Denisov and R. A. Pushkina, *Opt. i. Spectroskopiya*, 6, 491 (1959).
10. S. H. Marcus and S. I. Miller, *J. Am. Chem. Soc.* 88, 3719 (1966).
11. M. L. Josien, P. Dizabo and P. Saumagne, *Bull. Soc. Chim. France* 423, (1957); M. L. Josien, C. Castinel and P. Saumagne, *ibid.* 48, (1957).
12. M. Saunders and J. B. Hyne, *J. Phys. Chem.* 31, 269 (1959).
13. J. R. Crook and K. Schug, *J. Am. Chem. Soc.* 86, 4271 (1964).
14. M. M. Rousselot, *Comp. Rend. Acad. Sc. Paris Ser. C* 262, 26 (1966).
15. M. M. Rousselot and M. Martin, *ibid.* 262, 1445 (1966).
16. M. M. Rousselot, *ibid.* 263, 649 (1966).
17. H. L. Robinson, *Ph.D. Thesis*, Leicester, (1984).

18. V. Gutmann, *Coordination Chemistry In Non-Aqueous Solutions*, Wien-New York, Chapter 2, (1968).
19. N. J. Pay, *Ph.D. Thesis*, Leicester, (1981).
20. C. M. Huggins, G. C. Pimentel and J. N Shoolery, *J. Phys. Chem.* 60, 1311 (1956).
21. H. L. Robinson, *Unpublished Results*, Leicester.
22. R. Bicca de Alencastro and C. Sandorfy, *Can. J. Chem.* 50, 3594 (1972).
23. W. L. Jorgensen, *J. Phys. Chem.* 90, 6379 (1986).
24. U. Mayer, *Monatsh. fur Chem.* 106, 1235 (1975).
25. S. Hahn, W. M. Miller, R. N. Lichtenthaler and J. M. Prausnitz, *J. Solution Chem.* 14, 129 (1985).

Chapter 4

*Hydrogen Bonding in
2-Hydroxyethanethiol.*

4.1 Introduction

The extent to which thiols form hydrogen bonds to water in aqueous solutions was investigated, principally using IR and NIR spectroscopy. The thiols chosen for study were cysteine and 2-hydroxyethanethiol. The latter has the advantage of being soluble in a wide range of polar and non-polar solvents and is less likely to form intra-molecular hydrogen bonds.

4.2 Previous Work

It is remarkable that more than 45 years after Hunter et al.,¹ working here in Leicester, confirmed and generalised Auwers² observation that thioacetic acid is associated and forms hydrogen bonds of the type ($-S-H \cdots O$), work is still being carried out in the same laboratory to determine whether or not hydrogen bonds are formed between thiols and water.

This study was initiated as a result of the apparent contradiction between the assertion commonly made by biochemists, that thiol groups in proteins are hydrophobic, and the observation by many different techniques, of hydrogen bonding between thiols and a wide range of bases. For a review of literature reporting evidence of hydrogen bonding between thiols and non-aqueous bases see chapter 3 and references therein.

In 'The Hydrogen Bond', Pimentel and McClellan³ reviewed developments in the field of hydrogen bonding and posed the question; '*Do sulfur (sic) compounds form hydrogen bonds?*' They concluded by noting that '*It is clear that the S-H group does*

show the specific H bond association behavior with some strong bases and it seems likely that the relative weakness of the S-H as a proton donor accounts for the absence of H bonds in some systems.''

Vinogradov and Linnell⁴ considered methionine (Met) as a hydrophobic group which does not take part in hydrogen bonding. Whereas, cysteine (Cys) was described as possibly a hydrogen bond donor, but probably not a hydrogen bond acceptor.

Data for the transfer free energy of various amino acids from organic solvents to water, measured by Nozaki and Tanford⁵ (table 4.1), was used by Kanehisa and Tsong⁶ to introduce a scale of local hydrophobicity in proteins. The local hydrophobicity of a residue (i) in an amino acid sequence was defined as the sum of the Nozaki-Tanford values for the two nearest-neighbour residues on both sides of the residue, i.e. $i\pm 1$ and $i\pm 2$. The local hydrophobicity values were then correlated with helix and β -sheet formation in 47 proteins.

The first observation of absorption bands due to SH groups in a native protein, was reported by Alben, Bare and Bromberg.^{7,8} Using Fourier transform (FT) IR to study human oxy- and deoxy-haemoglobin, they found in each case two overlapping bands (see table 4.2 for frequencies and assignments) in the 2500-2600 cm^{-1} region. They compared the intensity of these bands with those of simple thiols in various solvents which are known to hydrogen bond to the SH group, and found that both of the bands

Table 4.1

Amino acid	Nozaki - Tanford Values / kcal mol ⁻¹
Trp	3.4 ^a
Phe	2.5 ^a
Tyr	2.3 ^a
Leu	1.8 ^a
Val	1.5 ^b
Met	1.3 ^b
Cys	1.0 ^b
His	0.5 ^a
Ala	0.5 ^b
Thr	0.4 ^b

Nozaki-Tanford transfer free energy values refer to the transfer of an amino acid sidechain from 100% organic solvent to water at 25°C.

a - Average values for ethanol and dioxane. For histidine and leucine the values for ethanol are given double weighting because of their greater accuracy.

b - Value for ethanol only.

Table 4.2

Cysteine Residue	$\bar{\nu}$ S-H / cm ⁻¹
human oxyhaemoglobin	
-104	2553.8
-112	2567
human deoxyhaemoglobin	
-104	2557
-112	2564

observed have intensities consistent with SH groups which are strongly hydrogen bonded, probably to the carbonyl group of a peptide residue. It was suggested that FTIR spectroscopy of sulphhydryl groups may be a powerful tool for investigating the $\alpha_1\beta_2$ interface region of haemoglobin.

9
Isolated α -chains of haemoglobin were studied by Alben and Bare using FTIR spectroscopy. In particular they recorded spectra in the sulphhydryl region. No absorption bands were observed in that region, which indicated to them that *'...the β -112 cysteine -SH is not specifically hydrogen bonded in the isolated chain as it is in the $\alpha_2\beta_2$ tetramer but, rather, is exposed to solvent water and to a random local molecular environment...'*

10
Nakanishi et al. used the same technique to investigate sulphhydryl groups in heavy meromyosin. They contrasted the absorption band due to the SH group of cysteine in solution with that of SH groups present in heavy meromyosin. Cysteine was found to have a band at 2582 cm^{-1} whereas heavy meromyosin shows a band at around 2560 cm^{-1} which is 5.8 times more intense. Both of these observations are consistent with thiol groups in heavy meromyosin being hydrogen bonded. The high frequency of the SH stretching absorption of cysteine solutions would appear to suggest that the SH group is free of any hydrogen bonding.^{11,12}

In an IR study of hydrogen bonding in proteins, Kristof and Zundel¹³ observed the effect upon the S-H band of $(\text{L-Cys})_n$ ($n = 44$), of both adding salts and increasing the degree of

hydration. They found that upon addition of NEt_4OH to pure $(\text{L-Cys})_n$ a continuous absorption grows in the region $2600\text{-}1750\text{ cm}^{-1}$ with a ν_{max} at 2200 cm^{-1} . They interpret this as being due to the formation of very long, easily polarisable hydrogen bonds, i.e. $\text{SH}\text{---}\text{S}^- \rightleftharpoons \text{S}^-\text{---}\text{HS}$. This continuum replaces the stretching vibration at 2552 cm^{-1} which they assign to non-hydrogen-bonded SH groups.

The effect of increasing the degree of hydration was to break the $\text{SH}\text{---}\text{S}^- \rightleftharpoons \text{S}^-\text{---}\text{HS}$ bond and therefore increase the intensity of the band at 2552 cm^{-1} . They thus concluded that "*...these bonds can only be present in hydrophobic regions of proteins.*"

The assignment of the stretching vibration at 2552 cm^{-1} to non-hydrogen-bonded SH groups would, in the light of many IR studies of thiols which conclude that free SH groups have a stretching frequency of between 2590 and 2580 cm^{-1} , seem to be erroneous. However, the spectra are of dry films of $(\text{Cys})_n$ and therefore may not be comparable with spectra recorded in solutions.

From the above studies it is clear that there is a certain amount of ambiguity over the environment of SH groups responsible for absorptions in the $2550\text{-}2560\text{ cm}^{-1}$ region. Indeed, the question of whether hydrogen bonds are formed between thiol groups and water molecules is still unclear.

4.3 Experimental

4.3.1 Infra-red Spectra

IR spectra were recorded on a Perkin-Elmer 681 double beam spectrometer. Demountable cells with Teflon spacers and calcium fluoride plates were used for the sample solutions. In order to obtain the best baselines possible a separate spectrum was recorded of the reference solvent in the same cell as the sample spectrum had previously been recorded in. Both spectra were stored as data files on floppy disks, and a percentage of the reference spectrum was subtracted from the sample spectrum, such that a flat baseline resulted. For non-aqueous samples, cells with a pathlength of 1 mm were used, aqueous samples were recorded using cells with a 0.025 mm pathlength. Spectral band wavenumbers were measured using a peak finding routine in the computer software (see chapter 2).

4.3.2 Nuclear Magnetic Resonance Spectra

Spectra were recorded at 25°C. on a Bruker AM300 FT NMR spectrometer operating at 300.134 MHz. A dual-nuclear probehead with a 5 mm diameter probe was used. TMS was used as an internal reference.

4.3.3 First Overtone Near Infra-red Spectra

First overtone spectra were recorded on a Perkin-Elmer 340 spectrometer at 25°C. 0.5 mm pathlength cells were used, spectra being recorded against a reference cell containing pure water.

4.3.4 Purification of Materials

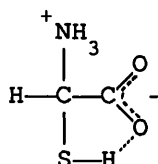
L-(+)-cysteine and 2-hydroxyethanethiol, used without further purification, were obtained from Aldrich Chemical Company Ltd. at

97% and 98% purity respectively. Water was deionised and then passed through a millipore 'Milli-P' system. Other solvents were purified by fractional distillation over CaH_2 and stored over CaH_2 or molecular sieves.

4.4 Results and Discussion

Figure 4.1 shows an IR spectrum of a 0.5 M aqueous solution of L-cysteine (pH = 6.4) in the sulphhydryl region, the peak having a ν_{max} at 2575 cm^{-1} . The spectrum is slightly complicated by a sloping baseline caused by the low frequency wing of the N-H stretching absorbance around 3300 cm^{-1} . A computer subtraction of this band was performed in order to obtain ν_{max} . The frequency observed is 7 cm^{-1} lower than that reported by Nakanishi *et al.* (2582 cm^{-1}). The spectrum recorded by Nakanishi *et al.* was of cysteine in an aqueous solution with a pH of 8.0. This may explain the difference in ν_{max} observed in the two systems.

It is concluded from the above result that some form of hydrogen bonding is taking place. Cysteine (I) has the capability to form intramolecular hydrogen bonds of the type shown and it may be that these are responsible for the observed shift in frequency of $\nu \text{ SH}$ from that of 'free' SH groups. However, for these hydrogen bonds to form hydrogen bonds between the carboxylate group and water must be broken.



(I)

Heating (figure 4.2) induces no significant changes in $\nu \text{ SH}$. It

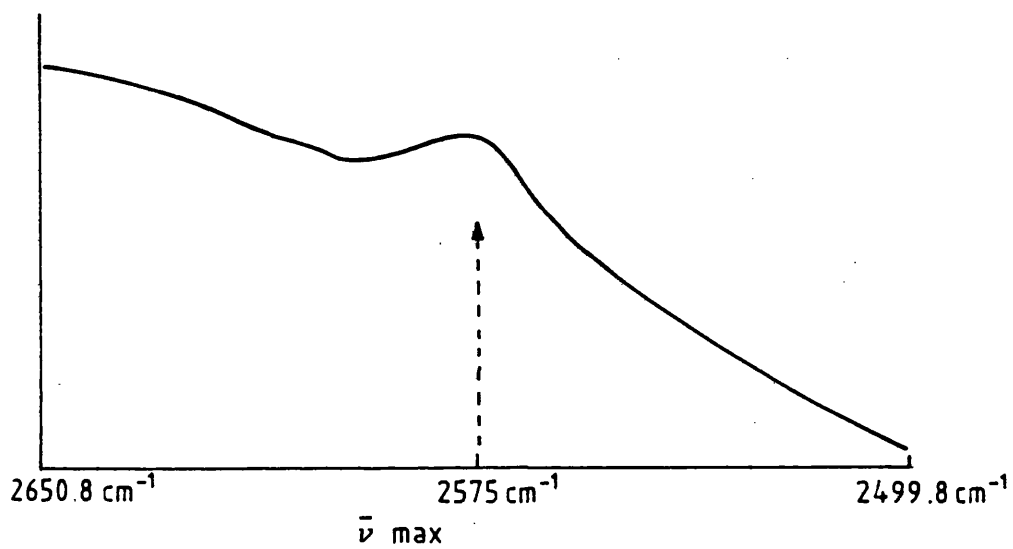


Fig. 4.1. Infrared spectrum of a 0.5M aqueous solution of (p.H. = 6.4) of L-Cysteine in the sulphydryl region.

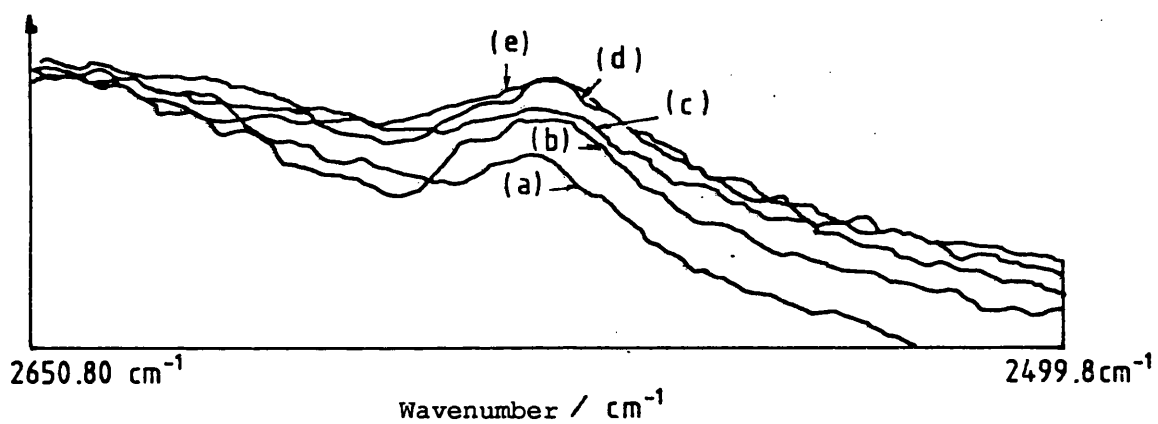
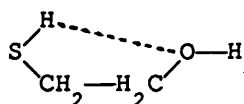


Fig. 4.2. Temperature dependency of the ν S-H band of a 0.3 M aqueous solution (p.H. = 6.4) of L-Cysteine. (a) 30°C., (b) 50°C., (c) 60°C., (d) 80°C., (e) 90°C.

was expected that if hydrogen bonding is present between water molecules and the SH group, heating would disrupt it and therefore ν SH would shift to a higher frequency. Why this might not be observed is discussed later.

2-hydroxyethanethiol (II) is likely ²⁸ to be able to form intramolecular hydrogen bonds of the type shown but it has the advantage of being soluble in a wider range of solvents than cysteine. It was therefore decided to concentrate upon this thiol for the remainder of the study.



(II)

Figures 4.3a, b and c, show spectra of increasingly concentrated solutions of 2-hydroxyethanethiol in CCl_4 in the ν SH region. In the most dilute solution ν_{max} occurs at 2592 cm^{-1} . As the concentration increases ν_{max} shifts to lower frequency, and when the concentration is 2.0 M it absorbs at 2577 cm^{-1} . These results suggest that as the concentration is increased, intermolecular hydrogen bonds are formed between thiol groups (III), or more probably, because of the greater donor/acceptor properties of OH groups, between thiol and hydroxy groups (IV). Both of these types of hydrogen bond have been shown to exist in other systems ¹⁴⁻¹⁷ by previous studies and it is likely that both exist in this system.

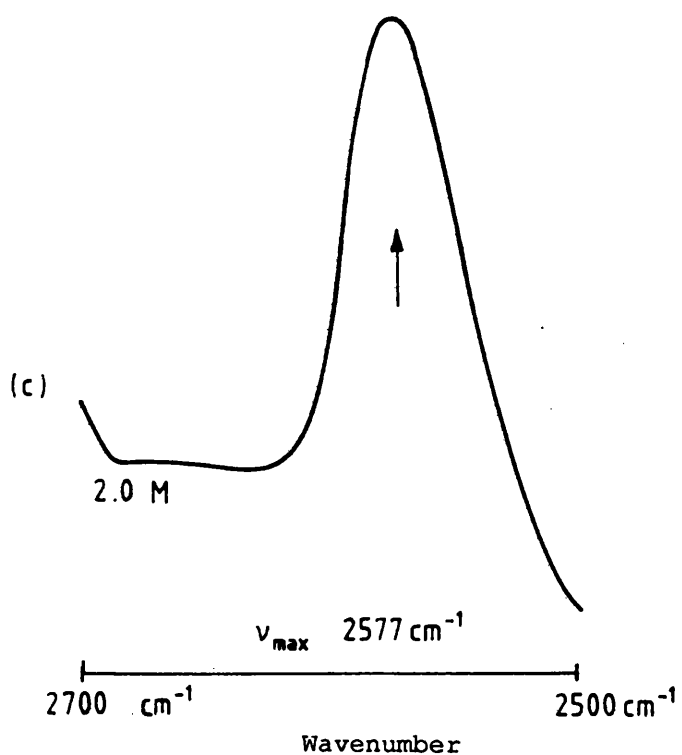
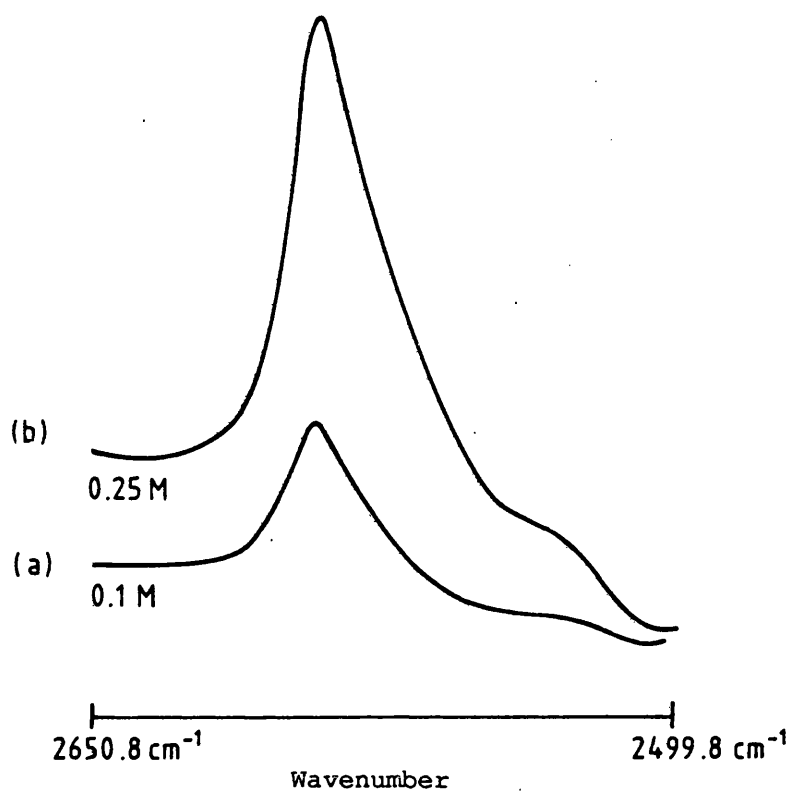
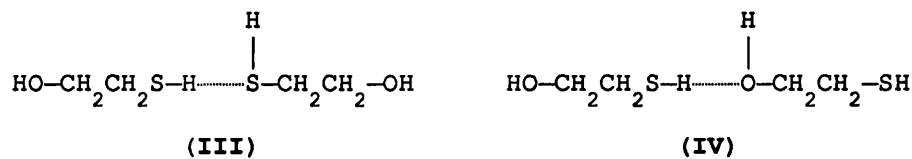


Fig. 4.3. Infrared spectra of solutions of 2-Hydroxyethanethiol in CCl_4 in the sulphhydryl stretching region. (a) 0.1M, (b) 0.25 M, (c) 2.0 M.



In order to probe the ability of sulphur to act as a proton acceptor it was decided to compare SH stretching frequencies in solutions of 2-hydroxyethanethiol in CCl_4 and chloroform (CHCl_3). CHCl_3 has an acidic proton with an acceptor number (AN) of 23.1 and, providing sulphur is capable of accepting a hydrogen bond, should be able to form a hydrogen bond with the sulphur atom. There are several examples in the literature of CHCl_3 being used as a probe in this way.

A 0.1 M solution of 2-hydroxyethanethiol in CHCl_3 gave the spectrum shown in figure 4.4, ν_{max} occurs at 2585 cm^{-1} which is 7 cm^{-1} lower than in CCl_4 (figure 4.3a). This is consistent with the formation of a hydrogen bond between sulphur and the acidic proton of CHCl_3 , which would be expected to strengthen intramolecular hydrogen bonding to the S-H bond.

The above findings are supported by a simple NMR experiment in which spectra of dilute solutions of 2-hydroxyethanethiol in CCl_4 and CHCl_3 were recorded and the chemical shift of the sulphydryl proton measured relative to that of an internal reference (TMS). The SH proton chemical shift was found to occur at 1.20 in CCl_4 and 1.39 in CHCl_3 . This downfield shift induced by CHCl_3 is explained by the sulphydryl proton being partially withdrawn from its electronic environment as a result of the S-H bond being weakened and therefore lengthened by a strengthening of the

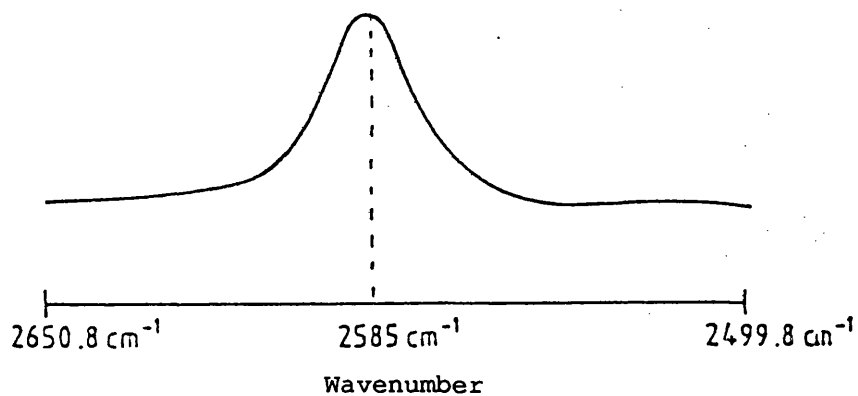


Fig. 4.4 Infrared spectrum of solutions of 0.1 M 2-hydroxyethanethiol in CHCl₃ in the sulphhydryl stretching region.

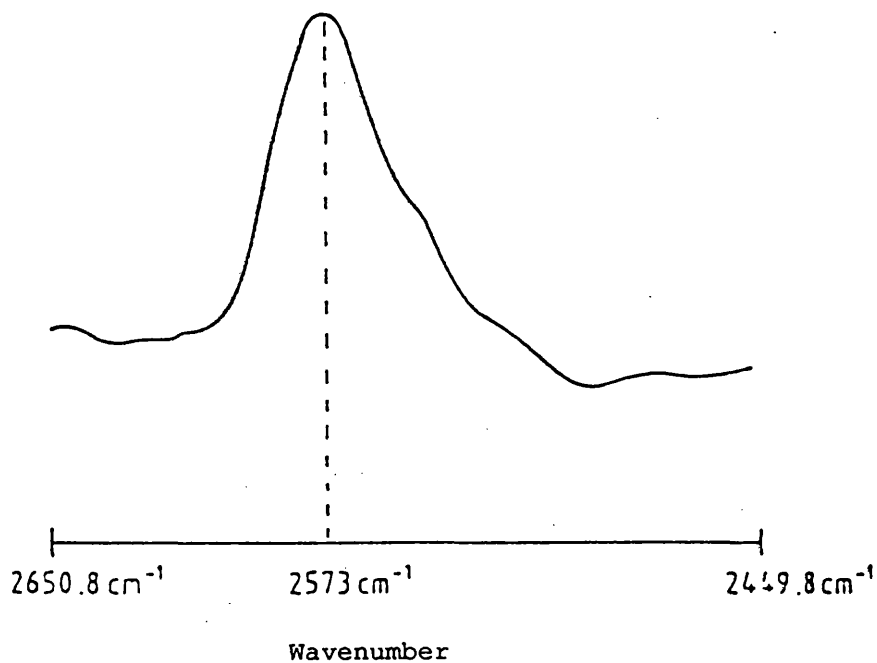


Fig. 4.5. Infrared spectrum of solutions of a 0.1 M aqueous solution of 2-hydroxyethanethiol in the sulphhydryl stretching region.

hydrogen bond between the proton of the thiol group and the oxygen of the hydroxyl group (II).

One of the greatest difficulties encountered when IR spectra of aqueous systems are attempted is the nature of the spectrum of water itself, which consists of broad and very intense absorption bands. The intensity of these bands is such that in order to obtain spectra it is necessary to use pathlengths no longer than 25 microns. Fortunately, ν SH occurs in a region which is a 'window' in the water spectrum. However, the weakness of its absorbance makes it necessary to accumulate spectra in order to obtain acceptable signal/noise levels.

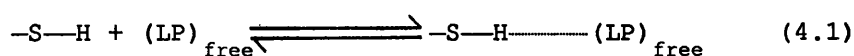
In the case of the variable temperature experiment, because the NaCl plates of the outer jacket also absorb a fraction of the beam, and more importantly tend to reflect a further fraction, it is necessary to use a higher thiol concentration than is ideal if solute-solute interactions are to be avoided. Having said this, although in CCl_4 solutions intermolecular hydrogen bonds are observed at 2.0 M concentration, there is much evidence to suggest that the high dielectric constant of water may effectively screen electrostatic interactions between 2-hydroxyethanethiol molecules thereby preventing aggregation from occurring. This should allow higher concentrations to be used without the complication of solute-solute hydrogen bonds having to be considered.

Figure 4.5 shows a spectrum of 1.0 M 2-hydroxyethanethiol in H_2O

which shows a ν_{max} at 2573 cm^{-1} . The extinction coefficient for $\nu \text{ SH}$ in H_2O is measured from figure 4.6 and found to be $84.2 \text{ mol}^{-1} \text{ dm}^2$. This compares with an extinction coefficient of $13.3 \text{ mol}^{-1} \text{ dm}^2$ in CCl_4 (figure 4.7). From previous studies^{11,12,25} it is clear that both the shift in frequency and increase in absorbance are consistent with hydrogen bond formation.

On heating, the $\nu \text{ SH}$ band of a 2.0 M 2-hydroxyethanethiol solution was found to shift towards lower frequency (figure 4.8). This is contrary to what had been anticipated. It had been thought that if the temperature is increased any hydrogen bonding between thiol groups and water would be weakened and ultimately broken, as in equilibrium (4.1). The effect of this would be to increase the strength of the S-H oscillator and therefore an increase in the frequency of $\nu \text{ SH}$; experimentally, the opposite is observed.

The observed spectral changes may be explained by taking into account the effect that heating has upon the structure of 'bulk'^{26,27} water. According to Symons, water may be described in terms of three species; $(\text{OH})_{\text{free}}$, Lone Pair $(\text{LP})_{\text{free}}$ and $(\text{OH})_{\text{bulk}}$. The former two of these are formed in equal concentration whenever a hydrogen bond is broken (equilibrium (4.2)) and are thought to be the reactive species responsible for solvating both electrolytes and non-electrolytes which interact with water. A more detailed description of this scheme is portrayed in chapter 1.



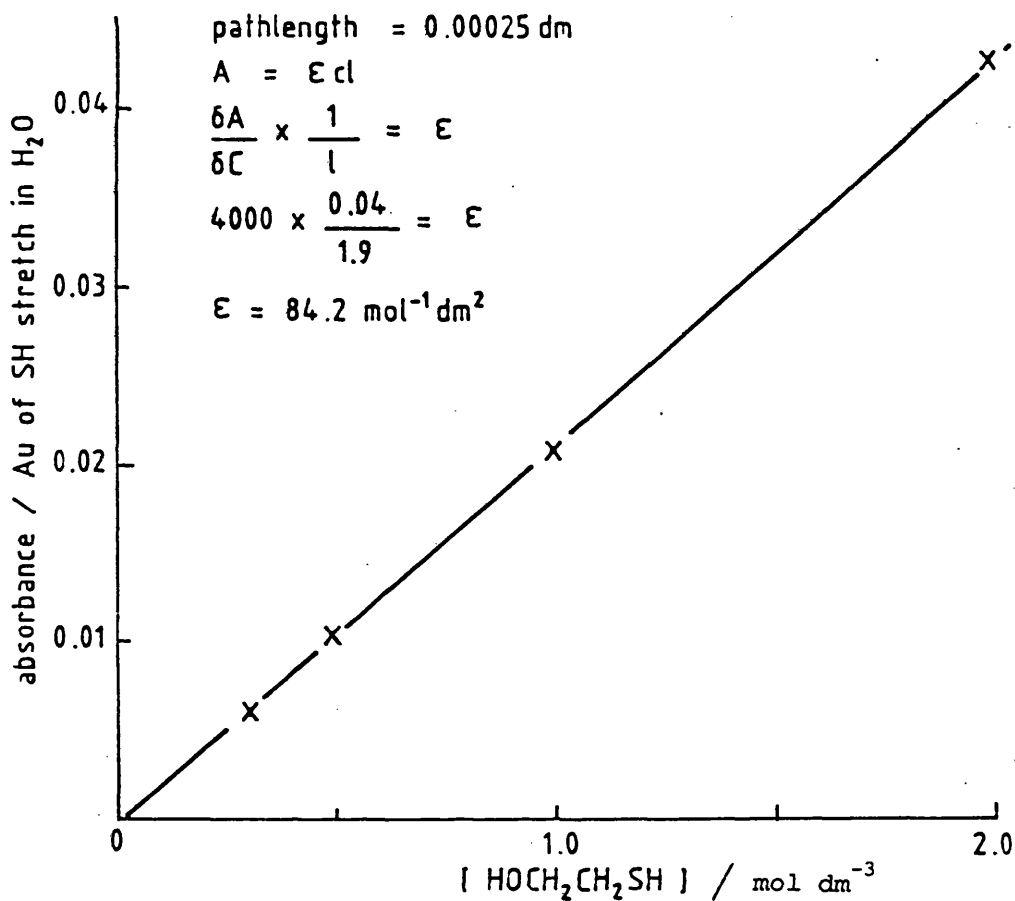


Fig. 4. 6. A Beer's law plot of the ν S-H band of aqueous solutions of 2-hydroxyethanethiol at 25° C.

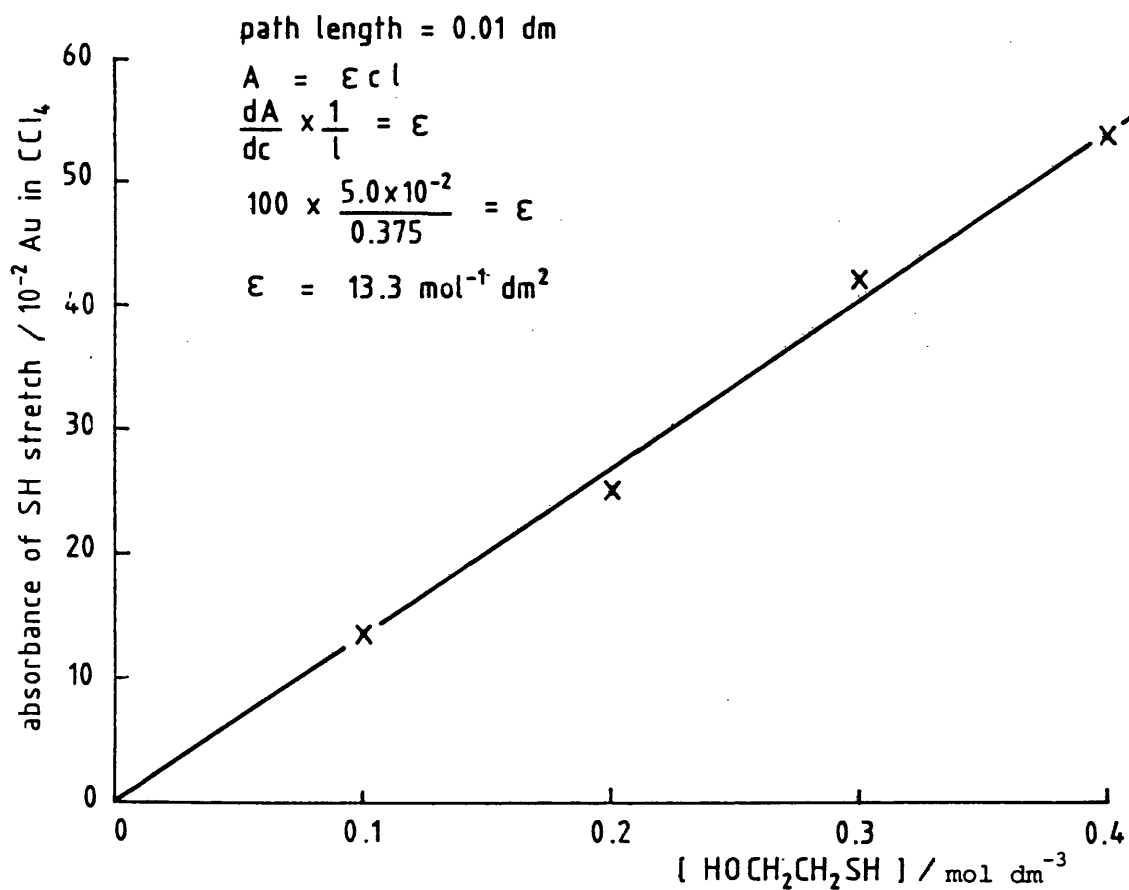


Fig. 4.7. A Beer's law plot of the ν S-H band of 2-hydroxyethanethiol in CCl_4 at 25°C .

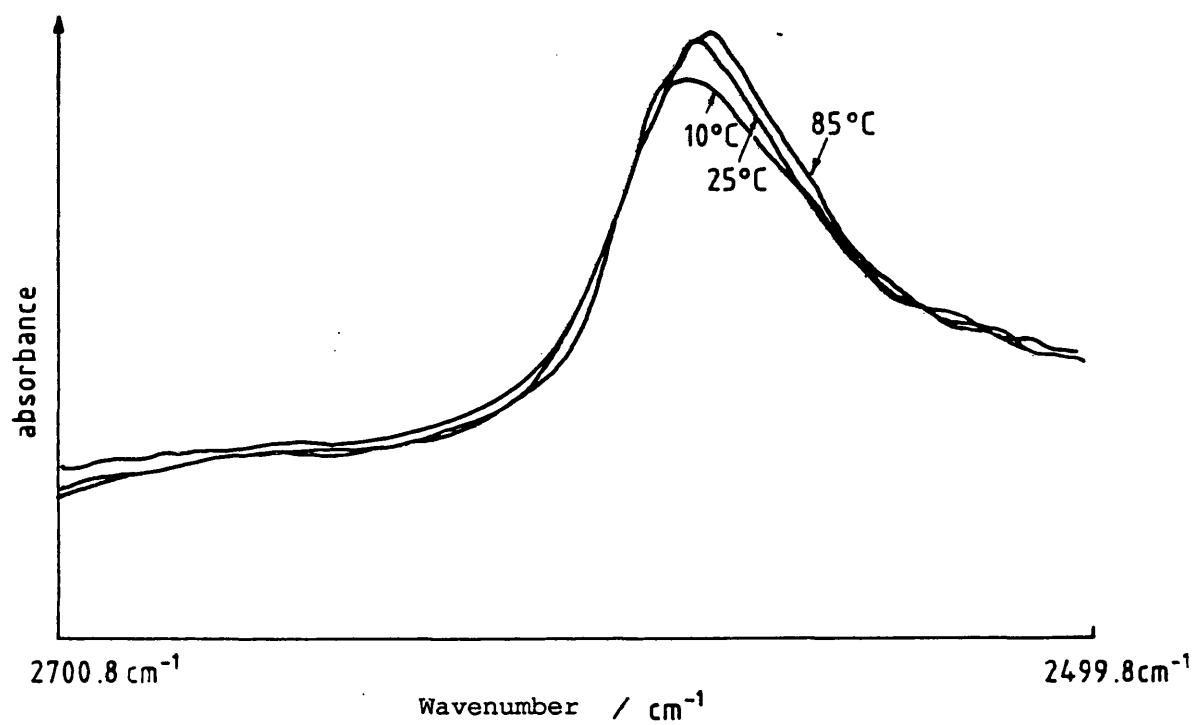


Fig. 4.8. Effect of temperature changes upon the sulphydryl stretching band of 2.0 M aqueous solutions of 2-hydroxyethanethiol.

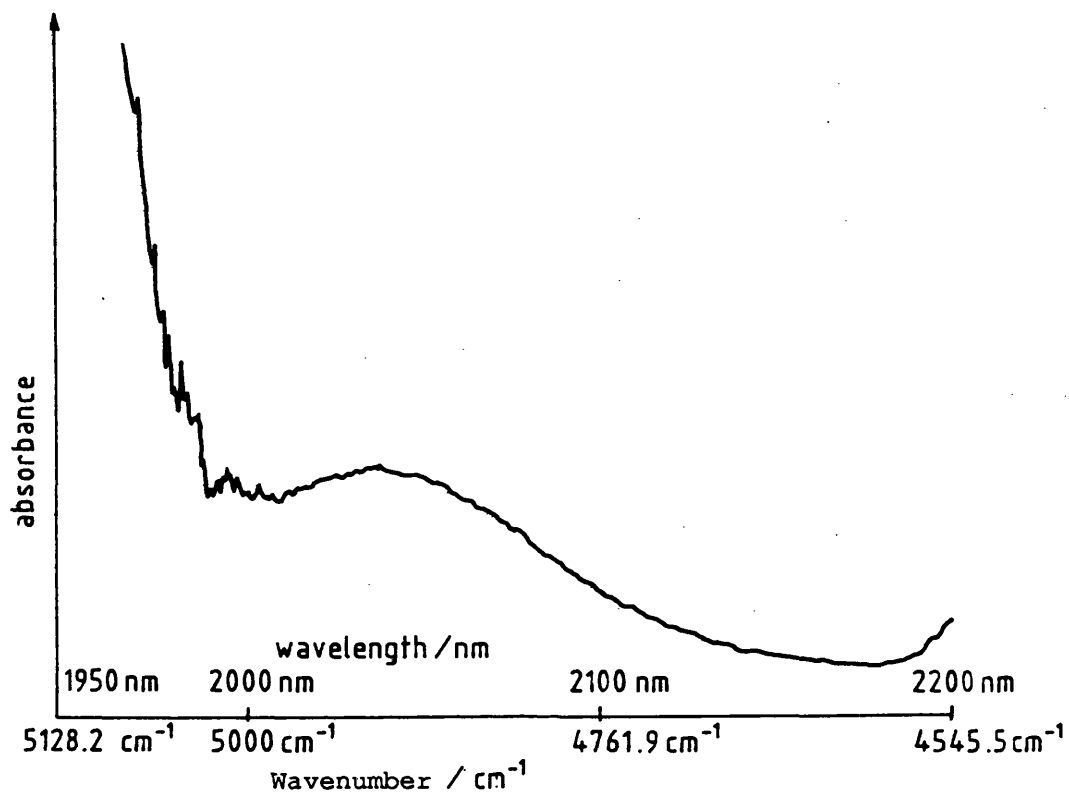


Fig. 4.9. Near infrared spectrum of a 0.5 M aqueous solution of 2-hydroxyethanethiol in 2 v S-H region.

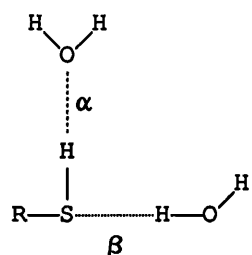
As the temperature is raised hydrogen bonds between water molecules are broken leading to increased concentrations of the reactive species $(OH)_{free}$ and $(LP)_{free}$ which in turn forces equilibrium (4.1) to the right hand side. Thus, by taking into account the effect that heating has upon both equilibria it is possible to rationalise the observed low frequency shift in ν SH.

Further evidence for hydrogen bonding between water and thiols is provided by the NIR spectrum of a 0.5 M aqueous solution of 2-hydroxyethanethiol in the 2ν SH region (figure 4.9). In this region there is no sign of a narrow band due to free SH groups which has been shown to absorb at 5056 cm^{-1} in pure EtSH. A broad band is observed with a ν_{max} around 4920 cm^{-1} which suggests¹² that all the thiol groups are participating in hydrogen bonds.

4.5 Concluding Remarks

The above results are consistent with hydrogen bonds (α) being formed between the SH group of 2-hydroxyethanethiol and the oxygen atom of water molecules. It is harder to prove whether or not a second hydrogen bond (β) is formed between water and the sulphur atom of thiols (ν). However, the fact that $CHCl_3$ lowers ν SH relative to the band in CCl_4 , coupled with the evidence of thiol dimer formation presented in chapter 3 and chemical shift data obtained in this study, shows that it is possible to form hydrogen bonds between sulphur and acidic protons. These results cast⁴⁻⁶ doubt over the assignment made by various workers, that Met is hydrophobic and incapable of forming hydrogen bonds with proton

donors.



It is difficult to see, bearing in mind these results, how the stretching vibration at 2552 cm^{-1} which Kristof and Zundel¹³ observed in (L-Cys)_n can be assigned correctly to 'non-hydrogen-bonded SH groups'. More likely, the band observed arises from SH groups which are hydrogen bonded to amide or carbonyl groups.⁸

The confusion which arises in the literature over the hydrophobicity of thiol residues in proteins and other systems, may be clarified simply by explaining that although thiol groups tend to be situated in hydrophobic regions of proteins, the SH group itself is not hydrophobic.

References for chapter 4

1. T. G. Heafield, G. Hopkins and L. Hunter, *Nature* 149, 218 (1942).
2. Auwers, *Z. Phys. Chem.* 30, 529 (1899).
3. G. C. Pimentel and A. L. McClellan, *The Hydrogen Bond*, W. H. Freeman, San Francisco, (1960), p 201.
4. S. N. Vinogradov and R. H. Linnell, *Hydrogen Bonding*, Van Nostrand Reinhold, New York, (1971), p 234.
5. Y. Nozaki and C. Tanford, *J. Biol. Chem.* 246, 2211 (1971).
6. M. I. Kanehisa and T. Y. Tsong, *Biopolymers* 19, 1617 (1980).
7. G. H. Bare, J. O. Alben and P. A. Bromberg, *Biochemistry* 14, 1578 (1975).
8. J. O. Alben, G. H. Bare and P. A. Bromberg, *Nature* 252, 736 (1974).
9. J. O. Alben and G. H. Bare, *J. Biol. Chem.* 255, 3892 (1980).
10. M. Nakanishi, T. Yamada, H. Shimizu and M. Tsuboi, *Bioc. Biop. Acta* 671, 99 (1981).
11. R. A. Spurr and H. F. Byers, *J. Phys. Chem.* 62, 425 (1958).
12. R. Bicca de Alencastro and C. Sandorfy, *Can. J. Chem.* 50, 3594 (1972).
13. W. Kristof and G. Zundel, *Biopolymers* 19, 1753 (1980).
14. M. M. Rousselot, *Comp. Rend. Acad. Sc. Paris Ser.C* 262, 26 (1966).
15. M. M. Rousselot and M. Martin, *ibid.* 262, 1445 (1966).
16. M. M. Rousselot, *ibid.* 263, 649 (1966).
17. M. O. Bulanin, G. S. Denisov and R. A. Pushkina, *Opt. i. Spectroskopiya* 6, 491 (1959).
18. V. Guttman, *The Donor-Acceptor Approach to Molecular*

Interactions, Plenum Press, New York, (1978).

19. S. Hahn, W. M. Miller, R. N. Lichtenthaler and J. M. Prausnitz, *J. Solution Chem.* 14, 129 (1985).
20. L. Lunazzi and F. Taddei, *Spectrochim. Acta* 24A, 1479 (1968).
21. P. Biscarini, L. Lunazzi and F. Taddei, *Boll. Sci. Fac. Chim. Ind. Bologna* 22, 67 (1964).
22. S. H. Marcus and S. I. Miller, *J. Am. Chem. Soc.* 88, 3719 (1966).
23. S. Bone and R. Pethig, *J. Mol. Biol.* 181, 323 (1985).
24. S. Bone, *Bioc. Biop. Acta* 916, 128 (1987).
25. A. Burneau, J. Limouzi, E. Marechal, J. Perchard and G. Zuppiroli, *Mol. Phys.* 41, 1373 (1980).
26. M. C. R. Symons, *Acc. Chem. Res.* 14, 179 (1981).
27. M. C. R. Symons, In *Water and Aqueous Solutions*, (ed. G. W. Neilson and J. E. Enderby), Bristol, Adam Hilger, p.41 (1986).

Chapter 5

*Solvent and Salt
Effects upon the
Dimethylphosphate and
Dimethylthiophosphate
Anions.*

5.1 Introduction

In this study ion-pairing between metal ions and the dimethylphosphate anion was investigated, principally using infra-red (IR) spectroscopy. The resulting spectra were then analysed and the conclusions compared with those of previous ³¹P nuclear magnetic resonance (NMR) and theoretical studies.

5.2 Previous Work

It is becoming apparent that hydration and cation binding play a central role in the determination of nucleic acid structures¹⁻⁵, and therefore, affect such nucleic acid functions as transcription and translation. It was determined relatively early on that the phosphate group interactions dominate both the hydration of, and binding of metal cations to, nucleic acids.

Falk, Hartman and Lord in an IR study of deoxyribonucleic acid concluded that each phosphate group is hydrated by up to six water molecules⁶. When this result is put into the context of their gravimetric studies⁷ which showed that between twenty and twenty four water molecules hydrate each base pair of calf thymus DNA, it can be seen quite how dominant the role of the phosphate group is in hydration of DNA.

Although there have been several studies investigating metal binding to nucleotides⁸⁻¹¹, the exact nature and site of such binding is still open to debate. Haake and Prigodich⁸, reported a method for the determination of phosphate anion - cation association constants from ³¹P chemical shifts. This utilised

equation (5.1);

$$K = \frac{C}{(P - C) M} = \frac{1}{(P/C - 1) M} \quad (5.1)$$

Where: K - Association constant

C - Concentration of cation - phosphate complex

P - Total phosphate anion concentration

M - Total cation concentration

when the total cation concentration is much larger than the total phosphate concentration, the free cation concentration can be approximated to the total cation concentration.

As they found only a single sharp ^{31}P resonance for any of the phosphates studied, cation exchange was fast on the NMR timescale. Therefore, the chemical shift data could be related to the variable (P/C);

$$\delta_{\text{obs}} = \frac{C}{P} \delta_{\text{C}} + \frac{P - C}{P} \delta_{\text{P}} \quad (5.2)$$

$$\frac{P}{C} = \frac{\delta_{\text{C}} - \delta_{\text{P}}}{\delta_{\text{obs}} - \delta_{\text{P}}} = \frac{\Delta\delta_{\text{max}}}{\Delta\delta_{\text{obs}}} \quad (5.3)$$

Where: δ_{obs} - Observed chemical shift of phosphate anion

δ_{C} - Chemical shift of the complex

δ_{P} - Chemical shift of the uncomplexed anion

This can then be substituted into equation (5.1) and rearranged to give;

$$\frac{1}{\Delta\delta_{\text{obs}}} = \frac{1}{K \Delta\delta_{\text{max}}} \left(\frac{1}{M} \right) + \frac{1}{\Delta\delta_{\text{max}}} \quad (5.4)$$

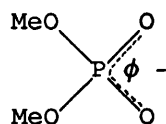
which is an equation of the form $y = mx + c$, where $1 / \delta_{\text{obs}}$ is a

function of $1 / M$. Thus K was found, the values obtained are presented in table 5.1 along with those calculated by other workers.

They concluded that their "...NMR method is revealing inner-sphere complexation." This conclusion was drawn from the effects that individual cations had upon the direction of change in chemical shift. They observed that $(\text{CH}_3)_4\text{N}^+$, Mg^{2+} and Ca^{2+} cause upfield shifts, whilst monocations such as Li^+ , Na^+ and K^+ , induce downfield shifts. In explaining these observations they referred to the relationship between bond angle and chemical shift proposed by Gorenstein^{12,13}.

Gorenstein¹² compiled almost all the X-ray crystallographic data then available on phosphates for which a ^{31}P chemical shift was known. The O-P-O angle between the two phosphate oxygen atoms which are either protonated or esterified was then plotted against the chemical shift (see figure 5.3).

The data shows that for acyclic monophosphates, as the RO-P-OR bond angle increases so the chemical shift moves upfield. Haake and Prigodich⁸ refer, not to changes in the O-P-O angle between the esterified oxygens, but rather the O-P-O angle between the anionic oxygens (ϕ). They then assume that an increase in the RO-P-OR bond angle will result in a decrease in ϕ (see scheme I).



(I)

Table 5.1

<u>Reference</u>	<u>Anion</u>	<u>Cation</u>	<u>Association Constant / M⁻¹</u>
8	(CH ₃ O) ₂ PO ₂ ⁻	Mg ²⁺	3.6 (0.1)
	"	Ca ²⁺	4 (1)
	"	Li ⁺	0.22 (0.02)
	"	Na ⁺	0.29 (0.02)
	"	K ⁺	0.15 (0.03)
23	(CH ₃ O) ₂ PO ₂ ⁻	Mg ²⁺	6
24	H ₂ PO ₄ ⁻	Ca ²⁺	11.9 (0.6)

standard deviations are in parentheses.

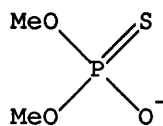
Using these relationships, Haake and Prigodich explain the upfield shifts caused by Ca^{2+} and Mg^{2+} , as being due to the formation of strong electrostatic interactions with the anionic oxygens and a resulting compression of ϕ . The upfield shift which results from the addition of the $(\text{CH}_3)_4\text{N}^+$ ion is due to decrease in ϕ . This is explained in terms of an increase in the strength of hydrogen bonding in the solvation shell of the phosphate. This being a consequence of the 'iceberg'¹⁴ effect. The downfield shifts caused by the addition of Li^+ , K^+ and Na^+ are rationalised by considering the formation of an inner-sphere complex between the monocation and the phosphate anion, which thereby disrupts the solvation of the anionic oxygens by water molecules. This leads to an increase in the ionisation of the anionic oxygens and therefore to increased repulsive forces between them with a corresponding increase in ϕ .

Using SFC ab initio calculations Berthod and Pullman investigated direct and through-water (solvent-separated/shared) interactions between Na^+ and DMP^- and found that "...The binding energy found (solvent-shared) is sufficiently close to the energy of direct binding to indicate that the binding of the cation through a molecule of water has an appreciable probability to occur."

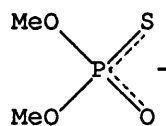
In this laboratory Patel investigated solvation of DMP^- , monomethylphosphate (MMP^-) and DMSP^- using the technique of IR spectroscopy. In his conclusions he reported that DMP^- is solvated by five or six water molecules in the primary solvation

shell. In methanolic solutions the primary solvation shell consist of five methanol molecules. These conclusions are lent theoretical support by Langlet ¹⁷ et al. who reach the same conclusion as to the number of water molecules in the primary shell. This figure is the same as that reached by Falk, Hartman ⁶ and Lord for the hydration of the phosphate group in DNA.

¹⁶ Patel also concluded that DMSP^- is solvated by up to three water molecules at the anionic oxygen, though he was not able to comment upon solvation which may occur at sulphur because of difficulties posed by solvent bands which mask the $\nu\text{P-S}$ band. The question of bond order and charge localisation in nucleoside phosphorothioates, was the subject of a thorough review by Frey and Sammons ¹⁸. They concluded that the weight of the evidence did not support the commonly held belief that the $\nu\text{P-O}$ and $\nu\text{P-S}$ bond orders in thiophosphate anions, are 1 and 2 respectively, with the bulk of the anionic charge centred on the oxygen (as represented in structure (II)). They suggested that the $^{31}\text{P}-^{17}\text{O}$ coupling constants ¹⁹ for thiophosphate diester monoanions were consistent with structures having P-O and P-S bond orders closer to 1.5, structure (III).



(II)



(III)

¹⁶ Patel also reported the effects that the addition of dications have upon the P-O stretching vibrations of DMP^- and DMSP^- in solutions of water, methanol and dimethylsulphoxide (DMSO),

however he was not able to offer any detailed explanations for the observed high frequency shifts in the ν_3 P-O vibration of DMP^- in solutions of methanol and DMSO. The main conclusion from the study was that *"...in aqueous solutions, solvent-separated ion-pairs are the favourable species."* This conclusion would appear to be in direct contradiction with that reached by Haake and Prigodich⁸ using their ^{31}P NMR method.

It is in view of this apparent contradiction that further work has been undertaken into metal binding to phosphate and thiophosphate monoanions. The results of which are reported and discussed herein.

5.3 Results and Discussion

5.3.1 Solvation of the Dimethylthiophosphate Anion

¹⁶Patel reported that DMSP^- is solvated by up to three water molecules around the anionic oxygen. However, he felt unable to comment upon the the possibility of further solvation occurring at sulphur. He was not able obtain IR spectra in the $\nu\text{P-S}$ ($850\text{-}700\text{ cm}^{-1}$) region. The main obstacles to recording spectra in this region are solvent absorbance bands which overlap, and therefore mask, the very weak $\nu\text{P-S}$ absorbance. This hindrance was overcome by using combinations of the following three 'tricks':-

- i) MeOD and D_2O were found to be more transparent in the $\nu\text{P-S}$ region and therefore, were used as solvents in place of methanol and water.

- ii) The signal to noise ratio of the spectra was improved by averaging several (typically eight) recordings.
- iii) Small differences in the sample and reference cells were corrected for using computer subtraction techniques.

Figures 5.1a, b and c show the IR spectra ($850-700\text{ cm}^{-1}$) obtained for DMSP^- in D_2O , MeOD and DMSO respectively. Each spectrum shows two broad overlapping bands which subsequently were partially resolved with the aid of a computer. The frequency of band (A), ca. 768 cm^{-1} , is insensitive to changes in solvent, whereas band (B) varies in frequency from 814 cm^{-1} in D_2O through to 748 cm^{-1} in DMSO, figure 5.2. It would appear therefore, that band (B) is due to the P-S stretch. The fact that a high frequency shift accompanies the change of solvent from the aprotic (non-hydrogen bonding) DMSO to protic (hydrogen bonding) MeOD and D_2O , can be rationalised in the following manner.

Hydrogen bonds which are formed by MeOD and D_2O to the P-O bond withdraw negative charge from the P-O bond which in turn withdraws negative charge from the P-S bond thereby decreasing the anionic character at sulphur. This leads to a strengthening of the P-S bond and therefore a high frequency shift in the P-S stretch, as observed. If there had been hydrogen bonding directly to sulphur the P-S stretch would have shifted to lower frequency.

Another observation which supports the above conclusion, is that

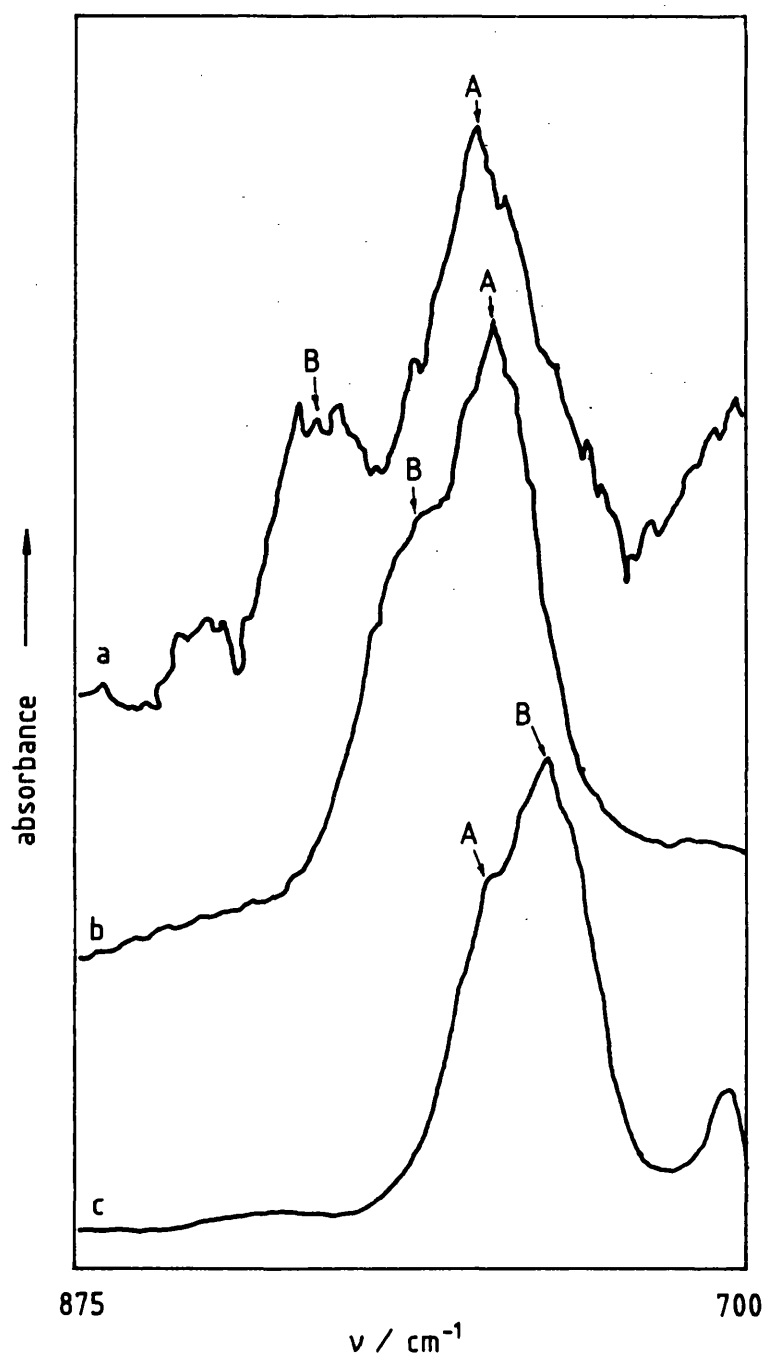


Figure 5.1.

Infrared spectra of NaDMSP solutions in the $\nu\text{P-S}$ region.
(a) D_2O , (b) MeOD and (c) DMSO.

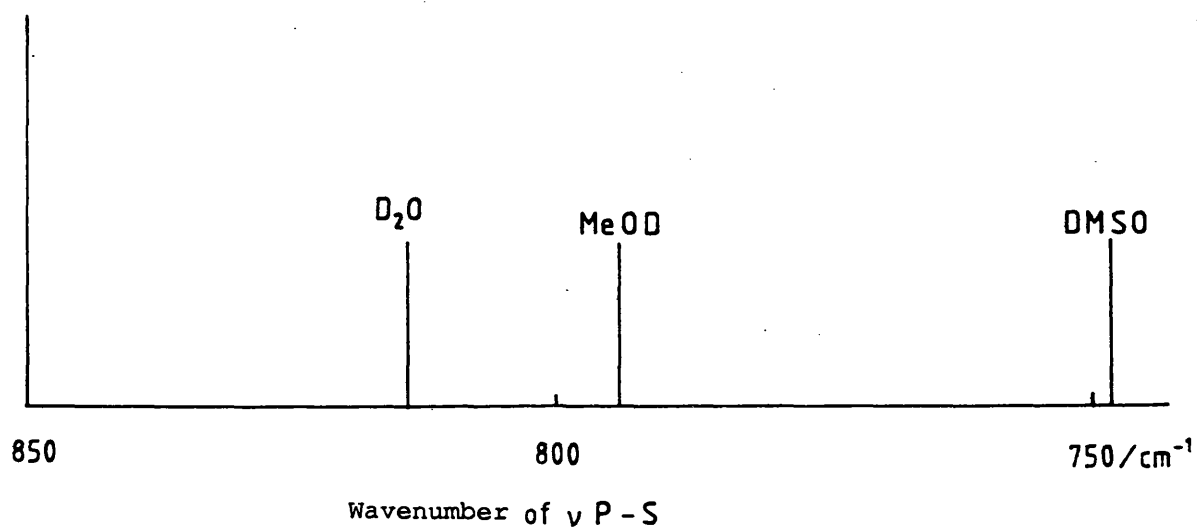


Figure 5.2.

Diagram showing the frequency of the ν P-S band of NaDMSP in DMSO, MeOD and D₂O. Curve analysis techniques were used to resolve the overlapping bands.

intensity of the $\nu_{\text{P-S}}$ band increases relative to band (A) in the order; $\text{D}_2\text{O} < \text{MeOD} < \text{DMSO}$. Since intensity of IR bands depends on the degree of bond polarisation, this observation indicates that the P-S bond is polarised to a greater extent in DMSO than in the protic solvent. This would not be expected if hydrogen bonds are formed to sulphur.

5.3.2 Metal Binding to Dimethylthiophosphate and Dimethylphosphate Anions

In principle there are at least two distinct types of ion-pair interactions:-

- a) the 'solvent separated' or 'outer sphere' ion-pair, in which the ions are separated by one or more layers of solvent molecules.
- b) the 'contact' or 'inner sphere' ion-pair in which the ions are in direct contact with each other.

In order to be able to understand the complicated and apparently anomalous high frequency shifts which dications induce in the $\nu_3\text{P-O}$ stretching band of DMP^- in solutions of methanol and DMSO, it was found to be helpful to look first at the factors which may affect the stretching frequency. These factors can be split into three main groups:-

- i) Solvation / Desolvation - the degree to which the P-O bond(s) are solvated has been shown to alter the $\nu_3\text{P-O}$ stretching

frequency. The addition of dications may affect the level of solvation.

- ii) Degree of Coupling - the extent to which the ν_3 P-O and ν_1 P-O stretching vibrations are coupled affects their vibrational frequencies. Changes in induced by metal binding are likely to affect the degree of coupling, and therefore, the ν_3 P-O stretching frequency.
- iii) Metal Ion Interactions - the electrostatic interaction between metal dications and the phosphate group will have an effect upon P-O bond strength, possibly resulting in a change in the ν_3 P-O stretching frequency.

Having identified the factors which can affect the IR spectra of phosphates and thiophosphates, it is then necessary to determine which of them apply for each individual anion-cation-solvent system. Table 5.2 shows which factors might apply for each system upon addition of dications.

From table 5.2 it is clear that effect of dications upon the $\text{DMSP}^- / \text{DMSO}$ system should have the least complicated spectral changes, and for this reason it was chosen as the first system to be studied.

Table 5.2

<u>System</u>	<u>Coupling</u>	<u>Desolvation</u>	<u>Mono/Bidentate</u>
DMSP ⁻ /DMSO	No	No	No
DMSP ⁻ /MeOH	No	Yes	No
DMSP ⁻ /H ₂ O	No	Yes	No
DMP ⁻ /DMSO	Yes	No	Yes
DMP ⁻ /MeOH	Yes	Yes	Yes
DMP ⁻ /H ₂ O	Yes	Yes	Yes

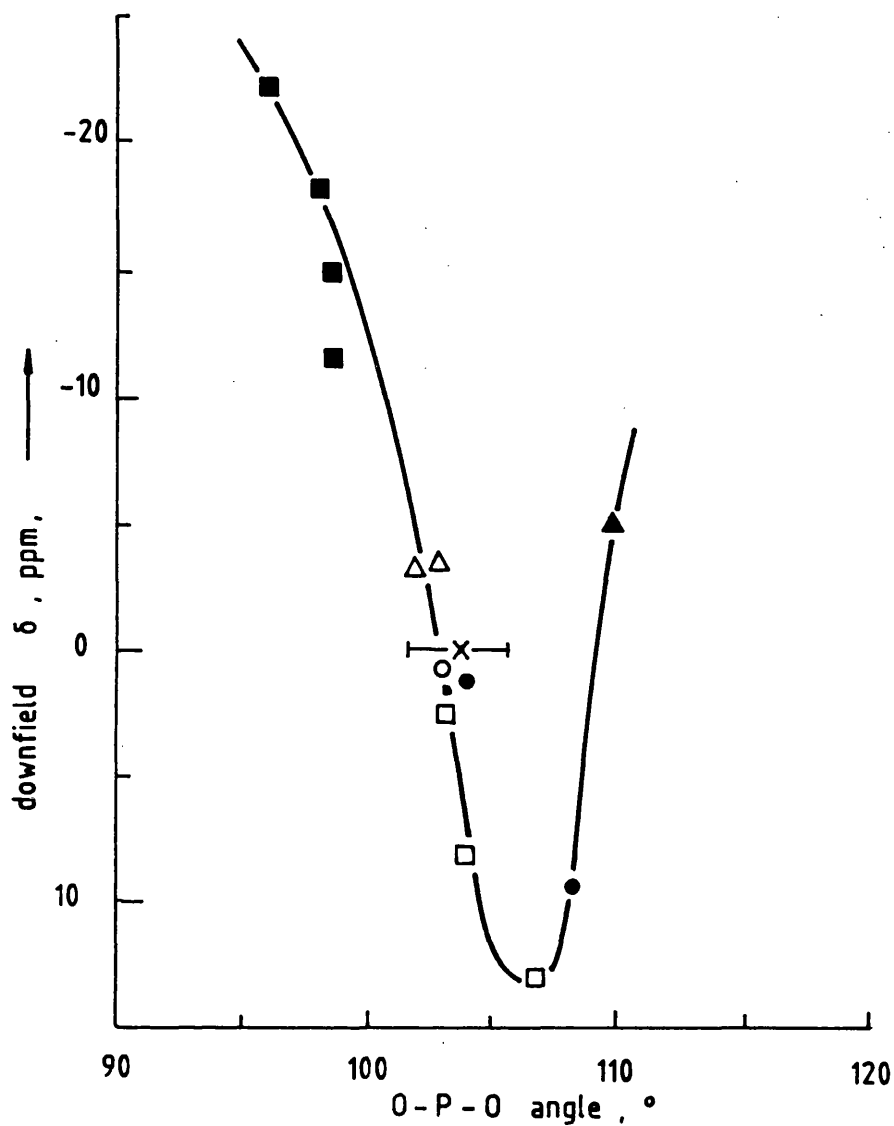
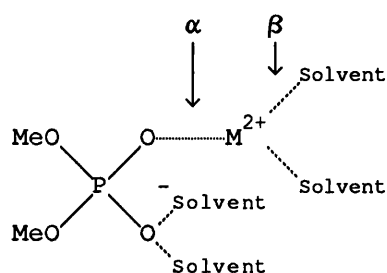


Figure 5.3.

^{31}P chemical shifts of phosphate esters versus the O -P-O bond angle between the esterified or protonated oxygen atoms.¹²
 (■, five-membered cyclic esters : △, monoester dianions : X, monoester monoanions : ○, acyclic diester monoanions : ●, acyclic diester acids : □, six-membered cyclic esters : ▲, Li_3PO_4).

The spectrum obtained from a solution of DMSP^- in DMSO is shown in figure 5.4a, from this it can be seen that the P-O stretch occurs at 1185 cm^{-1} . Upon addition of Mg^{2+} and Ca^{2+} this stretch shifts to 1180 cm^{-1} and 1162 cm^{-1} , respectively (see figures 5.4b and c). Thus, it can be seen that metal ions do induce low frequency shifts in the P-O stretch in the absence of any complicating factors, such as solvation / desolvation or, in DMP^- , changes in the degree of coupling. It is interesting to note that Ca^{2+} induces a greater shift in frequency than Mg^{2+} . This suggests that Ca^{2+} binds to DMSP^- more strongly than does Mg^{2+} . This conclusion is not shared by Pullman et al.²¹ whose theoretical studies led them to conclude that "The order of the binding energy is $\text{Mg}^{2+} > \text{Ca}^{2+} \dots$ ". One explanation for these differing conclusions may be the effect of solvent molecules upon dications, a factor which is not taken into account in the theoretical studies. This effect, the opposite of cooperativity, is illustrated below;



The effect of interaction (β) is to weaken the anion-cation interaction (α). Therefore if Ca^{2+} is less strongly solvated than Mg^{2+} , this will have the effect of strengthening the Ca^{2+} - anion interaction relative to the corresponding Mg^{2+} - anion interaction. This may be sufficient to reverse the normal trends observed upon increasing atomic weight.

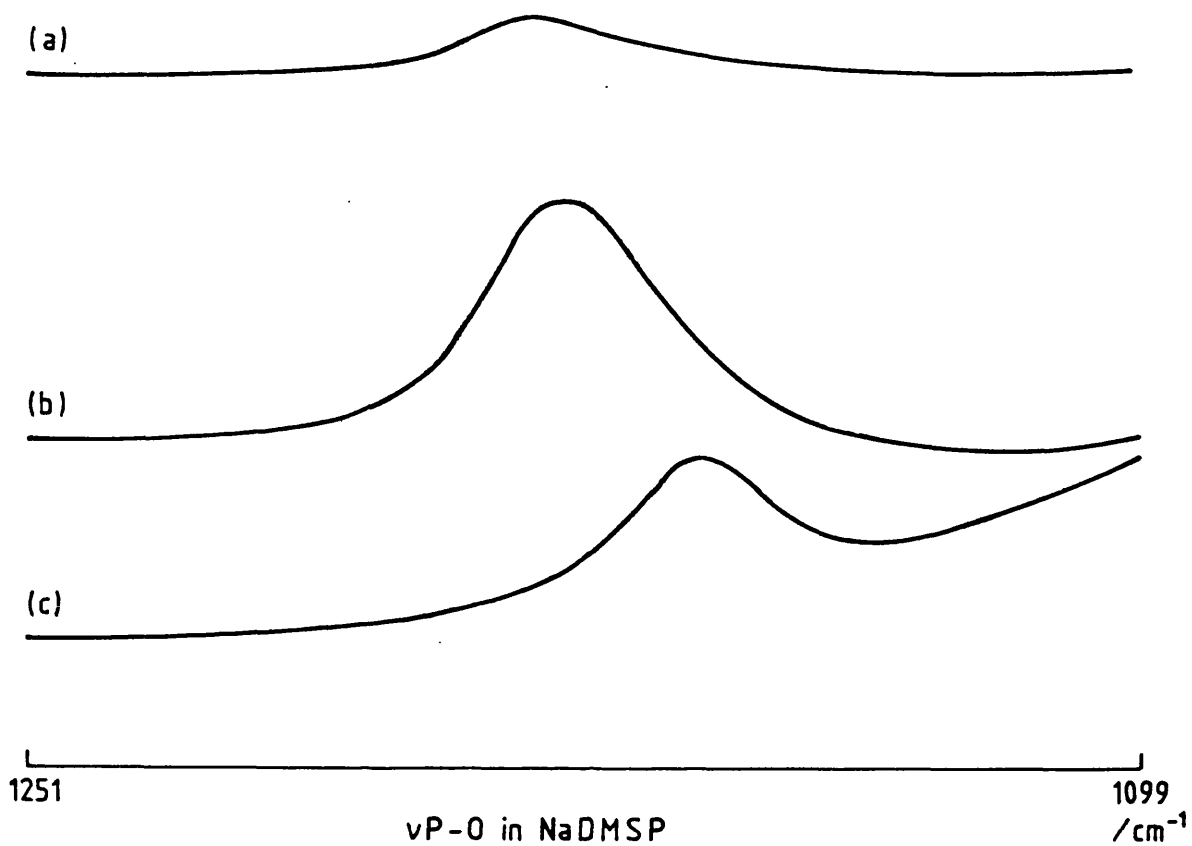
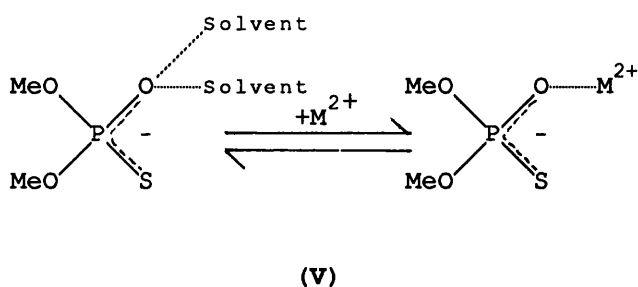
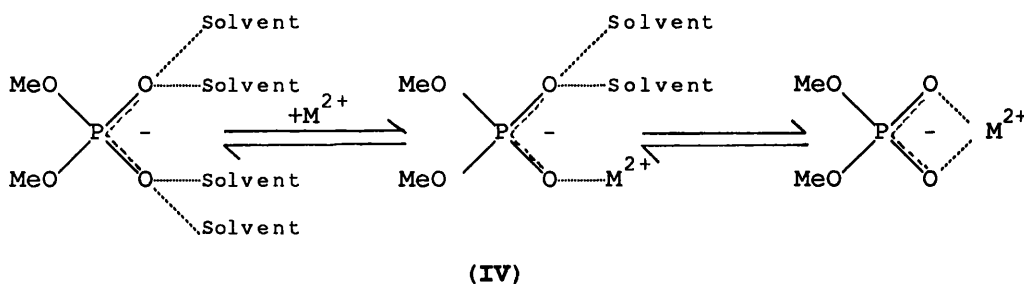


Figure 5.4.

Effect upon the infrared spectrum of NaDMSP (ν P-O region) of the addition of divalent cations. (a) No added salt, (b) + $\text{Mg}(\text{ClO}_4)_2$ and (c) + $\text{Ca}(\text{ClO}_4)_2$. Solvent = DMSO.

The $\text{DMSP}^- / \text{MeOH} / \text{dication}$ system was studied next. Figure 5.5a shows the spectrum obtained from a solution of DMSP^- in MeOH. The effect of Mg^{2+} and Ca^{2+} upon the spectrum is shown in figures 5.5b and c. In this system the effect dications have upon the P-O stretch is different to that observed in DMSO, the P-O stretch is shifted to higher frequency. The frequencies of these new bands are almost identical to those of the respective stretches in DMSO, suggesting that the same type of ion-pair might be formed in both systems. The high frequency shift in P-O stretch which is observed in MeOH solutions can be explained by desolvation, which would have to occur in order to form a contact ion-pair, as is now proposed (see scheme IV and V).



Systems containing the DMP^- anion are all complicated by the effect that ion-pairing may have upon bond angle, and therefore, the degree of coupling between the $\nu_3\text{P-O}$ and $\nu_1\text{P-O}$ stretching modes. The effect of changes in bond angle upon coupling between

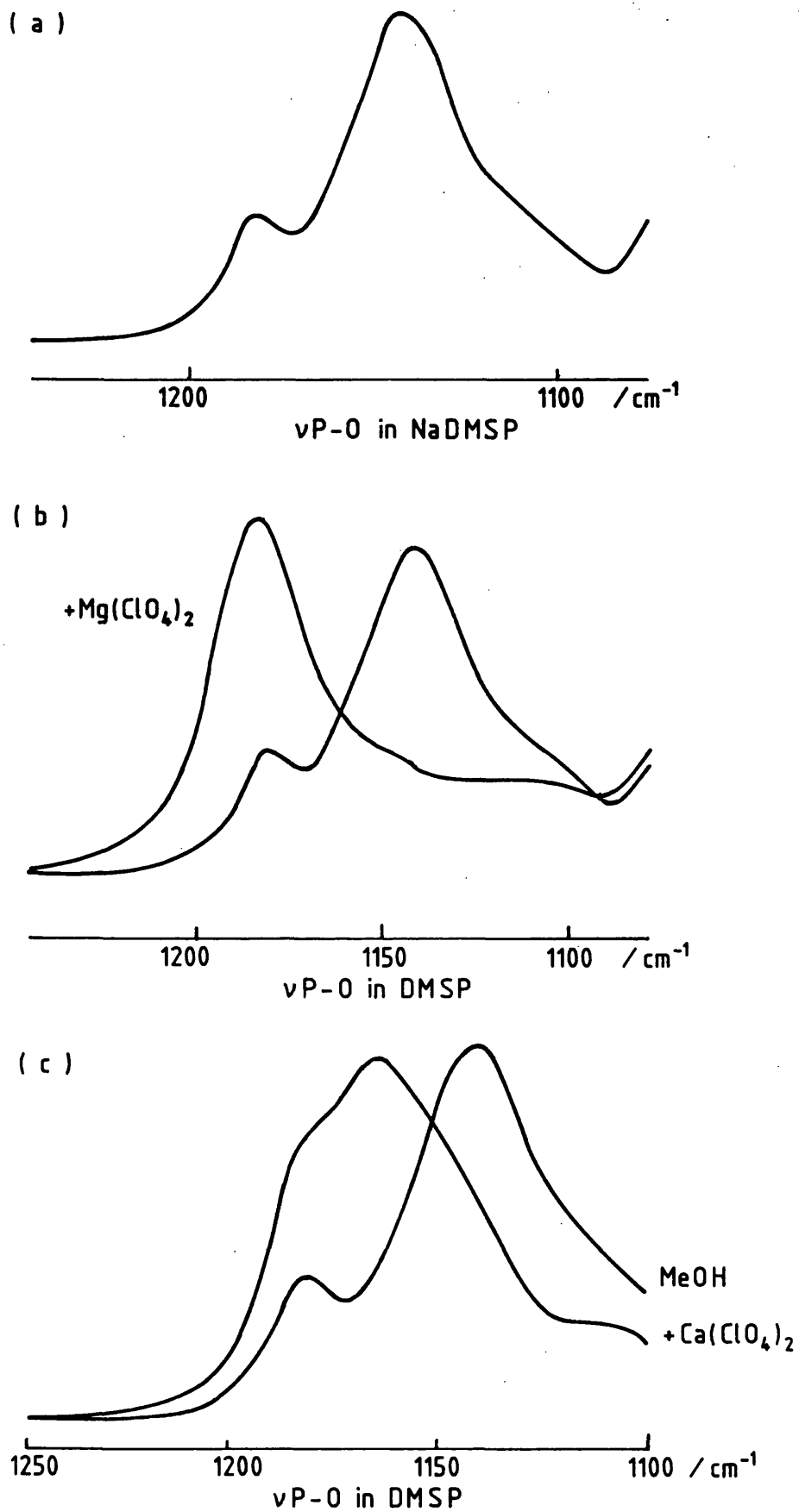


Figure 5.5. Effect upon the infrared spectrum of NaDMSP in MeOH (vP-O region) of the addition of divalent cations. (a) No added salt, (b) + Mg(ClO₄)₂ and (c) + Ca(ClO₄)₂.

the ν_s O-H and ν_{as} O-H stretching modes of solutions of H₂O in tetrachloromethane (CCl₄) was investigated by Bellamy, Blandamer, Symons and Waddington²². They concluded that as the H-O-H bond angle approaches 90°, so vibrational coupling between the ν_s and ν_{as} modes tends towards zero.

The spectrum of DMP⁻ in DMSO is shown in figure 5.6a. ν_3 P-O absorbs at 1253 cm⁻¹ the band is virtually symmetrical and, relative to the same band in H₂O and MeOH solutions, narrow. This points to an absence of strong solvent-anion interaction. As additions of Mg²⁺ and Ca²⁺ are made the ν_3 P-O stretch shifts to 1285 and 1259 cm⁻¹ respectively. This high frequency shift must be in some way related to a change in the degree of coupling between the ν_3 P-O and ν_1 P-O modes (the corresponding shifts for the DMSP⁻/DMSO systems are to lower wavenumber). The fact that the ν_3 P-O is shifting to higher frequencies upon additions of dications suggests there is an increase in the degree of coupling between ν_3 P-O and ν_1 P-O modes. This in turn suggests an increase in ϕ .

In order to understand how the above change in bond angle may come about it is necessary to propose a structure for the resultant ion-pairs. In general, the stronger the interaction between the ions and the solvent, the greater the chance of solvent-separated ion-pairs being formed. With DMSO as solvent, it is very unlikely that solvent-separated species dominate, and therefore the ion-pair formed is either a monodentate or bidentate contact ion-pair. Theoretical studies have shown the bidentate species to

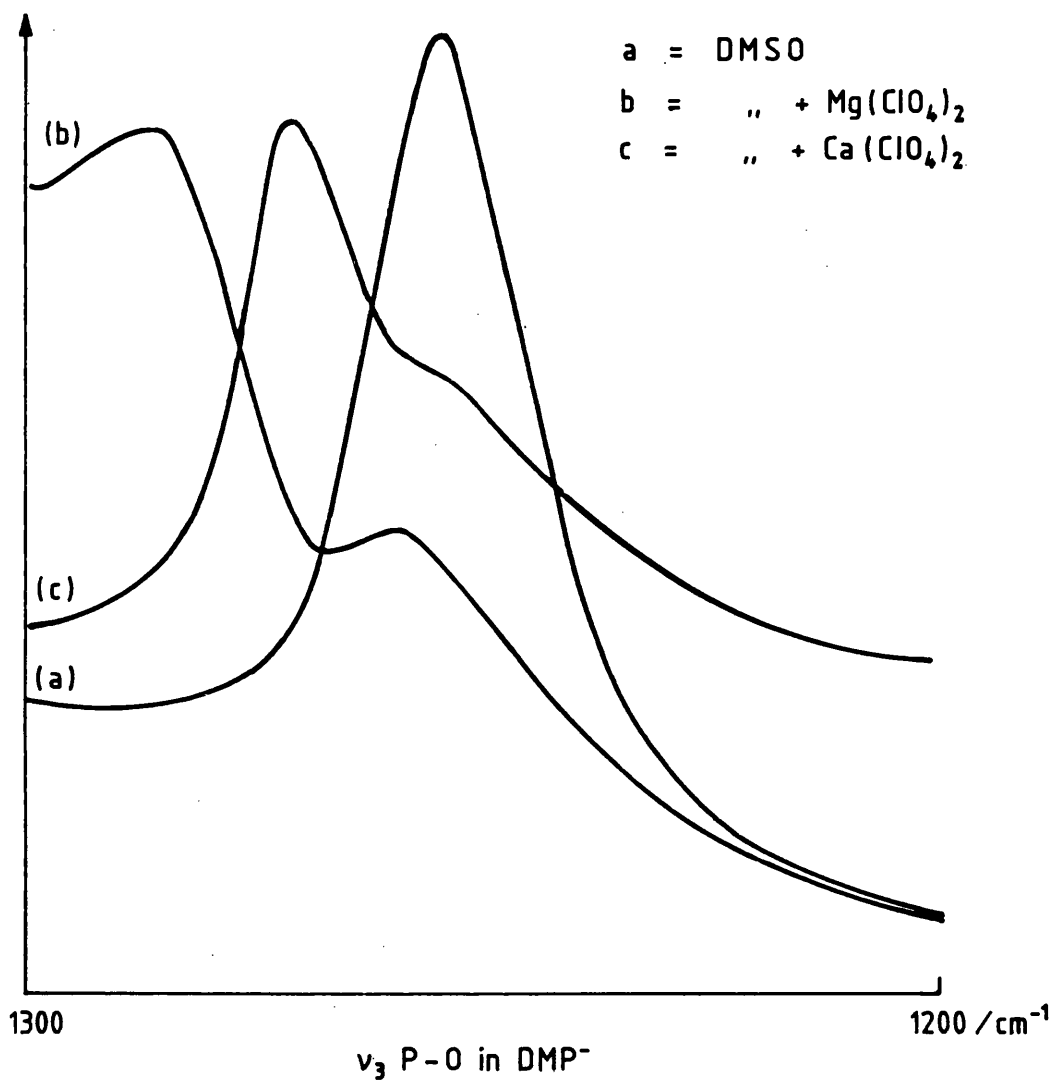


Figure 5.6.

Effect upon the infrared spectrum of NaDMP in DMSO ($v_3 \text{P-O}$ region) of the addition of divalent cations. (a) No added salt, (b) + $\text{Mg}(\text{ClO}_4)_2$ and (c) + $\text{Ca}(\text{ClO}_4)_2$.

be favoured in the absence of any strong solvent-anion interactions, therefore in DMSO it is proposed that the dominant ion-pairing is the bidentate contact ion-pair.

Having proposed that bidentate contact ion-pairs dominate in DMSO, the conclusion that can be drawn from the high frequency shifts in $\nu_3\text{P-O}$, is that the formation of the bidentate contact ion-pair is accompanied by an increase in ϕ . Previous studies have concluded that ϕ decreases upon formation of bidentate contact ion-pairs. A discussion of the relative merits of the evidence supporting each of these conclusions is included in the concluding remarks of this chapter.

Figure 5.7a shows the $\nu_3\text{P-O}$ band due to DMP^- in MeOH, the max occurs at ca. 1208 cm^{-1} . Addition of dications gives two new features in the $\nu_3\text{P-O}$ region of the IR spectra. These new bands occur at ca. 1240 and 1285 cm^{-1} with additions of Mg^{2+} , and ca. 1223 and 1258 cm^{-1} with additions of Ca^{2+} .

Once again, dications have induced high frequency shifts in $\nu_3\text{P-O}$. This time however, two new bands have been formed and the possibility of desolvation of the phosphate group has to be considered in addition to changes in the extent to which the two stretch modes are coupled. The effect of solvation upon the $\nu_3\text{P-O}$ stretch is shown in figure 5.8.

The observation that two new bands are formed when dications are added is interesting and points to mono- and bidentate contact ion-pairs being formed in equilibrium. As can be seen from scheme

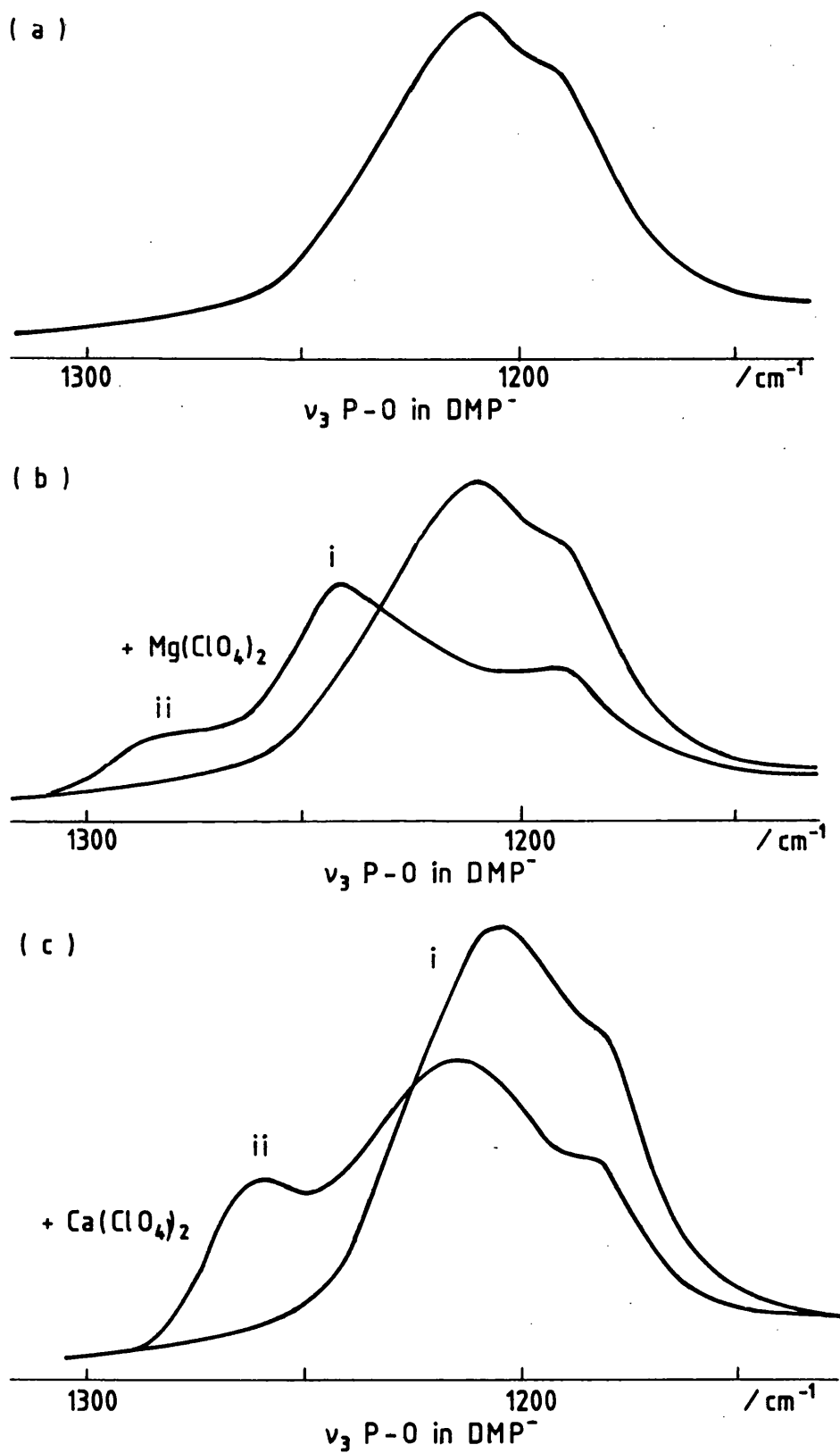


Figure 5.7.

Effect upon the infrared spectrum of NaDMP in MeOH (ν_3 P-O region) of the addition of divalent cations. (a) No added salt, (b) + $\text{Mg}(\text{ClO}_4)_2$ and (c) + $\text{Ca}(\text{ClO}_4)_2$.

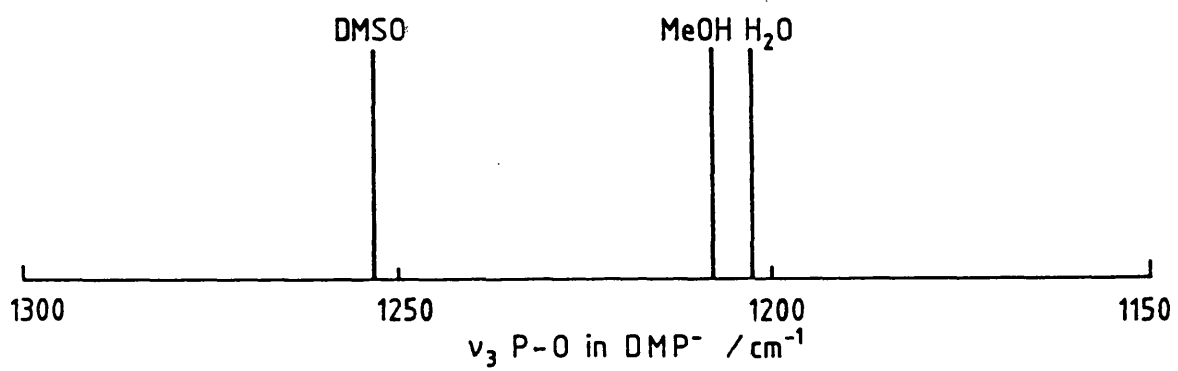


Figure 5.8.

Diagram showing the frequency of ν_3 P-O band of NaDMP in DMSO, MeOH and H₂O .

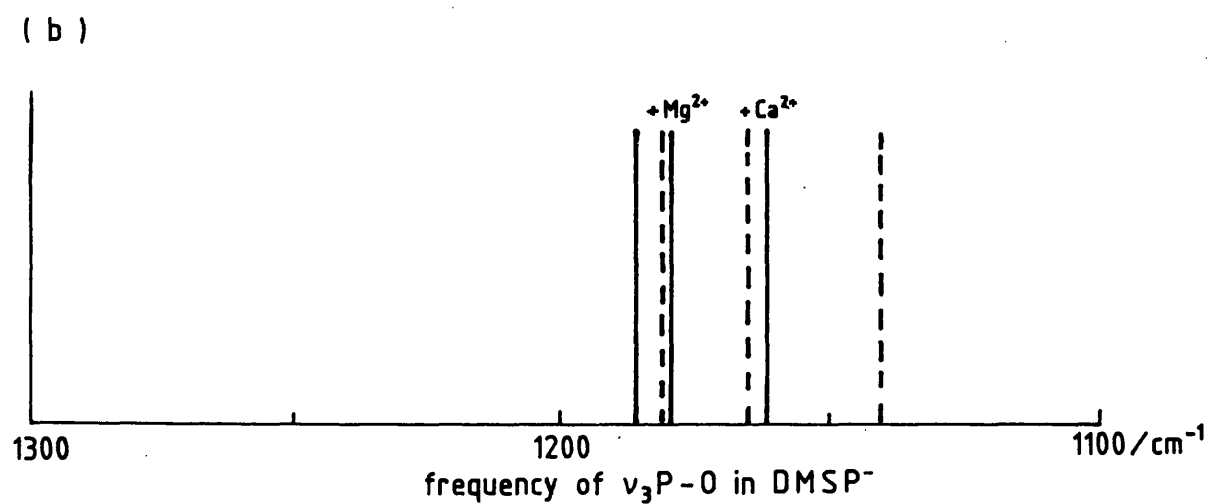
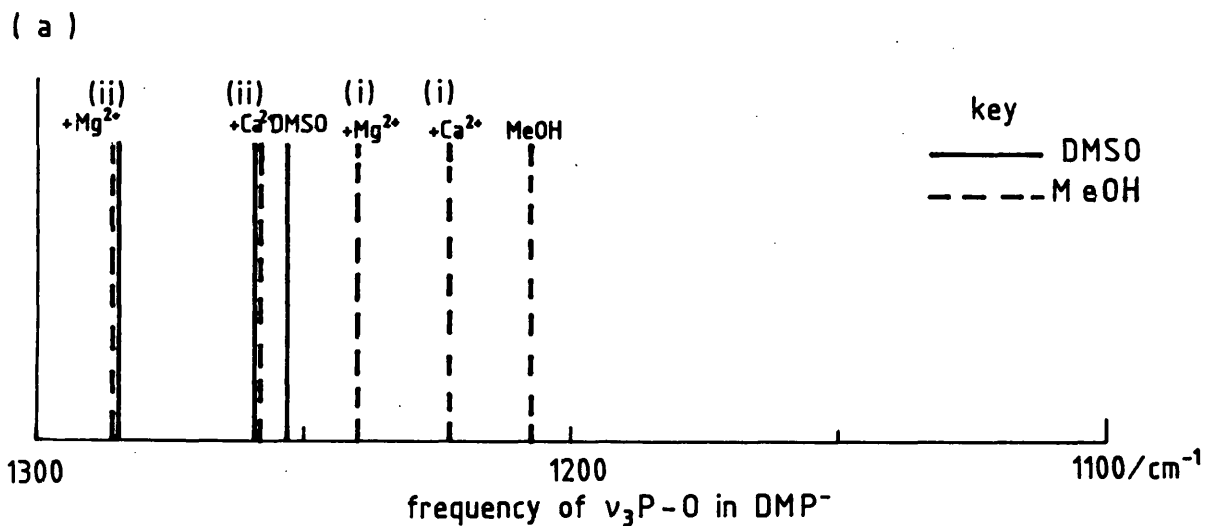


Figure 5.9.

Diagram showing an 'overview' of :-

(a) ν_3 P-O stretching frequencies for NaDMP in different solvents and with additions of divalent cations.

(b) ν P-O stretching frequencies for NaDMSP in different solvents and with addition of divalent cations.

(IV), in order for DMP^- to form contact ion-pairs a degree of desolvation must occur. This would result in a high frequency shift in $\nu_3\text{P-O}$. The bidentate species requires a greater degree of desolvation to occur, than does the monodentate. It might be expected, therefore, that the bidentate species is responsible for higher frequency of the two new bands (ii) in each case. Further evidence for this assignment is to be found if the frequencies of the bands formed upon addition of dications to DMP^- in both DMSO and MeOH are compared (see figure 5.9a). This overview clearly shows that the bands formed by additions of dication to DMP^- in DMSO, are almost coincident with the respective higher frequency bands formed when dications are added to DMP^- in MeOH. The secondary effect that solvent molecules exert upon the anion through the dication could lead to the frequency of band (ii) varying with solvent, but the fact that the frequency of the bands observed when dications are added to DMSP^- are very similar (see figure 5.9b) in DMSO and MeOH, indicates that this secondary effect is not significant.

5.4 Concluding Remarks

This work shows that IR spectroscopy is a useful tool for investigating metal binding to phosphates and thiophosphates. It has been possible to assign bands formed upon addition of Mg^{2+} and Ca^{2+} salts to specific ion-pairs. Furthermore, by exploring the effect of; solvation / desolvation, metal ion interactions and coupling between P-O modes, the shifts in frequency of the $\nu_3\text{P-O}$ and P-O stretches which occur, have been qualitatively rationalised.

The results suggest that in solutions of DMSO and MeOH, DMP^- and DMSP^- form contact ion-pairs with Mg^{2+} and Ca^{2+} . In the case of DMP^- in methanolic solutions a mono / bidentate equilibrium exists. In DMSO, this equilibrium, if it exists, lies heavily on the side of the bidentate species. The changes in the P-O stretch of DMSP^- are entirely consistent with the formation of contact ion-pairs with Mg^{2+} and Ca^{2+} and there is no evidence for the participation of sulphur in this ion-pair.

One of the conclusions that can be drawn from the high frequency shift that Mg^{2+} and Ca^{2+} induce in the ν_3 P-O stretch of DMP^- in DMSO, is that formation of bidentate contact ion-pairs increases bond angle ϕ . If this conclusion is correct, then it invalidates the explanation of changes in ^{31}P chemical shift observed by Haake and Prigodich⁸ which is based upon the relationship between bond angle and ^{31}P chemical shift proposed by Gorenstein¹². Therefore, it is necessary to determine whether this relationship can be applied correctly to the changes in ^{31}P chemical shift induced by metal binding to DMP^- .

Gorenstein related RO-P-OR bond angles (as measured by crystallography) to ^{31}P chemical shifts for a wide range of phosphates. As can be seen in figure 5.3, the bond angles of the phosphates varied between ca. 97 and 110° . The chemical shift varied over a range of ca. 25 ppm. Gorenstein¹² notes that "...bond angles in the solid state may significantly differ from those in solution due to crystal packing forces...", he then states that a Gillespie-Nyholm analysis of the compounds suggests

that the solid-state bond angles do at least represent the expected distortions from tetrahedral symmetry. He estimates the error in measuring the bond angles to be 0.5° .

In Haake and Prigodich's study the ^{31}P chemical shift of DMP^- varies over a range of only ca. 1.5 ppm. In view of the uncertainty inherent in estimating bond angles in solutions from solid-state data, and the error in measuring the solid-state data itself, it is difficult to see how Gorenstein's relationship between bond angle and ^{31}P chemical shift can sensibly be used to rationalise the chemical shift changes observed by Haake and Prigodich.

The basis for interpreting changes in the $\nu_3\text{P-O}$ stretch region of the IR spectrum of DMP^- in DMSO as being due to changes in the O-P-O bond angle, is a paper by Bellamy, Blandamer, Symons and Waddington²². In it they explored the relationship between the convergence of the $\nu_s\text{O-H}$ and $\nu_{as}\text{O-H}$ bands of H_2O and changes in the H-O-H bond angle. They concluded that convergence of the ν_s and ν_{as} is primarily a result of a decrease in the H-O-H bond angle. This would reach a limit when the bond angle reached 90° , when there should be no vibrational coupling between the two modes, and ν_s and ν_{as} should be coincident.

If this treatment is applied to DMP^- , it is clear that an increase in the separation of $\nu_3\text{P-O}$ and $\nu_1\text{P-O}$ would be indicative of an increase in bond angle ϕ . Unfortunately it was not possible to observe the $\nu_1\text{P-O}$ band because of solvent bands which absorb in

the region, however, an increase in the ν_3 P-O band of DMP^- in DMSO upon addition of Mg^{2+} and Ca^{2+} cannot be explained in terms of desolvation or simple metal ion interaction (cf. DMSP^- in DMSO) and therefore, an increase in ϕ is the most likely explanation. One reason for this may be the development of extra negative charge on the anionic oxygen atoms. This build up of negative charge would cause an increase in the repulsive forces between the oxygen atoms and thus an increase in ϕ .

Having satisfactorily explained the complex changes in ν_3 P-O stretch which are observed when dications are added to solutions of DMP^- in DMSO and MeOH, as being due to the formation of contact ion-pairs, it is now perhaps reasonable to attribute the insensitivity of the ν_3 P-O stretch to different cations in aqueous solutions of DMP^- , as being indicative of the dominance of solvent-separated/shared ion-pairs. This conclusion is in contradiction with that of Haake and Prigodich⁸ who envisage the formation of contact (inner sphere) ion-pairs, and use that hypothesis to calculate the association constants for the ion-pairs.

The IR spectra of the ν P-S band of DMSP^- in DMSO, MeOD and D_2O show that hydrogen bonds are not formed to sulphur even though it is expected to have considerable anionic character¹⁸. This is consistent with the idea of sulphur being a 'soft' base.

References for chapter 5

1. O. Kennard, *Pure and Appl. Chem.* 56, 989 (1984).
2. A. Mahendrasingam, V. T. Forsyth, R. Hussain, R. G. Greenall, W. J. Pigram and W. Fuller, *Science* 233, 195 (1986).
3. C. Migchelsen, H. J. C. Berendsen and A. Rupprecht, *J. Mol. Biol.* 37, 235 (1968).
4. R. Burton, S. Forsén and D. Reimarsson, *Nuc. Acids Res.* 9, 1219 (1981).
5. E. M. Bradbury, W. C. Price and G. R. Wilkinson, *J. Mol. Biol.* 3, 301 (1961).
6. M. Falk, K. A. Hartman and R. C. Lord, *J. Am. Chem. Soc.* 85, 387 (1963).
7. M. Falk, K. A. Hartman and R. C. Lord, *ibid.* 84, 3843 (1962).
8. P. Haake and R. V. Prigodich, *Inorg. Chem.* 23, 457 (1984).
9. D. K. Chatteraj and H. B. Bull, *Arch. Biochem. Biophys.* 142, 363 (1971).
10. K. Hamaguchi and E. P. Geiduschek, *J. Am. Chem. Soc.* 84, 1329 (1967).
11. M. Tsuboi, *J. Am. Chem. Soc.* 79, ? -1354 (1957).
12. D. G. Gorenstein, *J. Am. Chem. Soc.* 97, 898 (1975).
13. D. G. Gorenstein and D. Kar, *Bioc. Biop. Res. Comm.* 65, 1073 (1975).
14. C. Tanford, *The Hydrophobic Effect*, Wiley: New York, (1973).
15. A. Pullmann and H. Berthod, *Chem. Phys. Letts.* 46, 249 (1977).
16. K. Patel, *Ph.D. Thesis*, Leicester (1985).
17. J. Langlet, P. Claverie, B. Pullman and D. Piazzola, *Int. J. Quant. Chem.:Quant. Biol. Symp.* 6, 409 (1979).
18. P. A. Frey and R. D. Sammons, *Science* 228, 541 (1985).

19. R. D. Sammons, P. A. Frey, K. Bruzik and M-D. Tsai *J. Am. Chem. Soc.* 105, 5455 (1983).
20. L. J. Bellamy, *Advances in Infrared Group Frequencies*, Methuen, London (1968).
21. A. Pullman, B. Pullman, N. Gresh and H. Berthod, *Theoret. Chim. Acta* 44, 151 (1977).
22. L. J. Bellamy, M. J. Blandamer, M. C. R. Symons and D. Waddington, *Trans. Fara. Soc.* 67, 3435 (1971).
23. M. Cohn and T. R. Hughes Jr., *J. Biol. Chem.* 235, 3250 (1960).
24. T.-D. Son, M. Roux, M. Ellenberger, *Nucleic Acids Res.* 2, 1101 (1975).

Chapter 6

*Hydration of
Deoxyribonucleic Acid.*

6.1 Introduction

The hydration water of frozen dilute aqueous solutions of DNA is investigated in this study, using high field (300 MHz) fourier transform NMR spectroscopy. The results are interpreted in terms of changes in the extent to which DNA is hydrated at temperatures between -3 and -40°C. Comparisons are made with results obtained in previous NMR studies, and by investigations using other techniques. The ramifications this work has for probing the process by which DNA is damaged by γ -irradiation are also discussed.

6.2 Previous Work

The importance of the hydration of biomolecules has long been recognised and is reflected by the extent of literature pertaining to the subject. Accordingly, the techniques employed in investigating hydration are very diverse, including NMR, IR, UV, neutron diffraction, X-ray crystallography and gravimetric studies.

The problem of DNA hydration can be broken down into the following areas :-

- i) The extent to which DNA is hydrated, i.e. a measure of number of water molecules associated with each base-pair unit.
- ii) The determination of which sites in the DNA molecule are hydrated.
- iii) How hydration affects the secondary structure of DNA, in particular the transitions

between the different forms of DNA.

iv) What effect hydration has upon the nature of γ -irradiation induced damage of DNA.

Early IR studies^{1,2} concentrated upon assigning spectral bands to particular vibrational modes. Sutherland and Tsuboi³ reported changes in the spectra of solid films of DNA as a function of the relative humidity (r.h.) and by measuring the dichroic ratios of various bands concluded that the configuration of the phosphate group was not consistent with the Watson-Crick^{4,5} model, but was in agreement with the model proposed by Wilkins et al.⁶ Bradbury, Price and Wilkinson⁷ plotted the dichroic ratios of several bands against r.h. as well as the frequency of the O-P-O antisymmetric stretch. Their findings confirmed those of Wilkins et al.⁶ and added that "*the fast deuteration rate of salts of DNA...shows that the hydrogen atoms which take part in the hydrogen bonding mechanism between the bases are completely accessible to protons and possibly water molecules.*" This result has important repercussions for the interpretation of NMR experiments involving the γ -irradiation of DNA in H₂O / D₂O solutions^{8,9}.

In a series of three papers, Falk and co-workers¹⁰⁻¹² reported their results concerning DNA hydration. They employed gravimetric studies and IR and UV spectroscopy. The gravimetric study¹⁰ showed that DNA is hydrated by ca. 1.4 grams of water per gram of DNA, this equates to about 20 water molecules per base pair. The measurements were made at 21°C. and at 92% r.h. Additionally, DNA was found to be hydrated by the first two water molecules with an

energy of hydration approximately 2 kcal mol^{-1} higher than that of subsequent water molecules.

11

An IR study probed the effect of changes in r.h. upon characteristic vibrational bands arising from solid films of LiDNA and NaDNA. In particular they concentrated upon changes which provide information pertaining to the ranges of r.h. in which the different DNA subgroups become hydrated. These results, summarised, show that the phosphate group becomes hydrated in the 0 - 65% range. Between the r.h. range 60 - 75% a change in DNA structure occurs resulting in the helical B form. Above 75% the bases become hydrated at the C=O groups and ring nitrogen atoms. This process was found to be complete by 80% r.h. and further hydration was accompanied by swelling.

12

In the third of their papers, Falk et al. investigated structural changes associated with changes in r.h. especially those in the 75 - 55% range. In this range they observed a sharp increase in the UV dichroic ratios and absorbance at 260nm. This was concluded to be due to a reversible transition from the B configuration to a form in which the bases are neither stacked one above another nor perpendicular to the helical axis. It was therefore suggested "*...that the B configuration of DNA is stabilised by the stacking of the bases in the presence of water.*"

13

A later IR spectroscopy study by Falk, Poole and Goymour, concentrated upon quantifying the amount of hydration water associated with DNA and investigating the properties of this water

at low temperatures, i.e. whether the hydration shells are, to any extent, 'ice-like'. They studied the OH and OD stretching bands of isotopically dilute HDO in partially deuterated films of DNA. By varying the r.h., the number of water molecules per nucleotide (as calibrated using a previous gravimetric study¹⁰) was controlled and IR spectra in the OD stretching region (2700 - 2300 cm^{-1}) were recorded at temperatures between +25 and -130°C.

The spectra of DNA films with less than 10 water molecules per nucleotide, showed the following gradual and reversible changes upon cooling; a) an increase in peak intensity, b) a decrease in band half-width, c) a shift to lower frequency of the band. All of these changes are consistent with the cooling of water in condensed phases. In contrast, at temperatures less than -10°C. spectra of films in which the water content is slightly higher, around 14 water molecules per nucleotide, display a sharp, intense band "...within a few wavenumbers to that of pure ice at the corresponding temperature." Films of intermediate water concentration (10 - 13 water molecules per nucleotide) usually show no ice-like band when cooled, however, if cooled very slowly or left for several days at dry ice temperature, a small ice-like band grew in. These results were interpreted as being consistent with DNA having an inner layer of hydration water of upto 10 molecules which were incapable of crystallisation.

Early NMR studies concentrated upon trying to observe changes in water proton resonance brought about by solvation of DNA. Lubas and Wilczok¹⁴ measured proton relaxation times of DNA solutions by

utilising a spin echo technique . They concluded that DNA is hydrated by only about two molecules of nonrotationally bound water per base. This figure compares with that reported by Falk ¹⁰ et al. for the number of water molecules which are strongly bound to the phosphate group even at very low r.h. values. Since the quantity of hydration water is very small when compared with the total amount of water in DNA solutions, changes induced in the time averaged water proton resonance may not be easily detectable.

In an effort to avoid the 'swamping' effects of non-bound water in biomolecule solutions Kuntz ¹⁶ et al. recorded the proton resonance spectra of aqueous solutions of several biomolecules at temperatures between -5 and -35°C. and found that even at these temperatures there is a proton resonance due to a fraction of the total water concentration that remains unfrozen or mobile on the NMR timescale. Furthermore, they found that the area under this resonance varies linearly with macromolecule concentration. This suggests that these NMR signals are due to water which is associated with macromolecules. This unfrozen fraction was later ¹⁷ defined by Kuntz and Kauzmann as hydration water.

Not surprisingly, the above work by Kuntz ¹⁶ et al. led to several papers reporting examples of 'unfrozen' water being observed by NMR spectroscopy in various systems including; muscle, collagen, tissues, membranes and a wide range of macromolecule solutions. Particularly pertinent to the present study are those of Mathur de ^{8,9} Vre et al.

Mathur de Vre, Bertinchamps and Berendsen, addressed themselves to the question of to what extent DNA is hydrated and how this hydration water affects damage to DNA induced by γ -irradiation. They quantified the amount of 'unfrozen' water associated with solutions of DNA, poly(A), poly(C), poly(U), poly(A+U) and poly(A+2U). The extent of hydration ($H\%$) was defined as the number of grams of hydration water per 100g weight of DNA or polynucleotide. The area underneath the water proton resonance (Δ) at -5 and $+5^\circ\text{C}$. was measured and the plot of $(\Delta)_{-5} / (\Delta)_{+5}$ verses macromolecule concentration (C) was used to calculate ($H\%$). The results for DNA and other polynucleotides are presented in table 6.1. Mathur de Vre et al. ⁸ conclude that "...DNA is hydrated to a much greater extent than the single stranded polynucleotides or their molecular complexes." Their comparison of changes induced in the hydration water resonance linewidths of DNA and polynucleotides by γ -irradiation, led them to conclude "...that hydration water makes a distinct contribution to the overall radiation damage by indirect effects."

In the second of their papers, Mathur de Vre et al. ⁹ investigate isotopic effects upon the hydration of DNA, in particular how altering the ratio of $\text{H}_2\text{O} / \text{D}_2\text{O}$ in DNA solutions affects the linewidth of the hydration water resonance. They found that "... there is evidence that base rehydration with hydration water molecules occurs after an initial damage to the macromolecular chains in DNA caused by the direct or indirect radiation effects." Another observation was that temperature-dependent changes in hydration water resonance linewidths are dependent upon the $\text{H}_2\text{O} /$

Table 6.1

Hydration water content of various
⁸
 polynucleotides expressed as H%

Polynucleotide	Concentration / (g/100ml)	H%
Poly(A)	3.0	79
Poly(U)	3.0	110
Poly(C)	3.0	110
Poly(A + U)	1.5 + 1.5	125
Poly(A + 2U)	1.0 + 2.0	148
DNA	1.5	198

Table 6.2

A comparison of hydration water
 concentration as measured by various
 techniques.

Reference	Technique	Hydration Water Concentration (water molecules per base-pair)
Falk ¹⁰	Gravimetric	20 ^a
Mathur de Vre ⁸	NMR ^b	72
Wang ²⁵	Self-Diffusion Coefficient	13 ^c
Lubas & Wilczok ¹⁴	NMR ^d	4

(a) measured at 92% r.h.

(b) experiment measured the quantity
 of 'unfrozen' water in frozen aqueous
 system at -5°C.

(c) measured at 25°C.

(d) experiment measured the amount of
 water which is non-rotationally bound to
 DNA.

D₂O proportion. From this they deduced that the distribution of H and D nuclei in the hydration layer is non-random with the OD bonds participating in interactions between water and hydrogen bonding groups, whereas the electrostatic interactions of hydration water molecules are more likely to result from OH than OD bonds. It was argued that these preferences are a result of, respectively; the difference in the zero-point energy of H bonds and D bonds¹⁸ (approximately 1.2 - 1.5 kcalmol⁻¹), and the greater polarisability of H bonds as compared with D bonds¹⁹. They cited, in support of these conclusions, evidence^{18,20-22} that labile protons in DNA and other biomolecules are not deuterated in D₂O. However, as previously mentioned, IR studies by two groups^{2,7}, both show that these labile protons are readily exchanged for deuterons in D₂O. Therefore, this concept of preferential hydration sites for H and D nuclei must be, at least, open to question.

The above work and that of other workers, is discussed further by Mathur de Vre in an extensive review of NMR studies of water in biological systems²³.

Tunis and Hearst²⁴, in an excellent review of DNA hydration compared and contrasted the various values obtained for the extent of DNA hydration by different workers and methods. Their review of previous work concluded by stating that "Different types of experiments give different values for water of hydration." And that ... "this is not surprising when one realizes the wide variety of parameters being measured." They suggested that the

value of 6.5 molecules of hydration water per base obtained by
²⁵
Wang was the most reliable value for average hydration.

One technique which has great potential for obtaining structural information about oligonucleotides, including DNA, is single crystal X-ray diffraction crystallography. Using this technique it is possible to derive molecular structures of atomic or near-atomic resolution. In a survey of oligonucleotide structures, Kennard²⁶ reviewed structures of single crystals published between 1978 and 1984.

In the literature, Kennard²⁶ found several examples of A- and Z-type conformations. However, only one example of a single crystal showing a full turn of a B-type helix. This study by Dickerson et al.²⁷ was made upon the dodecamer d(CGCGAATTCGCG). The helix was found to be right handed with average global helical parameter similar to those found in previous studies. However, they found that "*...each base-pair has a propeller twist that increases the overlap between the base and its neighbours up and down the same chain...*". This observation supported both experimental²⁸ and theoretical studies²⁹ which suggested this kind of modification of the Watson-Crick structure.

Of most relevance to the present study is the information obtained about the hydration of B-DNA. It was found that "*...between one and three water molecules are found around most phosphate oxygens...*". Very few of the phosphate's esterified oxygens were found to be hydrated. This observation is to be expected, as both

IR and theoretical studies of the dimethylphosphate anion showed relatively little hydration of the phosphate ester oxygens as compared with the anionic oxygen atoms. In addition, they found a chain of nine linked water molecules extending along the minor groove. Towards either end of the helix, the primary hydration shell becomes less well ordered.

In summing up, Kennard suggests that water plays an important role in mediating conformational changes in DNA. However, further work is necessary before precise question about this role can be answered.

The concept of hydration water mediating conformation changes in DNA was extended and formalised by Saenger, Hunter and Kennard³² in an important paper entitled "*DNA conformation is determined by economics in the hydration of the phosphate groups*". As a result of further single crystal X-ray diffraction studies³³⁻³⁶ which concentrated upon the position of hydration water molecules and the phosphate groups, the following pattern emerges. When salts or non-polar solvents are added; "*...water molecules are withdrawn from the DNA and hydration therefore becomes more economical*". This occurs as a result of a change in conformation of the sugar residues which forces adjacent phosphate groups closer together, a fraction of water molecules which hydrate each phosphate group individually in the B-form, rearrange to form bridges between adjacent phosphate groups. Both the transition between conformation states, and formation of the water bridges are cooperative. The phosphate hydration patterns of A-, B- and

Z-type DNA are shown in figure 6.1 (reprinted from Saenger, Hunter
32
and Kennard).

Investigations into the mechanism by which γ -irradiation damages DNA have been, and continue to be, the subject of many studies, both in this laboratory and others, a review of recent work in the field was presented by Symons as the first Bruker lecture of the
37
Royal Society of Chemistry .

38
Two limiting mechanisms are generally agreed to account for the observed damage:-

a) Indirect Damage - In this process primary damage is to water molecules. The products of this damage; Hydrogen atoms (H^{\cdot}), Hydrated electrons (e_{aq}^{-}) and in particular, hydroxyl radicals (OH^{\cdot}), then attack DNA. This mechanism
39-41
has been widely studied using product analysis and pulse radiolysis. It is
38
concluded that this mechanism is appropriate to dilute aqueous systems which are irradiated at room temperature.

b) Direct Damage - In which primary electron loss and capture occur within the DNA molecule. In frozen systems this appears to be the
38
dominant mechanism . More importantly it may be argued that the frozen aqueous system is a good model for the situation in vivo. This is because within the cell nuclei the concentration

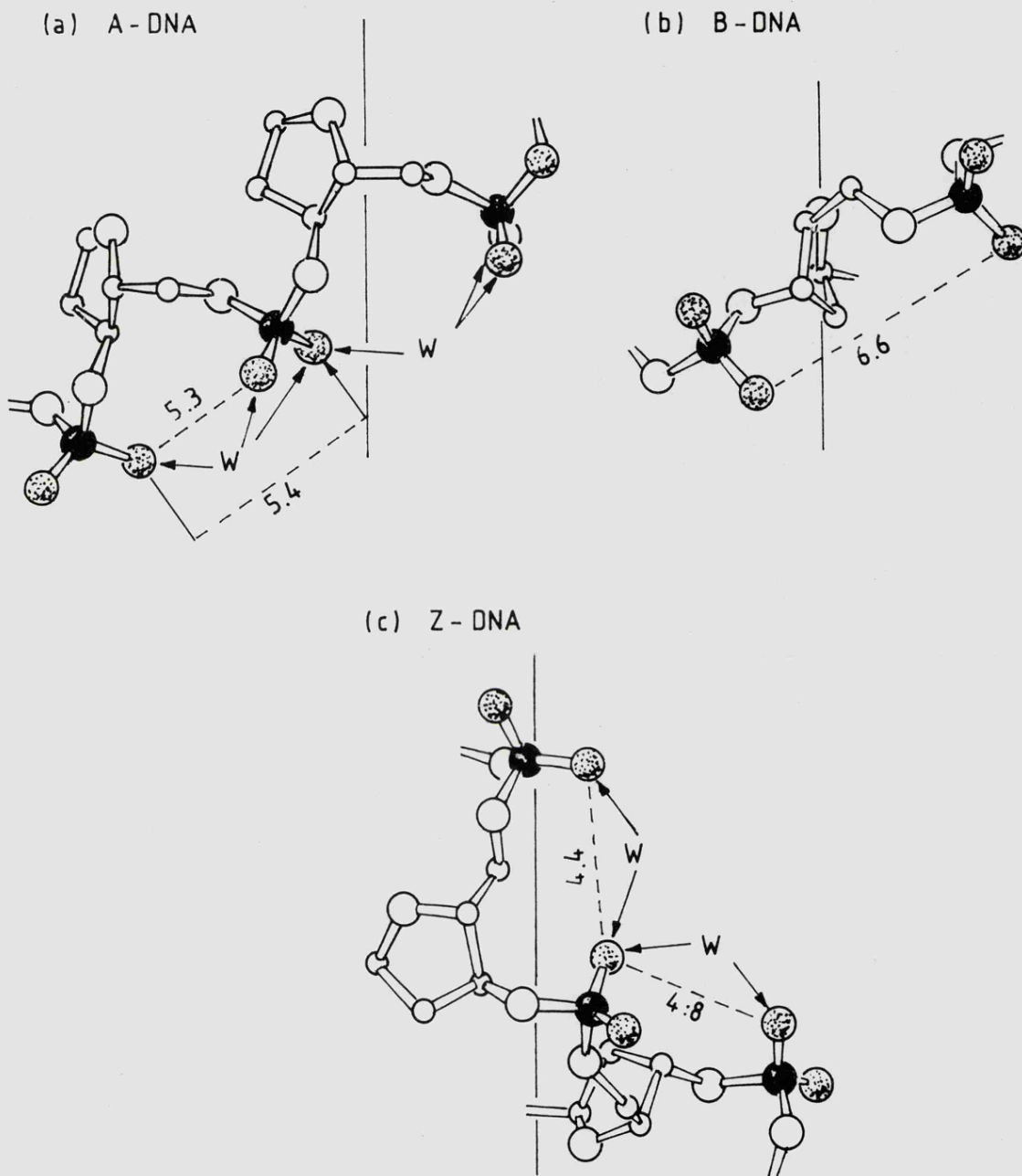


Fig.6.1. Comparison of hydration patterns³² of A-, B- and Z- type DNA. Vertical lines represent the helical axes ; phosphorous atoms indicated by solid spheres (●) and free phosphate oxygen atoms by shaded spheres (⊙). The shortest distances between free phosphate oxygen atoms are given. W represents water molecules which bridge free phosphate oxygens in A- and Z- DNA.

of water is relatively low consisting mainly of solvation water as opposed to 'bulk' water, which is separated from the DNA by the nuclear membrane. This is a situation which is analogous to that found in frozen aqueous systems in which the hydration water is the only mobile fraction.

Clearly, it is essential to know the concentration of hydration water, in order to be able to assess the relative importance of the above mechanisms in γ -irradiation induced DNA damage. It was in view of the somewhat contradictory evidence, as to the extent of DNA hydration (summarised in table 6.2), that the present NMR study was undertaken.

6.3 Experimental

6.3.1 Nuclear Magnetic Resonance Spectra

All spectra were recorded on a Bruker AM300 FT NMR spectrometer operating at 300.134 MHz. A multinuclear probehead with a 10 mm diameter probe was used in conjunction with a variable temperature controller unit. The latter was found to be stable to within 0.5°C. precise temperatures were measured by inserting a sample tube containing the probe of a pre-calibrated Comark electronic thermometer (type 1625) before and after each spectrum / measurement.

Measurements of T_1 were made using the inversion-recovery method, the $[180^\circ - \tau - 90^\circ \text{ (FID)} - T_d]_n$ pulse sequence (where T_d is a delay

time which allows the system to re-establish equilibrium before the next 180° degree pulse) was generated using a microprogram. 200 scans were accumulated for every spectrum with zero-filling used to improve digitisation. A built-in computer program which related signal intensity to the variable delay (τ), was used to calculate T_1 . The results presented are the average obtained from five separate samples. Error bands represent the extent of variability between samples.

6.3.2 Sample Preparation

Calf Thymus DNA (7.1% Na) was obtained from Sigma Chemical Company. Solutions were made up using deionised water which had been further purified using a millipore 'Milli-P' system. All samples except those used to determine the concentration dependence of the 'unfrozen' fraction, were made up to be 20 mg/ml.

6.4 Results and Discussion

When biological macromolecules are put into aqueous solution, weak macromolecule-water interactions occur which lead to the formation of a well defined hydration layer around the macromolecule. The water molecules which contribute to this layer are unlike 'bulk' water in that they are dynamically orientated and have had both their translational and rotational modes of motion reduced by the macromolecule-water interactions.

42

In the case of protein-water interactions in solution, Franks envisaged three distinct water molecule environments, as

represented in figure 6.2. Area A consists of water molecules which are in the neighbourhood of the protein's hydration sites, their motion is governed, to a large extent, by that of the protein molecule or localised groups with which they are interacting. Region C represents water molecules which are unperturbed by macromolecules, i.e. 'bulk' water. Region B is a result of the "... *incompatibility of the hydrogen bonding in regions A and C*". Franks⁴² suggested that water molecules in regions A and B represent the hydration layer and contribute to the 'unfrozen' fraction which is 'seen' by NMR. Whilst this model might not accurately describe non-frozen aqueous solutions (see chapter 1 for arguments), it does describe frozen aqueous systems fairly well and will be used to help interpret the results of the present study.

Since the NMR studies by Mathur De Vre et al.^{8,9} were performed, the introduction of high field Fourier transform (FT) NMR spectrometers has led to much greater sensitivity, it should therefore be possible to quantify the 'unfrozen' fraction more precisely. Accurately weighed amounts of calf thymus DNA were dissolved in water and left to equilibrate for at least 24 hours. The resulting gelatinous solutions were then transferred to a 10 mm (outer diameter) NMR tube. Into this was inserted a 5 mm NMR tube containing a solution of tetramethylsilane (TMS) in deuterated trichloromethane (CDCl₃) (see figure 6.3). Any air bubbles were removed at this stage by very gentle centrifugation.

A ¹H NMR spectrum with a sweep width of 10000Hz was then recorded

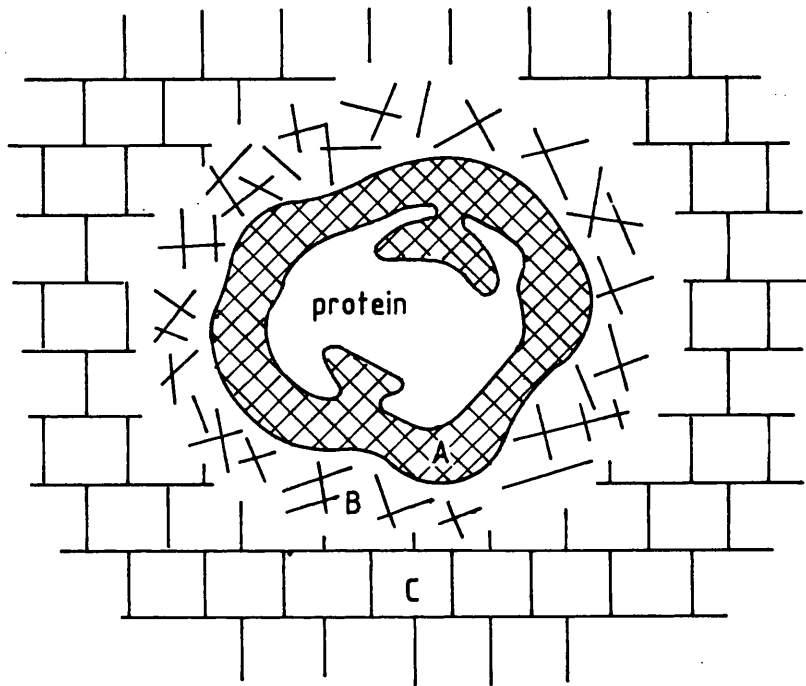


Fig. 6.2. Diagrammatic representation ⁴² of the protein environment in solution. The protein can be considered as having a primary hydration shell A in which the water molecules motions are largely determined by those of the polar protein sites. C is the unperturbed water structure and region B arises from The spatial and orientational mismatch between regions A and C.

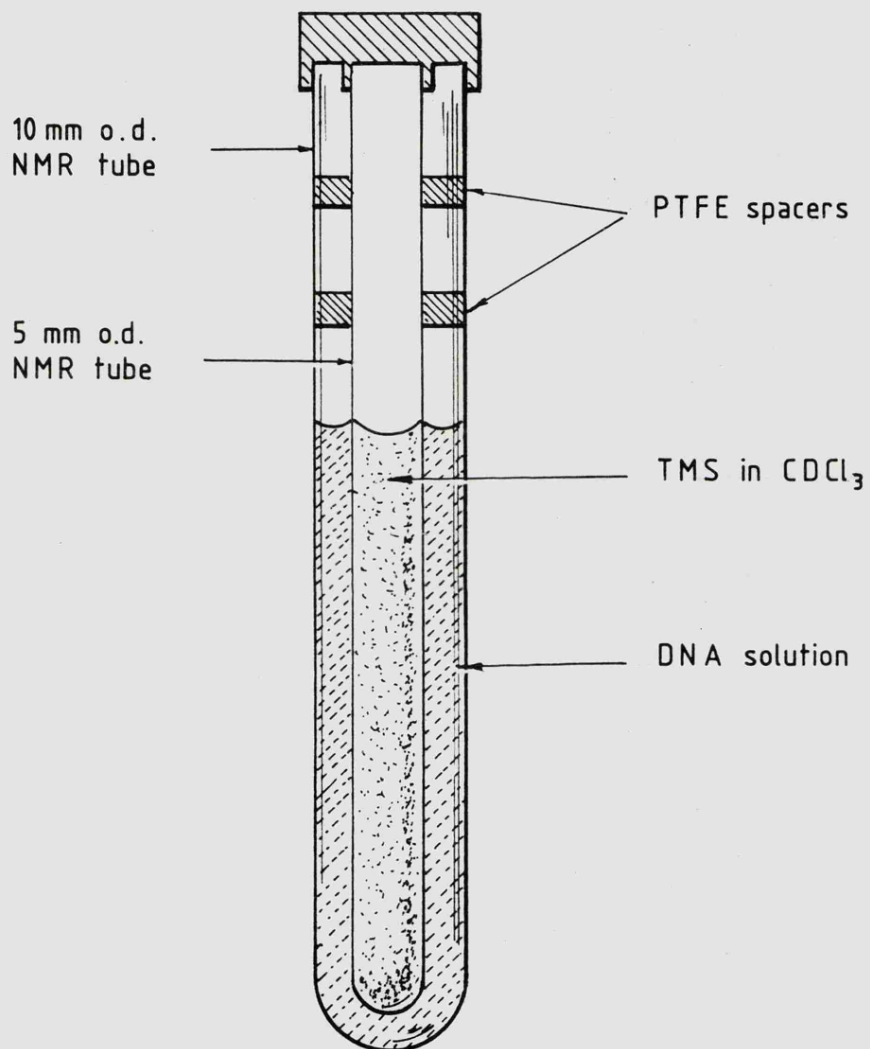


Fig. 6.3. Arrangement of inner and outer nmr tubes used in the experiments.

at +5°C. and the resulting water and TMS peaks integrated to obtain the relative area underneath the H₂O peak to that of the TMS peak (figure 6.4). The sample tube was then withdrawn and slowly frozen using an ice bath, from the bottom of the tube upwards. Care was taken to avoid displacement of the tubes relative to each other during this process. The sample tube was then re-inserted into the probe pre-cooled to -5°C. and the spectrum recorded again (figure 6.5). The relative areas of the, by now much diminished water peak, and the TMS peak were integrated. Because the area under the TMS peak is effectively constant it is thus possible, by normalising the area under the water peaks to the integral of the TMS peak, to relate the concentration of the 'unfrozen' water fraction at -5°C. to the total concentration of water at +5°C. Furthermore, since the absolute concentration of water in the DNA solutions are known, the absolute concentration of the 'unfrozen' fraction can be calculated.

Figure 6.6 shows that the concentration of 'unfrozen' water in the samples is proportional to DNA concentration as previously reported by other workers.

Figure 6.7 shows the effect upon the concentration of the 'unfrozen' hydration water, expressed as moles of water per molar base-pair (average MW = 662.15), of gently lowering the temperature. The results show that between -3 and -12°C. the amount of hydration water falls quite sharply. At -12°C. the unfrozen fraction consists of ca. 25 water molecules per

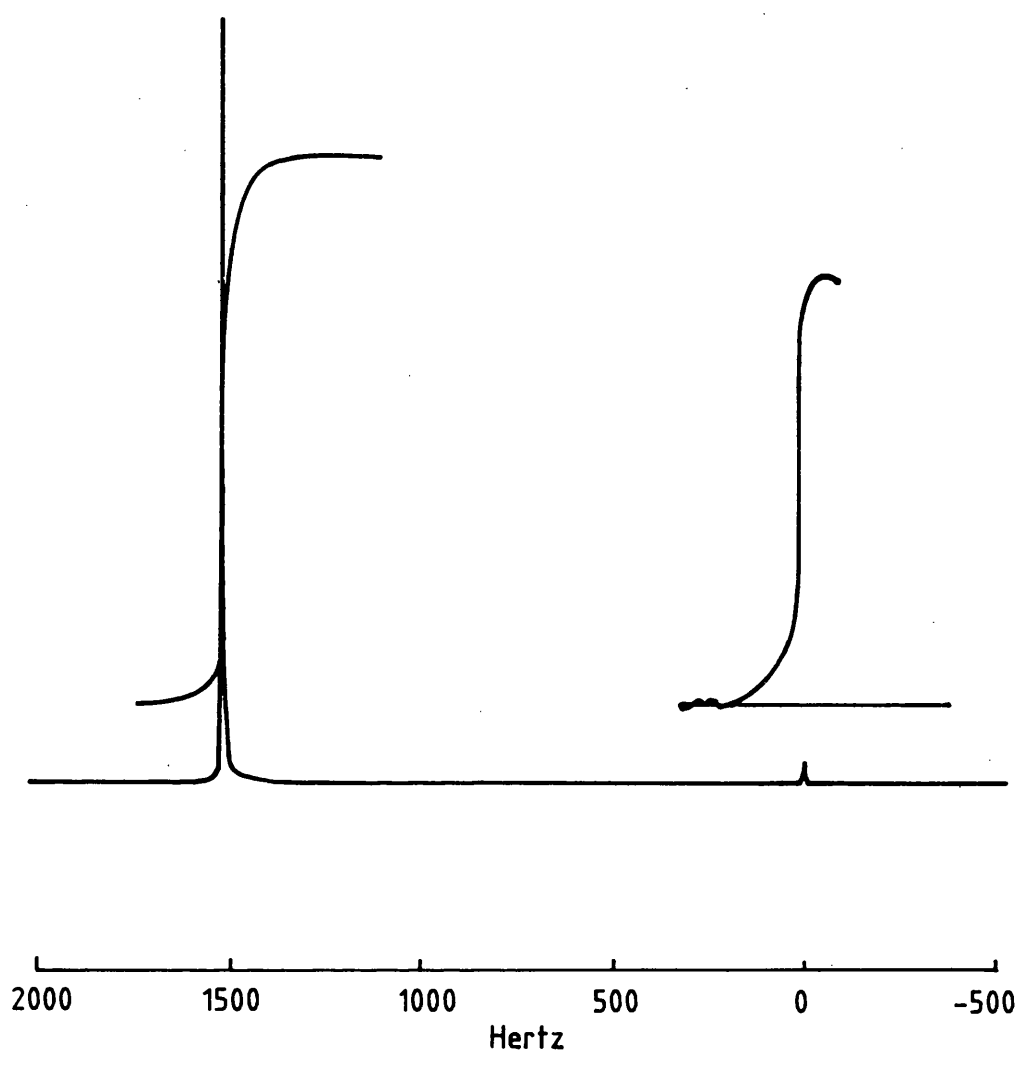


Fig. 6.4. Typical ^1H spectrum of 20 mg ml^{-1} DNA solution at $+5^\circ\text{C}$.

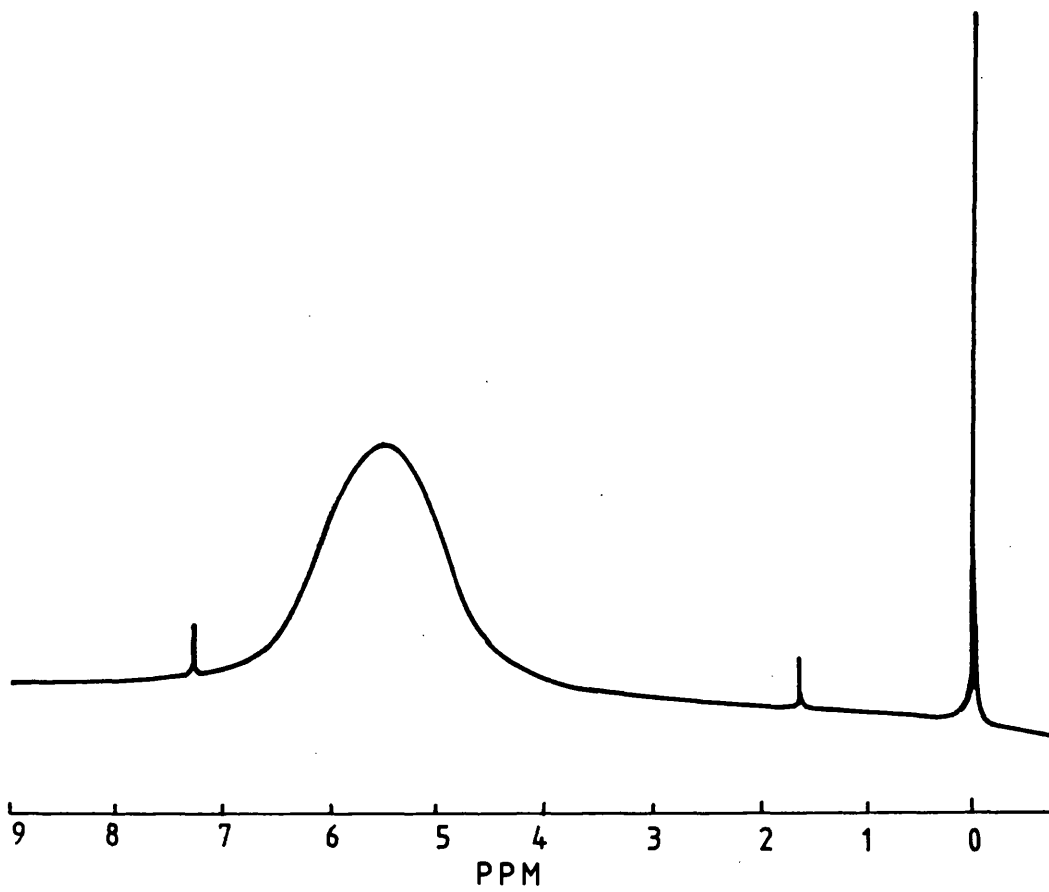


Fig. 6.5. Typical ^1H spectrum of 20 mg ml^{-1} DNA solution at -5°C .

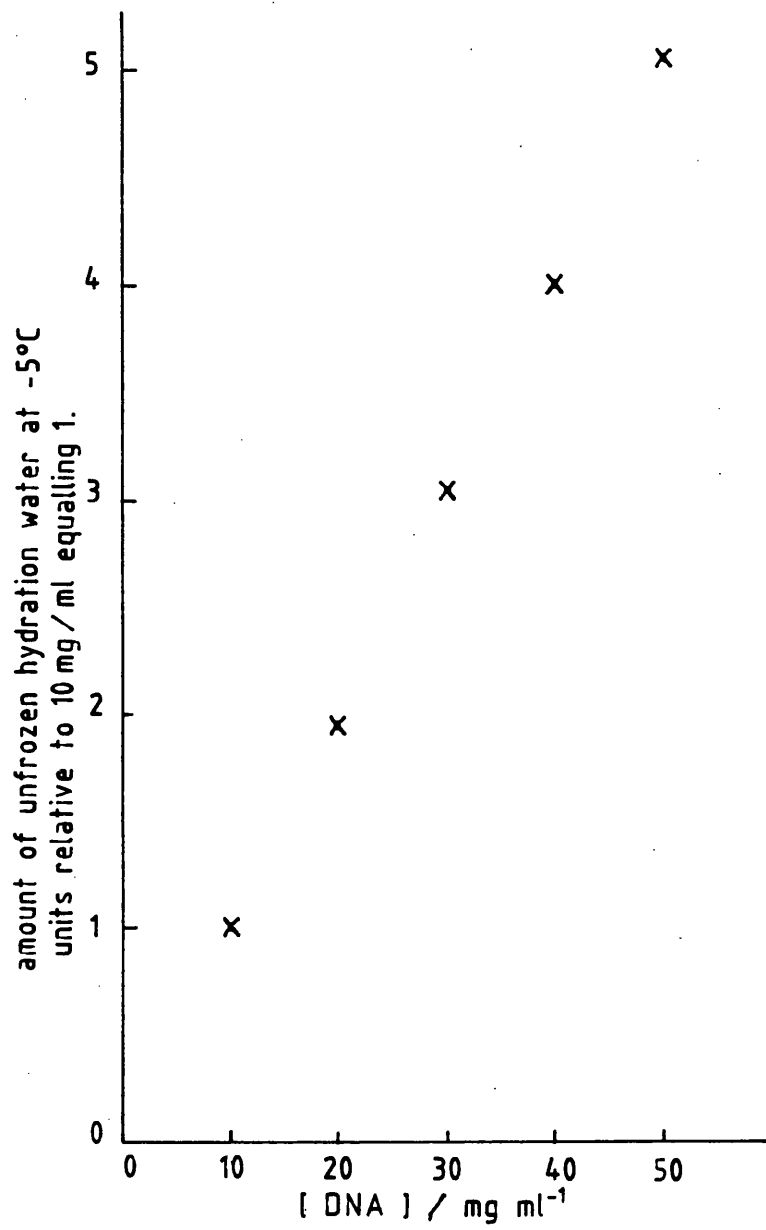


Fig. 6.6. Plot of area underneath the "unfrozen" water peak against DNA concentration.

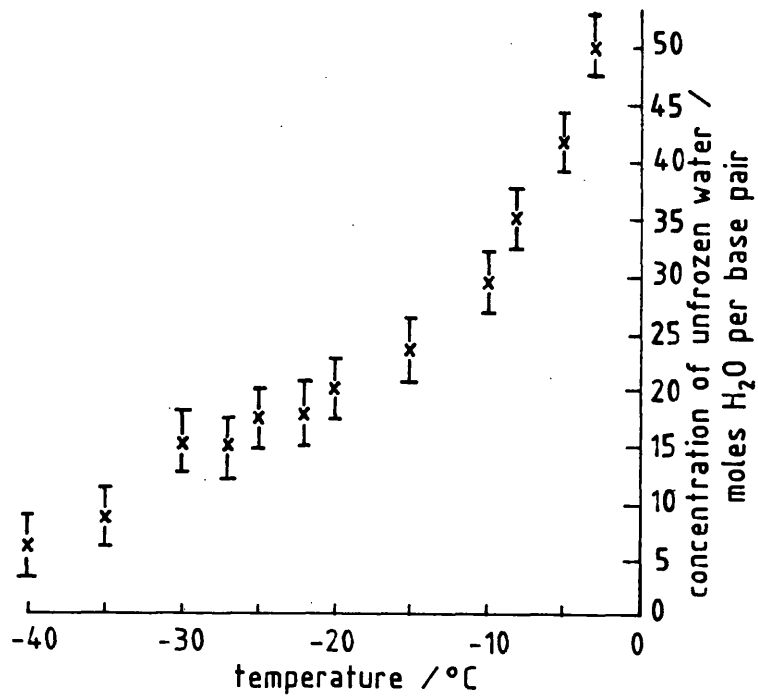


Fig. 6.7. Temperature dependency of the concentration of unfrozen water.

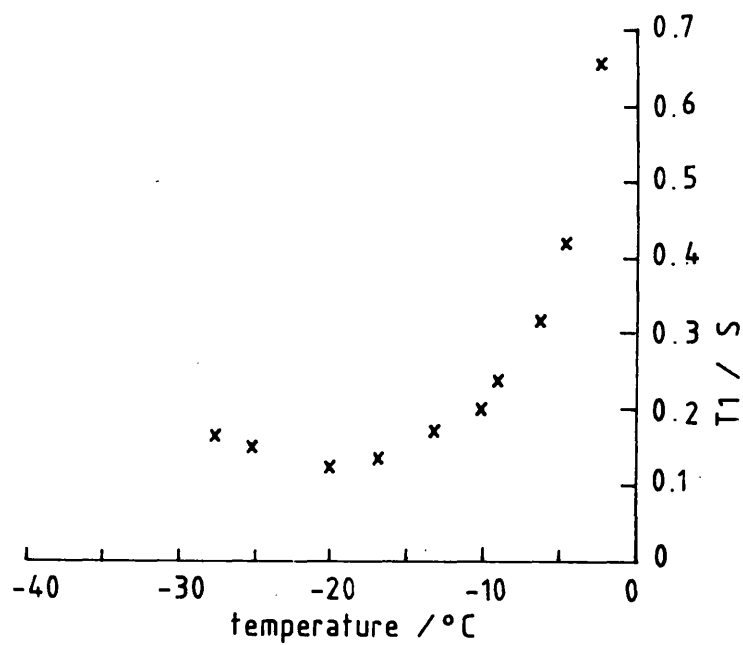


Fig. 6.8. Temperature dependency of the spin-lattice relaxation time (T_1).

base-pair. In contrast below -12°C . further cooling results in the concentration of hydration water falling regularly, but less sharply. Throughout the cooling cycle the width of the H_2O peak increases, and as a consequence the peak becomes increasingly difficult to integrate accurately. It is therefore difficult to assert, from these results alone, whether the shape of the hydration water concentration vs. temperature plot has any physical basis. Hence it was decided to measure the longitudinal relaxation time (T_1) (simply the inverse of the first order relaxation rate constant, measured in s^{-1}) of the 'unfrozen' fraction, and determine it's temperature dependency.

A detailed discussion of the theory of relaxation rates is not attempted here, (for this see Appendix I) however, in attempting to understand the physical meaning of T_1 measurements, it is useful to recall that longitudinal relaxation is often called spin-lattice relaxation. When nuclei are irradiated by, for example a 90 or 180° pulse the energy of the system is increased. To return the system to the situation of lowest enthalpy, this extra energy has to be transferred and dissipated. There are several relaxation mechanisms by which this can be done, the most important of which, for nuclei of spin $I = 1/2$, is dipolar relaxation. This process dissipates the excess energy through the changing electronic and magnetic dipoles of surrounding molecules. These fluctuating dipoles are a result of the vibration and rotation of bonds and atoms. The generic name for this surrounding framework is the 'lattice' and it is from this that the expression spin-lattice relaxation is derived.

From the above description of spin-lattice relaxation, it is possible to see that large changes in the nature of the 'lattice' will have a considerable effect upon T_1 . It was therefore hoped that measuring the T_1 of 'unfrozen' water at intervals between -3°C and -30°C . would detect any change in the environment of the hydration water, caused by cooling the sample.

The shape of the T_1 vs. temperature curve (figure 6.8) partially mirrors that of the hydration water concentration vs. temperature plot (figure 6.7). Between -3°C and approximately -10°C , the T_1 falls from 0.66 s to 0.2 s below -10°C . the T_1 continues to decrease, however, much more slowly. Where the similarity between plots ends is below -25°C . Below this temperature the concentration of hydration water continues to fall, whereas, the T_1 levels out and begins to increase.

The above T_1 results suggest that between -3°C and -10°C . the environment of the hydration water is altering, one explanation of this could be that as the system is cooled, some of the 'unfrozen' water molecules which are least affected by the DNA molecule are 'frozen out'. They thus become part of the bulk ice fraction. This would lead to a reduction in T_1 because the water molecules which have been 'frozen out' were those which were relaxed least efficiently by transfer of excess energy to the dipoles of the DNA molecule. Therefore the average spin-lattice relaxation time of the remaining 'unfrozen' fraction will be lowered.

Between -10°C and -25°C . cooling results in a gradual lowering of

T_1 which might be due to further small changes in the amount of hydration water. However, an alternative explanation may be that the strength of the DNA-hydration water interactions are increasing due to reduced thermal motion, and therefore dipolar relaxation with the dipoles of the DNA molecule is enhanced.

Below -25°C . T_1 begins to increase, this observation is consistent with reduced thermal motion of the DNA molecule, leading to a reduction in spin-lattice relaxation of the hydration water. This will have been occurring throughout the whole cooling process, however has been masked by the opposite, and presumably larger, influences upon relaxation rate caused by changes in the hydration shell.

The information obtained from T_1 measurements helps to confirm that the hydration shell surrounding DNA is changing, both in size and physical character as the sample is cooled between -3°C and -40°C . The greatest changes take place above -10°C . The changes can be best envisaged (with reference to figure 6.2) as region C encroaching upon region B.

6.5 Concluding Remarks

The figure of around 25 water molecules per base pair, obtained for the degree of DNA hydration at -12°C ., is in reasonable agreement with that of 20 water molecules per base-pair obtained for the primary hydration shell by gravimetric investigation. However, it must be borne in mind that differences exist between the structure of DNA in fibres, (even when in systems of high water activity) and

dilute aqueous solutions. In particular, in aqueous solutions of DNA, the B-helix is slightly underwound^{43,44} with a smaller rotation angle than that observed in fibre diffraction studies.

The changes in T_1 observed on cooling occur as a result of the secondary hydration shell being crystallised into the bulk ice phase. This process is largely complete at -12°C .

The observed temperature dependence of hydration shell size may be useful in determining the relative importance of direct and indirect mechanisms of γ -irradiation induced damage of frozen dilute aqueous solutions of DNA. Further work is suggested in this area.

References for chapter 6

1. E. R. Blout and M. Fields, *J. Biol. Chem.* 178, 335 (1949).
2. E. R. Blout and H. Lenormant, *J. Opt. Soc. Am.* 43, 1093 (1953).
3. G. B. B. M. Sutherland and M. Tsuboi, *Proc. Roy. Soc.* A239, 446 (1957).
4. J. D. Watson and F. H. Crick, *Nature* 171, 738 (1953).
5. F. H. Crick and J. D. Watson, *Proc. Roy. Soc.* A223, 80 (1954).
6. Wilkins *et al.* *Nature*, 175, 834 (1955).
7. E. M. Bradbury, W. C. Price and G. R. Wilkinson, *J. Mol. Biol.* 3, 301 (1962).
8. R. Mathur de Vre, A. J. Bertinchamps and H. J. C. Berendson, *Radiat. Res.* 68, 197 (1976).
9. R. Mathur de Vre and A. J. Bertinchamps, *Radiat. Res.* 72, 181 (1977).
10. M. Falk, K. A. Hartman and R. C. Lord, *J. Am. Chem. Soc.* 84, 3843 (1962).
11. M. Falk, K. A. Hartman and R. C. Lord, *ibid.* 85, 387 (1963).
12. M. Falk, K. A. Hartman and R. C. Lord, *ibid.* 85, 391 (1963).
13. M. Falk, A. G. Poole and C. G. Goymour, *Can. J. Chem.* 48, 1536 (1970).
14. B. Lubas and T. Wilczok, *Bioc. Biop. Acta* 120, 427 (1966).
15. H. V. Carr and E. M. Purcell, *Phys. Rev.* 94, 630 (1954).
16. I. D. Kuntz, T. S. Brassfield, G. D. Law and G. V. Purcell, *Science* 163, 1329 (1969).
17. I. D. Kuntz and W. Kauzmann, *Adv. Protein Chem.* 28, 239 (1974).
18. J. F. Thompson, *Biological Effects of Deuterium* p. 15,

Pergamon, New York, (1963).

19. A. Lewin, *Displacement of Water and Its Control of Biological Reaction* p. 3, Academic Press, New York, (1974).
20. H. L. Crespi and J. J. Katz, *J. Mol. Biol.* 4, 65 (1962).
21. H. R. Mahler, G. Dutton and B. D. Mehrotra, *Bioc. Biop. Acta* 68, 199 (1963).
22. A. Hvidt, *Dynamic Aspects of Conformational Changes in Biological Macromolecules* (C. Sadron, Ed.), pp. 103-115. Reidel, Dordrecht, (1973).
23. R. Mathur de Vre, *Prog. Biophys. Mol. Biol.* 35, 103 (1979).
24. M. B. Tunis and J. E. Hearst, *Biopolymers* 6, 1325 (1968).
25. J. H. Wang, *J. Am. Chem. Soc.* 77, 258 (1955).
26. O. Kennard, *Pure and Appl. Chem.* 56, 989 (1984).
27. R. Wing, H. Drew, T. Takano, C. Broka, S. Tanako, K. Itakura and R. E. Dickerson, *Nature* 287, 755 (1980).
28. M. Hogan, N. Dattagupta and D. M. Crothers, *Proc. Natn. Acad. Sci. U.S.A.* 75, 195 (1978).
29. M. Levitt, *Proc. Natn. Acad. Sci. U.S.A.* 75, 640 (1978).
30. K. Patel, *Ph.D. Thesis*, Leicester, (1985).
31. A. Pullman, H. Berthod, B. Pullman and N. Gresh, *Theoret. Chim. Acta* 85, 387 (1963).
32. W. Saenger, W. N. Hunter and O. Kennard, *Nature* 324, 385 (1986).
33. M. L. Kopka, A. V. Fratini, H. R. Drew and R. E. Dickerson, *J. Mol. Biol.* 163, 129 (1983).3).
34. O. Kennard *et al.*, *J. Biomolec. Struct. Dyn.* 3, 205 (1986).
35. E. Westhof, Th. Prange, B. Chevrier and D. Moras, *Biochimie* 67, 811 (1985).

36. B. Chevrier, A. C. Dock, B. Hartmann, M. Leng, D. Moras, M. T Thoung and E. Westhof, *J. Mol. Biol.* 188, 707 (1986).
37. M. C. R. Symons, *J. Chem. Soc., Faraday Trans. 1*, 83, 1 (1987).
38. P. M. Cullis, M. C. R. Symons, M. C. Sweeney, G. D. D. Jones and J. D. McClymont, *J. Chem. Soc., Perkin Trans. 2* 1671 (1986).
39. G. Scholes, *British J. Radiat. Biol.* 56, 221 (1983).
40. C. V. Sonntag, U. Hagen, A. Schon-Bopp and D. Schulte-Frohlinde, *Adv. Radiat. Biol.* 9, 109 (1981).
41. H. Kasai, H. Tanooka and S. Nishimura, *Gann.* 75, 1037 (1984).
42. F. Franks, *Phil. Trans. Roy. Soc.* B278, 89 (1977).
43. S. Bram, *J. Mol. Biol.* 58, 277 (1978).
44. W. Saenger, *Principles of Nucleic Acid Structure* Springer-Verlag (1983).

Appendix I

*Theory of N.M.R.
Relaxation Processes*

Appendix I - Theory of N.M.R Relaxation Processes¹

Classical mechanics can be used to predict the effect of an applied magnetic field (**B**) upon a macroscopic sample with spin angular momentum (**P**).

$$\frac{d}{dt} \mathbf{P} = -\mathbf{B} \wedge \mathbf{M} \quad (\text{I.1})$$

Since the magnetization **M** is related to the spin angular momentum **P** by

$$\mathbf{M} = \gamma \mathbf{P} \quad (\text{I.2})$$

where $-\gamma$ is the magnetogyric ratio

$$\frac{d}{dt} \mathbf{M} = -\gamma \mathbf{B} \wedge \mathbf{M} \quad (\text{I.3})$$

Nuclear moments precess about the field direction with angular velocity $\omega_i = -\gamma \mathbf{B}$. This corresponds to a frequency of $\gamma \mathbf{B} / 2\pi$, the Larmor frequency.

The placing of a sample in a magnetic field \mathbf{B}_0 causes the magnetic moment to change from 0 to \mathbf{M}_0 . For nuclei with spin = 1/2, \mathbf{M}_0 is given by

$$\mathbf{M}_0 = \frac{1}{4} N (\gamma \hbar)^2 \mathbf{B}_0 / kT \quad (\text{I.4})$$

From this it can be seen that there is a thermal component (kT) which is the origin of the relaxation processes. Bloch allowed the components of **M** parallel and perpendicular to \mathbf{M}_0 to relax with different time constants, T_1 and T_2 . Thus, if the **z** axis is chosen to be along \mathbf{B}_0

$$\frac{d}{dt} M_z = -(M_z - M_0) / T_1 \quad (\text{I.5})$$

$$\frac{d}{dt} M_x = -M_x / T_2 \quad (\text{I.6})$$

$$\frac{d}{dt} M_y = -M_y / T_2 \quad (\text{I.7})$$

The relaxation rates, T_1 and T_2 may differ because different nuclear spins may interact without transferring energy to the lattice. This process, which is exclusive to T_2 , is the reason why T_2 is sometimes known as the **spin - spin** relaxation time.

Fourier Transform NMR spectrometers use short pulses of radio frequency radiation. As a result of the Heisenberg uncertainty principle these pulses will have a range of magnetic field amplitudes. Therefore a pulse of around $10\mu\text{s}$ will give a range of frequencies great enough to excite any protons in a sample.

Information is obtained in the time domain and can be converted into the frequency domain using the mathematical procedure of fourier transformation.

$$F(\nu) = \int_{-\infty}^{\infty} f(t) \exp(+i2\pi\nu t) dt \quad (\text{I.8})$$

With a rotating frame of reference (that is to say a set of axes which rotate with the applied field such that it appears static) nuclear magnetization M precesses about the x axis for the duration of the pulse (τ_p). The rate of this precession in angular units is given by $\gamma B_1 \tau_p$.

If τ_p is set to a value of $\pi/2\gamma B_1$ the magnetization will be turned through 90° . Similarly, a pulse of $\pi/\gamma B_1$ will invert the

magnetization so that it lies in the -z direction. Following an 180° pulse magnetization returns to Boltzmann equilibrium by spin - lattice relaxation.

$$M_z(t) - M_0 = [M_z(0) - M_0] \exp(-t/T_1) \quad (\text{I.9})$$

A 90° pulse is followed by spin - spin relaxation

$$M_y(t) = M_y(0) \exp(-t/T_2)$$

Figure I.1 shows the dependence of T_1 and T_2 on the correlation time (τ_c). τ_c is a measure of the rate at which a molecule is reorientating. For solutions which consist of molecules randomly tumbling, τ_c is approximately equal to the time taken by an average molecule to reorientate through one radian. T_1 is related to τ_c by the following equation

$$T_1^{-1} = \gamma^2 [B_{XL}^0]^2 2\tau_c / (1 + \omega_0^2 \tau_c^2) \quad (\text{I.10})$$

from which it can be seen that when τ_c is very short (as is typical for mobile solutions) the above equation simplifies to

$$T_1^{-1} = 2\gamma^2 [B_{XL}^0]^2 \tau_c. \quad (\text{I.11})$$

In this case the solution is said to be in the extreme narrowing regime. If τ_c is similar to ω_0^{-1} then the term $\omega_0^2 \tau_c^2$ in equation I.10 cannot be ignored. From equation I.10 it is clear that T_1 will start to increase with τ_c . The resulting T_1 minimum will occur when $T_1^{-1} = \frac{\gamma}{\omega} [B_{XL}^0]^2$

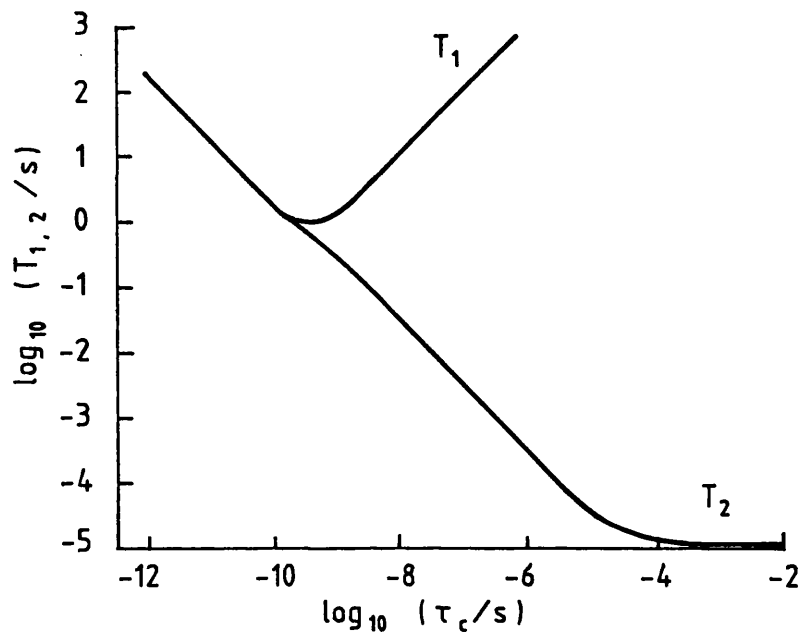


Fig. I.1. The dependence¹ of T_1 and T_2 on the correlation time τ_c . Operating frequency ν_0 is 400 MHz. r.m.s random field = 0.2 mT.

The spin - spin relaxation time does not go through any such minimum and continues to fall with increasing τ_c . This observation provides a useful method of determining whether or not nuclei are relaxing in the extreme narrowing regime, if T_2 is $\ll T_1$ then the relaxation is outside the extreme narrowing regime.

Reference for Appendix I

1. R. K. Harris, *Nuclear Magnetic Resonance Spectroscopy*, Pitman Books Ltd., London, (1983).

ABSTRACT

SPECTROSCOPIC STUDIES OF SOLVATION

PART 1 : SOLVATION OF THIOLS

PART 2 : HYDRATION OF DEOXYRIBONUCLEIC ACID

AUTHOR : GEOFFREY PHILIP ARCHER

The extent of hydrogen bonding in ethanethiol is determined using a correlation between the chemical shift of the sulphydryl proton and the stretching frequencies of the component bands of the ν_{S-H} infrared band. The component bands having stretching frequencies at 2585 cm^{-1} and 2570 cm^{-1} for non hydrogen bonded and mono-hydrogen bonded thiol groups respectively. It is calculated that the pure liquid at 22°C . contains ca. 49% free SH bonds. A dimerisation constant of $0.038\text{ dm}^3\text{ mol}^{-1}$ is estimated at 22°C .

2-Hydroxyethanethiol is used to investigate the strength of hydrogen bonding to the thiol group in aqueous solutions. The results of the IR and NIR studies are consistent with the formation of hydrogen bonds of S-H—O type between thiol and water molecules.

Salt and solvent effects upon the phosphate and thiophosphate groups of Sodium Dimethylphosphate (NaDMP) and Sodium Dimethylthiophosphate (NaDMSP) are investigated. Infrared spectra in the ν_{P-O} and ν_{S-P-O} of DMP and DMSP suggest that the order of strength of binding of metal ion to phosphate/thiophosphate group is $\text{Na}^+ < \text{Mg}^{2+} < \text{Ca}^{2+}$. The results indicate that solvent-separated ion pairs dominate in aqueous solutions, whereas, mono- and bi-dentate contact ion pairs are favoured in DMSO and methanol solutions. The thiophosphate group is solvated by methanol and water, primarily at the oxygen site. No evidence was found to support hydrogen bond formation to the anionic sulphur site. Infrared spectra were also consistent with Mg^{2+} and Ca^{2+} interacting with the Oxygen atom, but not the Sulphur atom.

DNA hydration is investigated using high field NMR spectrometry. Frozen aqueous DNA solutions were found to have a broad NMR signal due to hydration water. From this signal it is estimated that, at -12°C ., the DNA samples are hydrated by ca. 25 water molecules per base pair of DNA.

